OBJECTIVE PRELIMINARY ASSESSMENT OF OUTBURST FLOOD HAZARD FROM MORAINE-DAMMED LAKES IN SOUTHWESTERN BRITISH COLUMBIA

by

Robin James McKillop
B.Sc., University of British Columbia, 2001

THESIS SUBMITTED IN PARTIAL FULFILLMENT OF THE REQUIREMENTS FOR THE DEGREE OF

MASTER OF SCIENCE

In the
Department
of
Earth Sciences

SIMON FRASER UNIVERSITY

Fall 2005

APPROVAL

Name: Robin James McKillop

Degree: Master of Science

Title of Thesis: Objective preliminary assessment of outburst flood hazard from moraine-dammed lakes in southwestern British Columbia

Examining Committee:

Chair:

____
Dr. Peter Mustard
Associate Professor, Department of Earth Sciences

____
Dr. John Clague
Senior Supervisor
Professor, Department of Earth Sciences

____
Dr. Tracy Brennand
Supervisor
Associate Professor, Department of Georgraphy

____
Dr. Matthias Jakob
Supervisor
BGC Engineering Inc.

____
Dr. Jim O'Connor
External Examiner
U.S. Geological Survey

Date Defended: November 23, 2005

ABSTRACT

An objective, remote sensing-based procedure is proposed to evaluate the outburst flood hazard posed by moraine-dammed lakes in southwestern British Columbia. Outburst probability is estimated using an expression derived from statistical analysis of data collected from 175 moraine-dammed lakes in the southern Coast Mountains. Logistic regression identified four factors that correctly discriminate 70% of *drained* and 90% of *undrained* lakes: moraine height-to-width ratio, presence/absence of an ice core in the moraine, lake area, and main rock type forming the moraine. Objective methods, which incorporate empirical relations applicable to the study region, are used to predict outburst peak discharge and debris flow volume, travel distance, and area of inundation. Outburst flood hazard is especially sensitive to lake level fluctuations and is greatest for large lakes perched on valley sides behind narrow, ice-free moraine dams composed of sedimentary rock debris.

Keywords:

outburst flood, moraine-dammed lake, debris flow, hazard assessment, British Columbia

– To all who find happiness in mountains

ACKNOWLEDGEMENTS

Numerous people have helped make this thesis possible. In particular, I would like to thank my supervisor, John Clague, for always being approachable and enthusiastic, and for providing me with the opportunity to present preliminary results of this research at the European Geosciences Union conference in Vienna. My supervisory committee members, Tracy Brennand and Matthias Jakob, provided direction during the early stages of research and introduced me to a variety of data analysis techniques. Jim O'Connor kindly provided aerial photographs and maps of breached moraine dams in Washington and Oregon; Ian Bercovitz gave statistical advice; and Jennifer Butler helped locate photographs in the B.C. Aerial Photograph Warehouse.

I thank Michelle Hanson, Jeff Moore, Fred Touche, Dave Campbell, Tim Blair, Michael Morris, and Steve Yan-Klassen for their assistance in the field. Helicopter support was provided by John Goats (Pemberton Helicopters) and Mike King (White Saddle Air Services). I wish to thank Jasper Stoodley for GIS assistance and Nick Roberts for refreshing my photogrammetry skills. Christian Huggel, Andreas Kääb, and Jeffrey Coe offered valuable suggestions for this research.

Funding for this research was provided by an NSERC Discovery Grant to John Clague, and I was supported by an NSERC Postgraduate Scholarship, as well as a C.D. Nelson Memorial Scholarship and Graduate Entrance Scholarship from SFU.

Finally, I would like to thank my parents and my wife, Danielle, for their encouragement, support, and understanding.

TABLE OF CONTENTS

LIST OF FIGURES

LIST OF TABLES

CHAPTER 1:

INTRODUCTION

Moraine dams can fail suddenly and unexpectedly. Within hours or even minutes, an entire lake can drain, sending a slurry of water and debris many tens of kilometres downstream. In the past century, outburst floods from moraine-dammed lakes have claimed thousands of lives and caused hundreds of millions of dollars of damage (Richardson and Reynolds, 2000). Moraine dam failures have resulted in only minor damage in British Columbia (Blown and Church, 1985), but accelerated use and development of mountain valleys has increased the likelihood of impact on humans.

Given the destructive potential of outburst floods from moraine-dammed lakes, researchers are developing methods for predicting whether or not a particular lake is likely to drain catastrophically and, if so, what size of flood can be expected. This paper builds on published assessment methods and provides engineers and geoscientists with a remote sensing-based method for completing objective preliminary hazard evaluations of moraine-dammed lakes in southwestern British Columbia (Fig. 1-1). Such preliminary hazard assessments provide the basis for prioritizing hazardous lakes for more detailed field investigations.

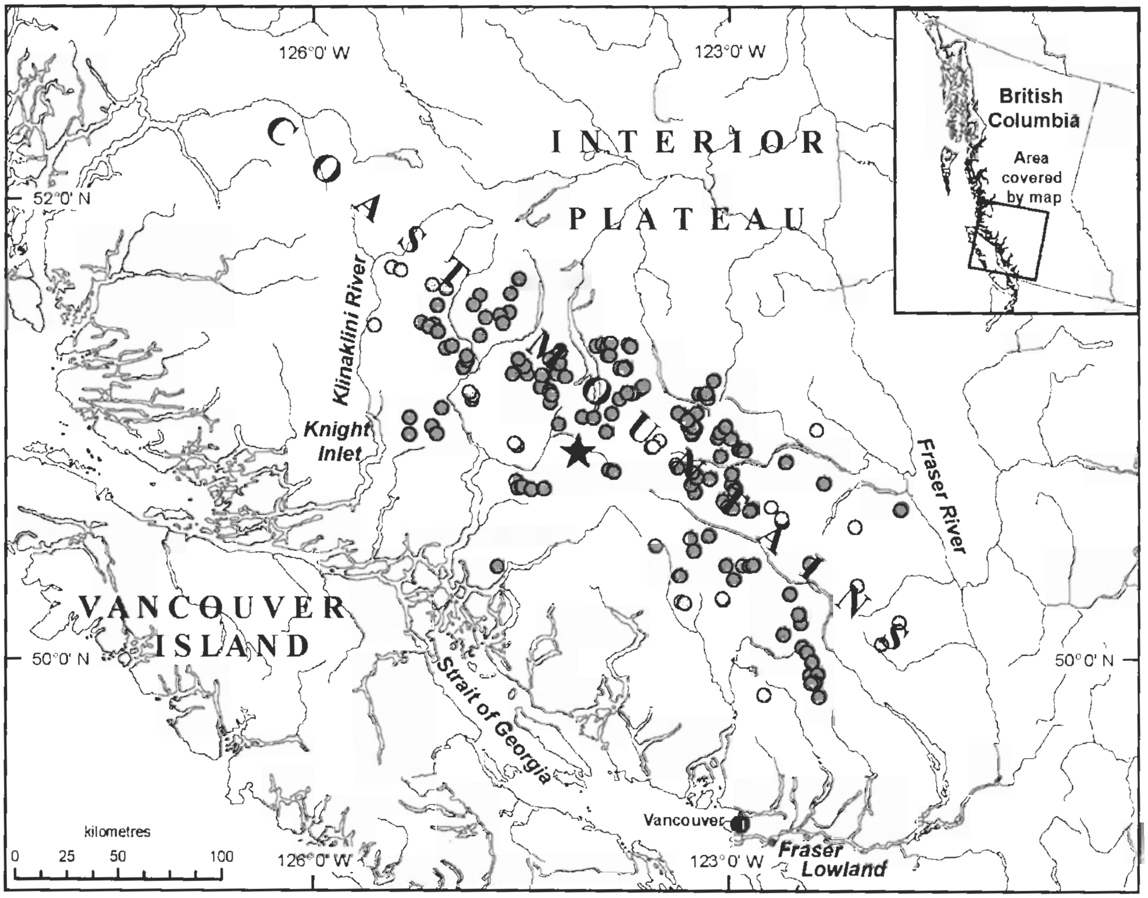

Fig. 1-1. Study area showing locations of 175 moraine-dammed lakes larger than 1 ha. An unnamed moraine-dammed lake (black star) is used to demonstrate the application of the predictive model (see Fig. 2-9). Map projection is BC Albers. Map data provided by, and reproduced with permission of, the Province of British Columbia.

1.1 Background

Moraine-dammed lakes have formed due to recent glacier retreat in high mountains throughout the world, including the Cordillera Blanca, Peru (Lliboutry et al., 1977), Himalayas (Richardson and Reynolds, 2000), Swiss Alps (Haeberli, 1983; Huggel et al., 2002), and the Cordillera of western North America (Clague and Evans, 2000; O'Connor et al., 2001). Lakes formed wherever moraines block valley drainage, but are most commonly situated between retreating glaciers and looped end moraines deposited near the end of the Little Ice Age (Matthes, 1939; Grove, 1988). Catastrophic drainage of such lakes is common because moraine dams are composed of unconsolidated sediment that may be rapidly eroded by anomalous lake outflows triggered by impact waves from rockfalls or ice avalanches or by high runoff events. The dams may fail catastrophically months to decades or more after they form (O'Connor et al., 2001), or they may gradually incise due to slow erosion.

Moraine-dammed lakes represent a special type of hazard for three reasons. First, because outburst floods from moraine-dammed lakes are generally non-recurrent, floods are unprecedented and thus unexpected. Second, the outburst floods originate from a point source but may travel tens to hundreds of kilometres downstream (Richardson and Reynolds, 2000) before attenuating to normal streamflow discharge. Thus, people and infrastructure far downstream from the source may be at risk. Third, the source of the hazard is known a priori. Because the flood source can be identified, disasters can be avoided through mitigation measures, for example by stabilizing moraine dams and lowering lakes levels (Lliboutry et al., 1977; Reynolds et al., 1998).

Given the cost of mitigative works, however, not all outbursts from moraine-dammed lakes can be prevented. Hazard analysts need a means of prioritizing the most hazardous lakes for detailed analysis and possible engineering works. Back analysis of outbursts has led to the development of empirical relations that may be used to predict the magnitude of future events. For example, outburst flood peak discharge may be estimated using an empirical relation based on lake volume and moraine dam height (Hagen, 1982; Haeberli, 1983; MacDonald and Langridge-Monopolis, 1984; Costa and Schuster, 1988; Huggel et al., 2002). However, selection of the most appropriate equation for use in a particular hazard assessment can be arbitrary, and the chosen formula may not be applicable to moraine-dammed lakes in a particular geographic area.

Existing methods of estimating outburst probability are qualitative and subjective. Lu et al. (1987) suggest numerical thresholds beyond which an outburst is likely based on data derived from 11 outburst floods in Tibet, Richardson and Reynolds (2000) schematically illustrate a lake's susceptibility to catastrophic drainage, and O'Connor et al. (2001) provide topographic criteria for a qualitative assessment of the "release potential" of a moraine-dammed lake. Huggel et al. (2004) provide the most systematic method to date for evaluating the probability of outburst from glacial lakes. They define five key indicators to which qualitative probabilities of low, medium, or high can be assigned: dam type, ratio of freeboard to dam height, ratio of dam width to height, frequency and magnitude of impact waves from rock and ice falls reaching the lake, and frequency of extreme meteorological events (Huggel et al., 2004, their Table 3). The effect of each indicator on outburst probability is considered independently, and the scoring is based on the experience of the analyst. Although systematic, Huggel et al's approach is subjective and based mainly on data from the Swiss Alps.

1.2 Research objectives

The purpose of this research is to develop a systematic and objective procedure for making preliminary assessments of outburst flood hazard from moraine-dammed lakes in southwestern British Columbia (Fig. 1-1). Engineers and geoscientists who perform hazard assessments in glacierized regions can benefit from this approach because it does not require field investigation or expertise in glacial hazard analysis. Statistical analysis, which is based on an inventory of all moraine-dammed lakes larger than one hectare in the southern Coast Mountains, is used to identify factors that most strongly influence outburst probability and to generate a formula from which the outburst probability of a particular lake can be estimated. I apply the assessment procedure to all lakes within the study area so that those responsible for hazard evaluation in southwestern British Columbia have a basis for prioritizing potentially hazardous lakes for more detailed investigation.

1.3 Terminology

Several terms used in this thesis are defined here to avoid uncertainty about their meaning. A "moraine" is defined herein as a conspicuous mound or ridge of rock debris deposited by a glacier. Both end and lateral moraines, ranging in height from just a few metres to over a hundred metres, impound lakes in the study area. Most moraines in the study area are composed of diamictons with grains ranging in size from clay to large boulders (Clague and Evans, 2000).

A "moraine-dammed lake" is defined herein as a substantial body of standing water whose existence in some way depends on damming by a moraine. The definition follows from, and complements, Blachut and Ballantyne's (1976) definition of "ice-dammed lake." Although the classic moraine dam has a definite ridge crest and is angular in cross-section, those lakes that are impounded by a low, rounded mound of morainal debris are also classified as moraine-dammed lakes (Fig. 1-2).

The term "catastrophic," as used in the phrases "catastrophic drainage" and "catastrophic failure," refers to a sudden and rapid process that generally lasts several hours. The Nostetuko Lake and Queen Bess Lake moraine dam breaches, which developed in five and eight hours, respectively (Blown and Church, 1985; Kershaw et al., 2005), are examples of catastrophic moraine dam failures.

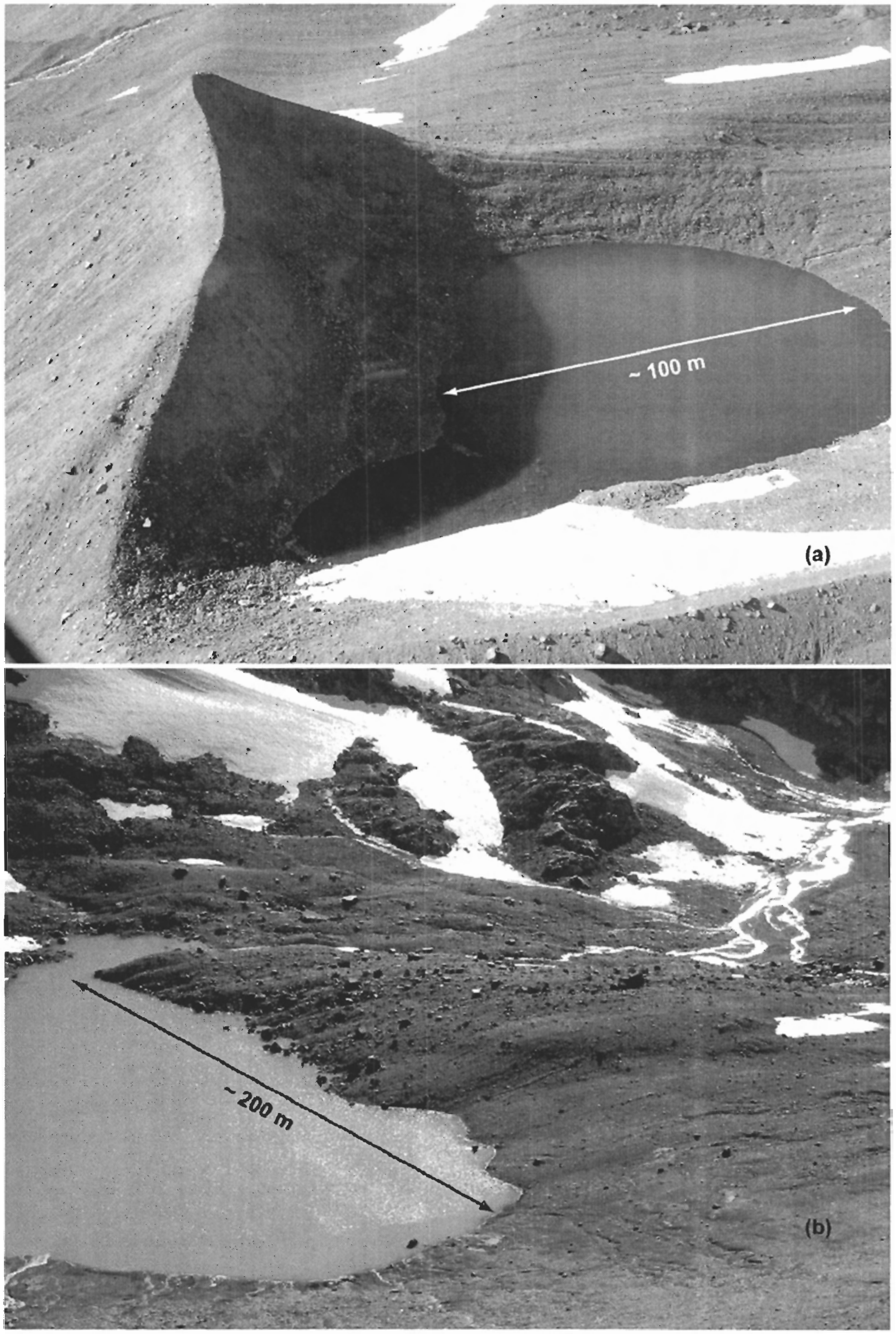

Fig. 1-2. Examples of two different moraine dam morphologies. (a) The classic narrow, sharp-crested moraine dam with an angular cross-section (location 123° 44' 22" W/50° 46' 42" N; photo taken July 31, 2004). (b) A low, rounded moraine dam that has been overridden by a glacier (location 123° 0' 24" W/50° 37' 22" N; photo taken July 17, 2004).

The term "outburst flood" is used in a broad sense throughout this thesis. In most instances, the term refers to a mixture of sediment and water that flows rapidly down a channel during and immediately after catastrophic failure of a moraine dam. Thus, a flood that forms a debris flow is still referred to as an outburst flood or, simply, an outburst. The term "outburst-generated debris flow" is used where the discussion refers specifically to material that behaves as a visco-plastic with high yield strength and non-turbulent flow (Costa, 1988).

1.4 Thesis overview

In addition to this introductory chapter, the thesis comprises two main chapters and a concluding chapter.

Chapter 2 describes the development of a statistical, remote sensing-based model for making preliminary estimates of outburst probability from moraine-dammed lakes in the southern Coast Mountains of British Columbia. Data for 175 moraine-dammed lakes between Fraser and Klinaklini rivers (Fig. 1-1) were collected for logistic regression analysis. Logistic regression is used to identify which factors best discriminate between *drained* and *undrained* lakes and, thereby, generate a formula for estimating the probability of catastrophic drainage from moraine-dammed lakes. The implications and applicability of the statistical model to other regions are discussed. This manuscript, which was prepared 90% by me and 10% by John Clague, is in review with *Global and Planetary Change* (McKillop and Clague, in review). Although John Clague helped improve the format and presentation of the paper, the intellectual content is entirely based on my ideas.

Chapter 3 incorporates the statistical model described in Chapter 2 into a framework for making objective preliminary assessments of the outburst flood hazard posed by moraine-dammed lakes in the southern Coast Mountains. The recommended methods for evaluating outburst flood and outburst-generated debris flow magnitude are based on aerial photographic analysis and, wherever possible, include existing empirical relations that are applicable to the study region. The chapter outlines procedures for estimating outburst peak discharge, maximum volume, maximum travel distance, maximum area of inundation, and probability. Three case studies demonstrate the application of the complete assessment, which yields reproducible results and enables prioritization of hazardous lakes for more detailed field investigation. This manuscript (90% prepared by me and 10% by John Clague) has been submitted to *Natural Hazards* (McKillop and Clague, submitted). Although John Clague helped improve the format and presentation of the paper, the intellectual content is entirely based on my ideas.

Chapter 4 summarizes the results of this research, its significance and its limitations, and recommends further research.

CHAPTER 2:

STATISTICAL, REMOTE SENSING-BASED APPROACH FOR ESTIMATING THE PROBABILITY OF CATASTROPHIC DRAINAGE FROM MORAINE-DAMMED LAKES IN SOUTHWESTERN BRITISH COLUMBIA

2.1 Abstract

Safe development of glacierized regions would benefit from a systematic and objective method for assessing the hazard posed by moraine-dammed lakes. Empirical relations exist for estimating outburst flood magnitude, but standardized procedures have yet to be developed for estimating outburst flood probability. To make quick and inexpensive preliminary assessments that are reproducible, a statistical, remote sensing-based approach is proposed to estimate the probability of catastrophic drainage of moraine-dammed lakes. A comprehensive inventory and analysis were completed of 175 moraine-dammed lakes in the southern Coast Mountains of British Columbia. By applying logistic regression analysis to the data set, the following four independent predictor variables that best discriminate drained lakes from undrained lakes were identified: moraine height-to-width ratio, presence/absence of an ice core in the moraine, lake area, and main rock type forming the moraine. The predictive model correctly classifies 70% of drained lakes and 90% of undrained lakes, for an overall accuracy of

88%. The model provides engineers and geoscientists with a tool for making first-order estimates of the probability of catastrophic drainage from moraine-dammed lakes in southwestern British Columbia.

2.2 Introduction

Moraine-dammed lakes are common in glacierized regions around the world (Lliboutry et al., 1977; Haeberli, 1983; Costa and Schuster, 1988; Clague and Evans, 2000; Richardson and Reynolds, 2000). They form between the snout of a glacier and its own end moraine and, less commonly, on the distal side of moraines where valley drainage has become blocked (Fig. 2-1). Moraine-dammed lakes are prone to catastrophic drainage, which can be attributed to the weak dam materials that typically fail rapidly through erosion and landsliding into the breach channel.

Outburst floods from moraine-dammed lakes have caused tens of millions of dollars of damage to infrastructure and killed thousands of people worldwide (Richardson and Reynolds, 2000). Floodwaters have damaged hydroelectric facilities (Vuichard and Zimmermann, 1987), washed out roads and bridges (Kattelmann, 2003), and destroyed houses and buildings (Huggel et al., 2003). Compared to the large amount of damage caused annually by floods and hurricanes, damage from outburst floods is relatively minor. Nonetheless, the potential severity of outburst flood damage warrants research into better understanding moraine dam failure processes, especially as development extends into alpine regions.

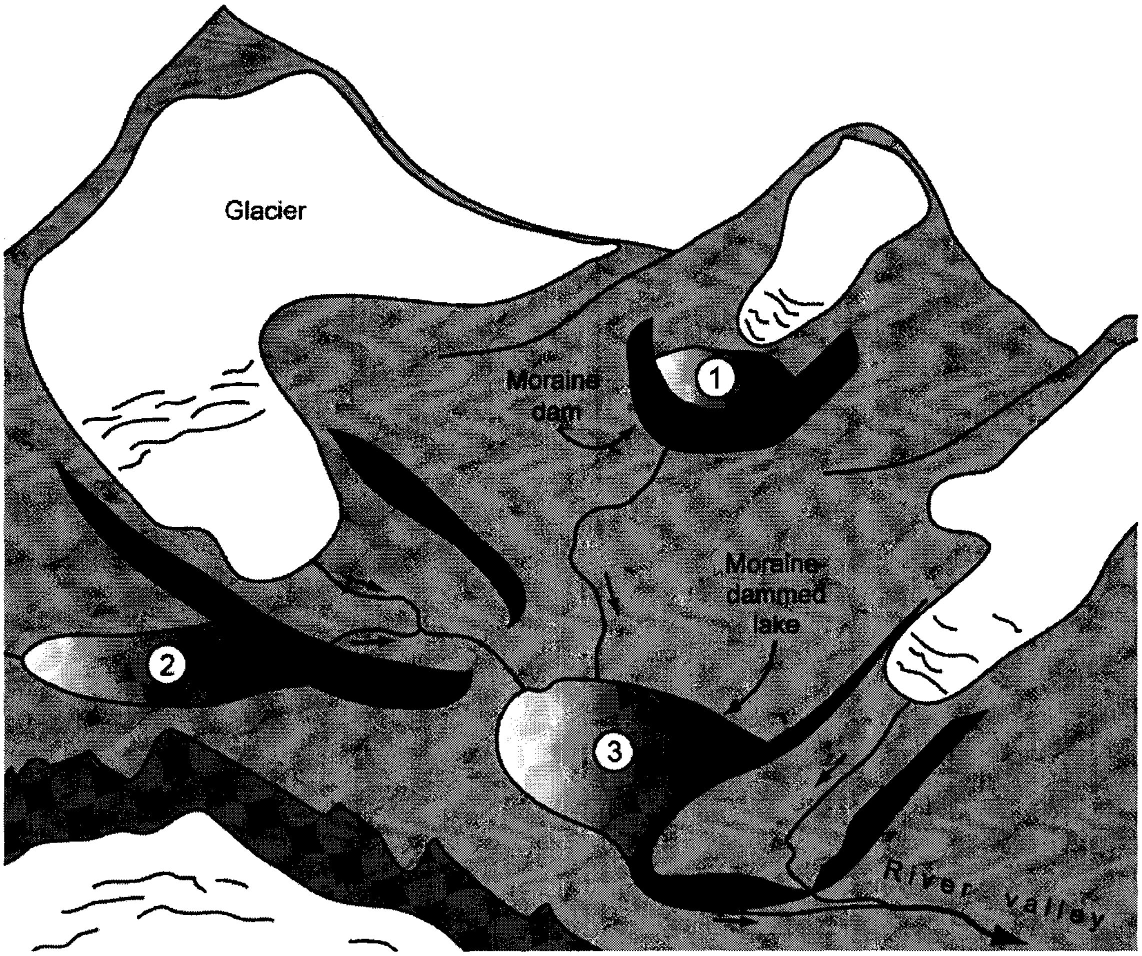

Fig. 2-1. Schematic showing three principal locations of moraine-dammed lakes (based on Clague and Evans, 2000, Fig. 6). (1) Impounded on proximal side of end moraine; (2) in tributary valley, impounded on distal side of moraine deposited by trunk glacier; (3) in trunk valley, impounded on distal side of moraine deposited by tributary glacier.

The hazard posed by moraine-dammed lakes differs from most other natural hazards. Whereas the locations of future earthquakes and tornadoes, for example, are not known with certainty, the sources of outburst floods from moraine-dammed lakes are obvious. The hazard source can be determined through aerial photograph or satellite image interpretation and confirmed in the field, and engineers and geoscientists have designed a variety of mitigation measures for preventing or reducing the potential size of outburst floods. In some cases, the hazard has been reduced by stabilizing moraine dams and their overflow channels (Lliboutry et al., 1977); in others, lakes have been partially drained (Reynolds et al., 1998). Such measures, however, are costly, time-consuming, and sometimes unsafe (Lliboutry et al., 1977), thus it is unreasonable to reduce the hazard posed by all moraine dams. Development of a systematic method for evaluating the risk of moraine dams failing would allow authorities to prioritize the most unstable lakes in a region so that the cost of mitigative engineering measures is minimized.

Hazard can be broadly defined as the product of magnitude and probability (Fell, 1994). Moraine dam hazard assessments, therefore, must include estimates of both outburst magnitude and outburst probability. A variety of different measures are used to quantify outburst magnitude, including total volume, travel distance, and downstream area of inundation. One of the most common measures of outburst magnitude, however, is peak discharge. Numerous empirical relations have been developed to estimate the peak discharge of outburst floods from moraine-dammed lakes (e.g., Costa and Schuster, 1988; Walder and O'Connor, 1997; Huggel et al., 2002). Peak discharge has a non-linear relation with lake volume, assuming complete drainage, which is "the most appropriate design analysis for planning possible mitigative measures" (Laenen et al., 1987). Not all outbursts, however, are floods; some transform into debris flows with very different runout and impact characteristics. Huggel et al. (2004) provide guidelines for estimating the probable maximum volume and travel distance of lake outbursts that transform into debris flows.

Although many authors discuss the factors that most likely predispose moraine dams for failure (e.g., Chen et al., 1999; Clague and Evans, 2000; Richardson and Reynolds, 2000; Huggel et al., 2004), no standardized, objective method yet exists for estimating outburst probability. In an attempt to improve the accuracy of estimates of outburst probability, several authors have specified criteria associated with moraine dam failure. Lu et al. (1987), for example, propose seven numerical "geographic conditions" that favour outburst floods, and both Richardson and Reynolds (2000) and O'Connor et al. (2001) schematically illustrate factors that they link to dam failure. Huggel et al. (2004) list five indicators of a lake's susceptibility to outburst floods, from which they derive a qualitative probability of dam failure.

Satisfactory methods have been developed for predicting outburst flood and debris flow magnitude, but few publications adequately address determination of outburst probability. The purpose of this paper is to provide an objective approach for estimating outburst probability. I use multivariate statistical analysis of remotely measured variables to derive a formula from which the probability of catastrophic drainage from moraine-dammed lakes in the southern Coast Mountains of British Columbia can be estimated.

2.3 Basis for a statistical, remote sensing-based approach

A statistical approach for estimating the probability of catastrophic drainage from moraine-dammed lakes was chosen over approaches based on deterministic analysis, return period, and a qualitative geomorphic analysis. Deterministic analysis requires complete understanding of failure mechanisms and prior knowledge of geotechnical properties of the moraine dam, which can only be determined through labour-intensive field work. Triggers of moraine dam overtopping and subsequent failure mechanisms are rarely known with certainty (Clague and Evans, 2000; Richardson and Reynolds, 2000) and would require detailed slope stability modelling. Financial and time constraints preclude regional field investigations.

A return period approach is commonly used in the probabilistic analysis of storm-induced debris flows (Hungr et al., 1984; Jakob, 2005b). Three factors, however, preclude use of this approach for estimating the probability of outburst floods from moraine-dammed lakes. First, glacial hazards change over time scales shorter than are required to derive frequency relations (Huggel et al., 2004). Second, the dates of past outburst floods are commonly not known with certainty. Third, most moraine-dammed lakes drain only once because the dams are destroyed.

The qualitative geomorphic approach has been used almost exclusively in moraine dam hazard assessments. Richardson and Reynolds (2000) and O'Connor et al. (2001), for example, compare a lake's topographic setting and dam morphology to those of lakes that have drained catastrophically to assess failure susceptibility. Unfortunately, the subjectivity of this approach can result in assessments that are inconsistent, depending on the expertise and biases of the geoscientist.

A more reliable and widely applicable approach for estimating outburst probability should meet four criteria. First, the approach has to be objective; results of assessments completed by different people ought to be similar. Second, the approach must be simple; hazard evaluation is standardized and follows a specific protocol so that geoscientists without expert knowledge can perform the assessment. Third, the approach should be practical; assessment procedures that minimize the necessary time and cost are preferred by consultants and their clients and are more readily completed. Therefore, wherever possible, inexpensive and publicly available data and software are used. Fourth, the approach has to be flexible; the model can be adapted for different data sources, and the conservativeness of the assessment can be adjusted to suit different applications. A statistical, remote sensing-based approach can satisfy these four criteria.

The successful application of multivariate statistical analysis of remotely measured parameters in landslide probability studies provides further justification for using a statistical, remote sensing-based approach. Dai and Lee (2003) and Ohlmacher and Davis (2003) used multivariate statistical analysis, in combination with geographic information systems software, to generate landslide probability maps. Their identification of similar predictor variables in different study areas demonstrates that a statistical approach may provide insight into the factors that control a moraine dam's susceptibility to failure. Based, in part, on their studies, the following prerequisites and assumptions should be met to ensure the validity of the model and appropriate interpretation of results: (1) moraine-dammed lakes that have produced an outburst flood (*drained*) can be distinguished from those that have not (*undrained*) with remote sensing methods; (2) lake parameters can be accurately measured; (3) sampled lakes represent all variability in the study area; (4) the same mechanisms that were responsible for past moraine dam failures will cause future failures; and (5) the sample size is large enough for statistical analysis.

Given these prerequisites and assumptions, a statistical model for estimating the probability of catastrophic drainage from moraine-dammed lakes in southwestern British Columbia cannot be based solely on the nine instances of moraine dam failure documented in the literature (Blown and Church, 1985; Clague et al., 1985; Evans, 1987; Ryder, 1991; Clague and Evans, 1992; Clague and Mathews, 1992; Clague and Evans, 2000; Kershaw et al., 2005). The sample size could be increased by including dam failures in other glacierized regions such as the Himalayas, Andes, or Alps. Although basing a statistical model on possibly morphologically distinct moraine dams in different mountain ranges may increase the model's spatial applicability, it would likely compromise the model's predictive capability within southwestern British Columbia. The lack of consistency of morphological data published in the literature further limits the use of existing data, at least without data homogenization. Furthermore, few quantitative data have been published on *undrained* moraine-dammed lakes. A statistical model cannot reliably identify lakes that are likely to drain catastrophically if it is based entirely on data collected from *drained* lakes.

2.4 Study area

I completed a comprehensive inventory of all drained and undrained moraine-dammed lakes larger than one hectare in British Columbia's southern Coast Mountains (Fig. 1-1). A lake area threshold of one hectare was used because outburst floods from lakes of this size have considerable destructive potential (e.g., Tats Lake, Clague and Evans, 1992) and can be reliably detected on 1:30 000- to 1:40 000-scale aerial photographs. The study area is 70 000 km^2 in size and is bounded on the south by the Strait of Georgia and Fraser Lowland, on the west by Knight Inlet and Klinaklini River, on the north by the Interior Plateau, and on the east by Fraser River. The Coast Mountains extend from the International Boundary about 1700 km northwest to Alaska and Yukon. The Coast Mountains are composed mainly of Late Jurassic to Early Tertiary granitic rocks, intermediate- to high-grade metamorphic rocks, and minor Cenozoic volcanic rocks (Monger and Journeay, 1994).

Elevations in the southern Coast Mountains range from sea level in coastal fjords to over 4000 m at the summit of Mount Waddington. Local relief is typically between 1000 and 2000 m. The high relief and rugged topography are largely the product of late Tertiary and Quaternary tectonic uplift and fluvial and glacial erosion (Parrish, 1983; Mathews, 1989). Many valleys have broad bottoms and steep sides, and contain thick Quaternary sediments. Contemporary glaciers range in size from small cirque glaciers to icefields up to 400 km^2 in area straddling the drainage divide of the Coast Mountains. Conspicuous late Holocene moraines, mostly deposited during the Little Ice Age (Matthes, 1939; Grove, 1988), occur near the margins of many glaciers throughout the study area. The moraines average about 30 m high, but some exceed 100 m in height. They are composed of unconsolidated diamicton and poorly sorted bouldery gravel (Fig. 2-2). The diamicton matrix is dominantly sand, but includes finer material.

Fig. 2-2. Example of poorly sorted bouldery till characteristic of most moraine dams in the southern Coast Mountains. Pit excavated July 17, 2004, into moraine dam located at 123° 0' 24" W/50° 37' 22" N. Ice axe is approximately 65 cm long.

Synoptic-scale climate ranges from wet maritime on the coast and windward western slopes to drier sub-maritime in the rain shadow of the Coast Mountains. Climate is orographically modified in alpine and subalpine regions where most moraine-dammed lakes are located. Mean annual precipitation on the lee side of the range is less than 500 mm, whereas the windward slopes and major icefields receive more than 3000 mm annually (Canadian National Committee for the International Hydrological Decade, 1978). Precipitation is generally heaviest in the late autumn when Pacific cyclones move onto the British Columbia coast. Flooding occurs in small to intermediate-size watersheds during intense rain-on-snow events in autumn and during the early summer freshet in large drainage basins such as that of Fraser River.

2.5 Database development

Moraine-dammed lakes were detected and measurements were made using aerial photographs (Table 2-1). Huggel et al. (2002) developed GIS-based algorithms for detecting glacial lakes using Landsat satellite imagery, which may be the more economical solution for study regions where recent aerial photograph coverage is incomplete, but I used aerial photographs for four reasons: (1) they have higher spatial resolution than most satellite images, which is sometimes needed to distinguish moraine- and bedrock-dammed lakes; (2) they are inexpensive, provide complete recent coverage of our study area, and can be viewed at no cost at provincial and federal aerial photograph libraries in Canada; (3) vertical relief and horizontal distances can be measured on aerial photographs; and (4) they are routinely used by geoscientists and engineers in hazard assessments. Where possible, 1:30 000- to 1:40 000-scale, post-1990 aerial photographs were used for lake detection. These aerial photographs facilitated

Table 2-1. Candidate predictor variables.

No.[a]	Variable	Code	Data source[b]	Data type[c]	Units[d]	Definition	Reference[e]
1	Lake freeboard	*Frbd*	AP	C	m	Elevation difference between lake surface and lowest point in moraine crest	Blown and Church (1985)
2	Lake freeboard-to-moraine crest height ratio	*FMht*	AP	C	-	Ratio between lake freeboard (#1) and moraine crest height (elevation difference between toe and crest of moraine dam)	Huggel et al. (2004)
3	Lake area	*Area*	TRIM	C	ha	Lake surface area	Chen et al. (1999)
4	Moraine height-to-width ratio	*Mhw*	AP	C	-	Ratio between moraine height (vertical distance from distal toe to lake surface) and moraine width (horizontal distance from distal toe to lakeshore)	Clague and Evans (2000); Huggel et al. (2002)
5	Moraine distal flank steepness	*Mdfk*	AP	C	°	Slope from crest to distal toe of moraine dam	Chen et al. (1999)
6	Moraine vegetation coverage	*Mveg*	AP	N	-	Vegetation (grass, shrubs, trees) on moraine dam - contiguous or discontiguous	Costa and Schuster (1988); Goldsmith (1998)
7	Ice-cored moraine	*IceC*	M & AP	N	-	Moraine dam type - ice-cored or ice-free	Kattelmann (2003)
8	Main rock type forming moraine	*Geol*	BCGS	N	-	Bedrock lithology surrounding and/or upstream of lake - granitic, volcanic, sedimentary, metamorphic	Blown and Church (1985); this study
9	Lake-glacier proximity (horizontal distance)	*LGpx*	AP	C	m	Horizontal distance between glacier snout and nearest lakeshore	Ding and Liu (1992); Chen et al. (1999)
10	Lake-glacier relief (vertical distance)	*RlfG*	AP	C	m	Elevation difference between lake surface and glacier snout	Slingerland and Voight (1982)
11	Slope between lake and glacier snout	*LGsp*	AP	C	°	Slope from glacier snout to nearest lakeshore	Ding and Liu (1992)
12	Crevassed glacier snout	*Crev*	AP	N	-	Lowermost 500 m of glacier - crevassed or crevasse-free	Ding and Liu (1992)
13	Glacier calving front width	*Calv*	AP	C	m	Horizontal distance between left and right margin of glacier in contact with lake	Lliboutry et al. (1977); Richardson and Reynolds (2000)
14	Glacier snout steepness	*SnSt*	TRIM	C	°	Slope of lowermost 500 m of glacier	Alean (1985)
15	Snow avalanches enter lake	*Snow*	AP	N	-	Evidence of snow avalanches entering lake (remnant avalanche debris, vegetation trimlines, or avalanche gully at lakeshore) - yes or no	Ryder (1998)

Table 2-1, cont.

No.[a]	Variable	Code	Data source[b]	Data type[c]	Units[d]	Definition	Reference[e]
16	Landslides enter lake	*Lsld*	AP	N	-	Evidence of landslides entering lake (coherent deposit of landslide debris) - yes or no	Evans (1987); Ryder (1998)
17	Unstable lake upstream	*UsLk*	AP	N	-	Upstream ice-dammed lake, moraine-dammed lake, landslide-dammed lake, or bedrock-dammed lake situated beneath hanging glacier - yes or no	Huggel et al. (2003)
18	Watershed area	*Wshd*	TRIM	C	ha	Watershed area above lake outlet	Clague and Evans (1994)
19	Lake type	*Lk*	AP	N	-	Lake type, based on location, as defined in Fig. 2-1 - type 1, 2 or 3	Clague and Evans (2000)

All measurements based on pre-outburst conditions.
[a] See Fig. 2-4 for schematic definition of predictor variables.
[b] AP = aerial photographs; TRIM = online 1:20 000-scale Terrain Resource Information Management topographic maps (Province of British Columbia, 2001); BCGS = online 1:250 000-scale British Columbia Geological Survey geological maps (Massey et al., 2005); M = 1:2 000 000-scale moraine type map (Østrem and Arnold, 1970).
[c] C = continuous; N = nominal.
[d] m = metres; ha = hectares (1 ha = 10 000 m^2); ° = degrees; - = unitless.
[e] Authors either directly cite variable as an important predictor of outburst probability or provide basis for its inclusion.

efficient detection of lakes over large areas and provided the most recent and complete coverage. Even lakes that drained completely and suddenly several decades earlier could be easily identified by the gaping V-notch in their moraine dams, a signature of catastrophic moraine dam failure. Both qualitative and quantitative measurements were made using 1:15 000-scale, post-1990 aerial photographs.

Photogrammetric measurements were made using a mirror stereoscope and parallax bar, following techniques outlined by Lillesand and Kiefer (2000). By computing the magnitude of relief displacement on a point-by-point basis, it was possible to plot features in their planimetrically correct positions and thereby accurately measure horizontal distances (Table 2-2). The relief displacement of features such as moraine dams enabled heights to be determined using standard photogrammetric methods, though percent error increased with decreasing object height (Table 2-2). Lillesand and Kiefer

Table 2-2. Comparison of aerial photograph-based photogrammetric measurements with field-based measurements.

No.	Lake	Terrain feature	Distance measure	Photogrammetric measurement (m)	Field-based measurement (m)	Percent error (%) [a]
2	Queen Bess	Narrow terminal moraine width	Horizontal	54	55	2
64	East Granite	Debris fan width	Horizontal	64	60	7
101	Boomerang	Moraine width	Horizontal	296	300	1
189	Soo Lower	Lake outlet to tributary lake outlet	Horizontal	511	500	2
285	Salal	Lakeshore to lateral moraine crest	Horizontal	111	120	8
306	Nichols	Lake length	Horizontal	176	185	5
306	Nichols	Moraine width	Horizontal	88	90	2
306	Nichols	Nearby lake length	Horizontal	44	47	6
2	Queen Bess	Lake surface to moraine crest	Vertical	48	50	4
2	Queen Bess	Freeboard of pond in lateral moraine	Vertical	4	5	20
2	Queen Bess	Freeboard of pond in terminal moraine	Vertical	2	5	60
64	East Granite	Moraine breach height	Vertical	18	21	14
189	Soo Lower	Moraine breach height	Vertical	22	30	27
285	Salal	Lake surface to moraine crest	Vertical	11	10	10
306	Nichols	Moraine height	Vertical	7	6	17
306	Nichols	Moraine height	Vertical	33	35	6

[a] Percent error = [|photogrammetric measurement – field measurement| / field measurement] * 100%

(2000) point out five assumptions implicit in the use of the method: (1) aerial photographs are truly vertical; (2) flying height is accurately known; (3) objects are clearly visible; (4) principal points are precisely located on the photographs; and (5) the measurement technique used has an accuracy consistent with the degree of relief displacement involved. To increase the precision and consistency of photogrammetric measurements, all parallax bar readings were repeated until three consecutive readings were within 0.05 mm of each other, which corresponds to a ground feature height uncertainty of about 2-3 m on 1:15 000-scale photographs.

Some measurements, including lake area and watershed area, were made from online 1:20 000-scale Terrain Resource Information Management (TRIM) topographic maps (Table 2-1) (Province of British Columbia, 2001), which are based on late 1980s to early 1990s aerial photographs of the study area. The use of TRIM maps, which, in some cases, were based on aerial photographs with different dates from those used for photogrammetric measurements, is justified for the measurement of lake and watershed area because changes in lake area within this period are negligible and watershed area is invariable. Although measurable through photogrammetric methods, glacier snout steepness was also measured from TRIM maps because only an approximate average gradient over the lowermost 500 m of the glacier was required. To verify that using photogrammetric measurements for such a coarse measurement is unnecessary, I changed a random selection of glacier snout steepness values and re-ran the statistical analysis. Because no major systematic differences in glacier snout steepness were observed between drained and undrained lakes, the changes had no effect on the model.

The main rock type forming each moraine dam, which was assumed to be the same as the upslope lithology, was determined from online 1:250 000-scale British Columbia Geological Survey (BCGS) geological maps (Table 2-1) (Massey et al., 2005). The relatively coarse level of detail provided by these maps was sufficient, given the study area's location within the Coast Plutonic Complex (Monger and Journeay, 1994), because most moraine dams are entirely surrounded by granitic bedrock. In the few cases where the BCGS maps indicated the presence of more than one bedrock lithology upstream of the moraine dam, a comparison of bedrock attributes visible in the aerial photographs with the BCGS map polygons confirmed the bedrock origin of rock debris forming the moraine.

Moraine dam type for about half of the lakes in the study area is based on Østrem and Arnold's (1970) 1:2 000 000-scale map of ice-cored and ice-free moraines in southern British Columbia (Table 2-1). For moraine dams that are not shown on Østrem and Arnold's map, assignment was based on a combination of several criteria they outline for distinguishing ice-cored from ice-free moraines using aerial photograph interpretation: (1) a moraine with a rounded surface with minor superimposed ridges, indicative of flow or creep, was assumed to be ice-cored; (2) a disproportionately large end moraine in front of a small glacier was suspected to be ice-cored; and (3) a narrow, sharp-crested moraine was interpreted to be ice-free (Fig. 2-3). Through ground truthing for a similar study in Scandinavia, Østrem (1964) found the assumptions concerning the presence or absence of an ice core "could generally be confirmed." Because few moraine dams in Østrem's (1964) study were misclassified using the criteria outlined above, I suspect a similarly small number of moraine dams in the study area were misclassified.

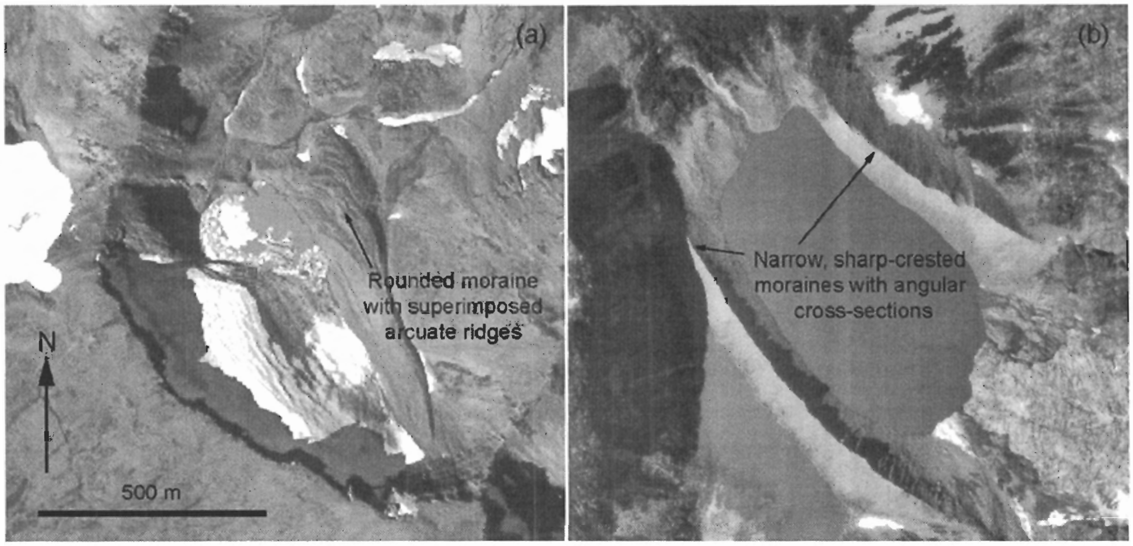

Fig. 2-3. Typical (a) ice-cored and (b) ice-free moraine dams in the southern Coast Mountains. Aerial photographs (a - 30BCC97175-156; b - 30BC79069-190) reproduced with permission of the Province of British Columbia.

To test the effect of misclassification of moraine type, I re-ran the statistical analysis after switching the moraine types of a random selection of 5% of the moraine dams. The main results did not change.

I conducted field investigations in the summer of 2004 to verify the aerial photograph observations and measurements, to quantify the error between field measurements and remotely sensed data, to assess changes in some lake-glacier systems since the aerial photographs were taken, and to make first-hand observations to better understand what conditions may predispose a moraine dam to fail. Twenty-five drained and undrained lakes, ranging in size from one hectare to about 200 hectares, were visited. Financial constraints and the remoteness of most lakes precluded detailed surveys of lake bathymetry and moraine dam morphology, thus the focus in the field was to ground truth remote measurements (Table 2-2).

I identified 175 moraine-dammed lakes in the study area (Appendices A-D). Ninety percent of the lakes are type 1, 7% are type 2, and 3% are type 3 (Fig. 2-1). Only 10 of the 175 lakes had drained or partially drained. Event occurrences (in this case drained lakes) are statistically more informative than non-occurrences (undrained lakes) (King and Zeng, 2001), thus the predictive capability of the statistical model would be compromised unless the number of drained lakes in the database could be increased. To address this problem, I could have expanded the study area until enough drained lakes had been identified to validate the statistical analysis. However, to increase the number of drained lakes to 20 would require roughly doubling the study area, which was not feasible. Time and financial constraints necessitated an expansion of the database with drained lakes from outside the initial study area, within the Pacific Northwest. Six drained lakes from British Columbia and four drained lakes and one undrained lake from Washington and Oregon were added (Appendix E). Qualitative and quantitative measurements for the 20 drained lakes and 166 undrained lakes provided the data set for statistical analysis.

2.6 Candidate predictor variables

A predictor variable is a variable that is used to predict the value of another variable. Thus, candidate predictor variables, which are selected given their potential for explaining lake status, are the initial list of variables on which statistical analysis is based. I chose candidate predictor variables on the basis of previously published accounts of moraine dam failures and field observations. Variables were only included if they met three criteria. First, variable measurement had to be objective. Repeat measurements should be consistent, and different analysts should obtain similar results. Second, only variables with a physical basis for inclusion were included. Third, variables could be measured on aerial photographs or maps.

Some potentially important predictor variables had to be excluded because they could not be measured remotely. Lake bathymetry, which influences the propagation and run-up of displacement waves caused by rock and ice falls (Kershaw et al., 2005), requires field surveys and thus was excluded. Geotechnical characteristics of the moraine dam, which may affect its resistance to erosion due to overflow, can also only be assessed in the field and lab. Seepage through the moraine dam, which can initiate piping failure (Lliboutry et al., 1977; Huggel et al., 2003), cannot reliably be observed on aerial photographs.

Remotely measurable variables that are either spatially homogeneous within the study area or are difficult to objectively quantify were also excluded. The seismicity of a region, for example, would intuitively be included as a candidate predictor variable. An earthquake can destabilize a moraine dam (Lliboutry et al., 1977) or trigger an ice avalanche or rockfall that may enter the lake and generate displacement waves capable of overtopping the dam. Seismicity, however, differs little throughout my study area (Anglin et al., 1990) and is similar in central Oregon (USGS, 2003), where the foreign lakes incorporated into the statistical analysis are located. Therefore, seismicity was excluded from the list of candidate predictor variables. Huggel et al. (2004) include the local frequency of "extreme meteorological events" (high temperature and precipitation) as a predictor variable in their subjective scheme for estimating a "qualitative probability" of outburst. Storm- and snowmelt-induced runoff have been cited by several authors as a trigger mechanism for moraine dam failure (e.g., Lliboutry et al., 1977;

Yamada, 1998). Unfortunately, however, isohyet maps of short-duration, intense rainstorms, which provide the best spatial quantification of "extreme meteorological events," are unavailable for moraine dams in British Columbia due to the scarcity of climate stations capable of measuring continuous rainfall (Canadian National Committee for the International Hydrological Decade, 1978). The sudden collapse of the snout of Diadem Glacier into Queen Bess Lake on one of the hottest days of the year (Kershaw et al., 2005) demonstrates the need for an expanded network of meteorological stations in southwestern British Columbia, particularly in areas where a lake outburst could impact humans.

After excluding predictor variables that require field measurement and those that are spatially homogeneous or difficult to objectively quantify, the number of candidate predictor variables was reduced to 19 (Table 2-1). Figure 2-4 provides a schematic definition of the 19 predictor variables. Four of the variables relate to the lake, five to the moraine dam, six to the glacier, and four to the basin. The candidate predictor variables include both continuous and nominal data (Table 2-1).

2.7 Development of the predictive model

The number of possible multivariate statistical procedures that can be applied to the data set is limited by the type and distributional form (e.g., normal or binomial) of the data. The simplest statistical prediction method uses contingency table analysis, in which the discrete categories of one or more predictor variables are cross-tabulated with each state of the dichotomous dependent variable (Ohlmacher and Davis, 2003), which is capable of having only one of two possible values. The proportion of tallies in each cell of the table can be interpreted as conditional outburst probabilities, given a state of the

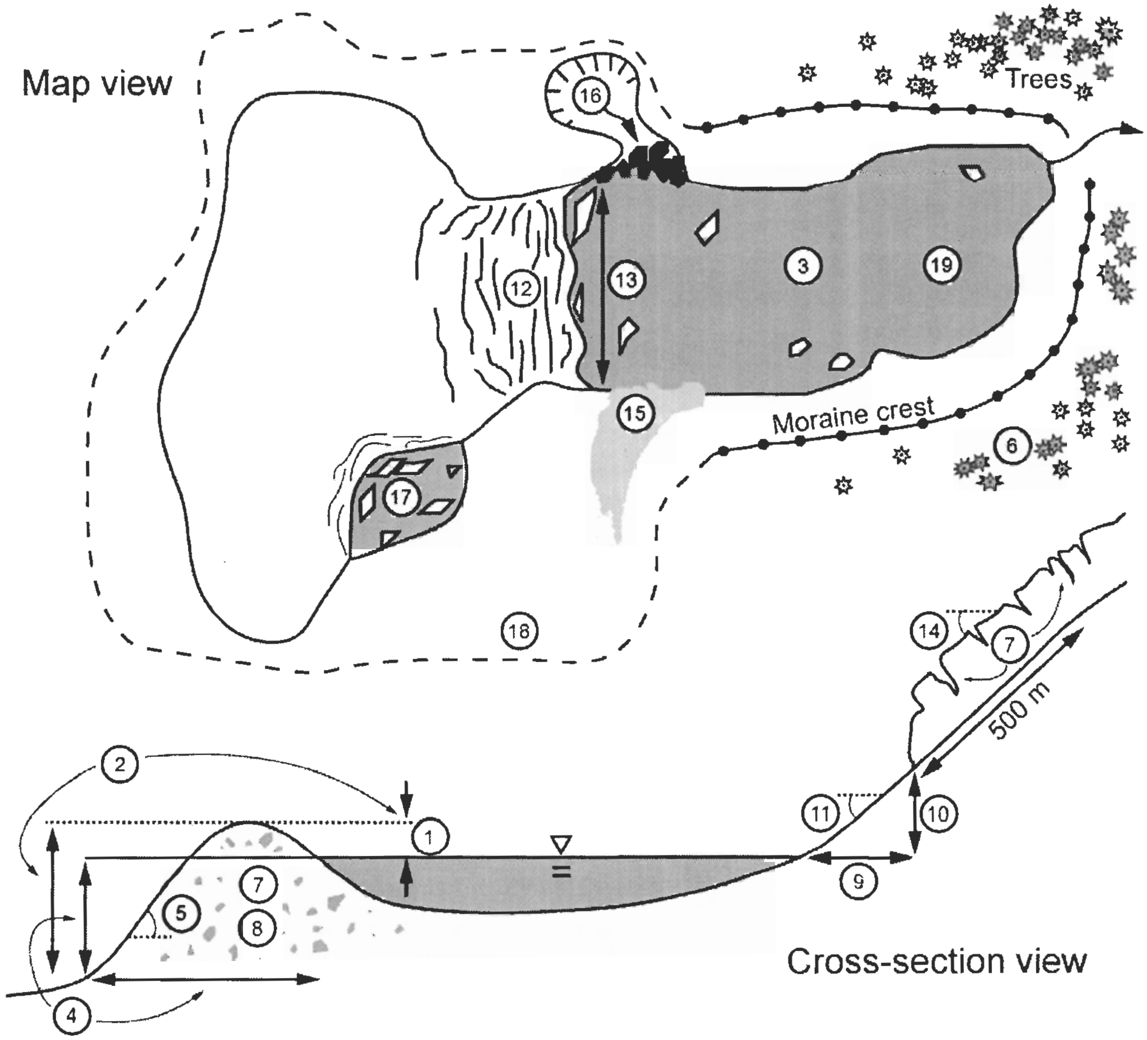

Fig. 2-4. Nineteen candidate predictor variables. Numbers are cross-referenced to those in Table 2-1: (1) lake freeboard, (2) lake freeboard-to-moraine crest height ratio, (3) lake area, (4) moraine height-to-width ratio, (5) moraine distal flank steepness, (6) moraine vegetation coverage, (7) ice-cored moraine, (8) main rock type forming moraine, (9) lake-glacier proximity (horizontal distance), (10) lake-glacier relief (vertical distance), (11) slope between lake and glacier, (12) crevassed glacier snout, (13) glacier calving front width, (14) glacier snout steepness, (15) snow avalanches enter lake, (16) landslides enter lake, (17) unstable lake upstream, (18) watershed area, and (19) lake type.

predictor variable. In this case, however, the large number of predictor variables makes contingency table analysis unwieldy.

Discriminant analysis classifies individuals into mutually exclusive groups on the basis of a set of independent variables (Dillon and Goldstein, 1984). Linear combinations of the independent variables are derived that will discriminate between groups by maximizing between-group variance and simultaneously minimizing within-group variance. Press and Wilson (1978) strongly discourage using discriminant analysis in situations, such as in this study, where at least one independent variable is nominal, thereby violating the assumption of multivariate normality.

Linear regression is perhaps the most commonly used method for predicting the value of a dependent variable from observed values of a set of predictor variables (Dillon and Goldstein, 1984). Although the method can be generalized to include nominal predictor variables, linear regression requires that the dependent variable be normally distributed and continuous. In situations such as this study, where the dependent variable is dichotomous and the predictor variables are either continuous (e.g., moraine height-to-width ratio) or nominal (e.g., main rock type forming the moraine), the most appropriate multivariate statistical method is logistic regression.

Logistic regression is an extension of linear regression, developed for situations in which the dependent variable is dichotomous rather than continuous. In linear regression, one estimates or predicts the mean value of the response corresponding to a particular set of values for the predictor variables (Pagano and Gauvreau, 2000). In this study, where the response is dichotomous, the objective is to estimate the probability that a lake will be classified into one category as opposed to another, given a particular set of predictor variables. Each lake can be represented by a dichotomous variable, Y, which indicates whether a lake is drained ($Y = 1$) or undrained ($Y = 0$), and n independent variables, X_1, $X_2, \ldots, X_n$. Because Y is dichotomous, the probability that $Y = 1$ is also the expected value of Y, given $X_1, X_2, \ldots, X_n$; that is, $P(Y = 1)$ is the regression against $X_1, X_2, \ldots, X_n$

(Dai and Lee, 2003). By definition, $P(Y = 1)$ is restricted to values between zero and one, and, because dichotomous categories are mutually exclusive, $P(Y = 0) = 1 - P(Y = 1)$.

I wish to estimate $P(Y = 1)$, given a set of independent variables. Therefore, an initial attempt is made to directly model $P(Y = 1)$ by regression:

$$P(Y = 1) = \alpha + \beta_1 X_1 + \beta_2 X_2 + \ldots + \beta_n x_n, \tag{1}$$

where α is the intercept and β_i are the regression coefficients estimated from the data. Such a model, however, can yield both positive and negative values outside the probability limits. This problem can be partly circumvented by regression modelling of the odds, which are defined as the ratio of the probability that something occurs to the probability that it does not occur:

$$\text{Odds}(Y = 1) = P(Y = 1)/[1 - P(Y = 1)] = \alpha + \beta_1 X_1 + \beta_2 X_2 + \ldots + \beta_n x_n \tag{2}$$

Although the odds are a ratio with no fixed maximum, they can have a minimum value of zero. This problem is circumvented by taking the natural logarithm of the odds, called the logit of Y, thereby producing a variable that has no numerical limits:

$$\text{logit}(Y) = \ln\{P(Y = 1)/[1 - P(Y = 1)]\} = \alpha + \beta_1 X_1 + \beta_2 X_2 + \ldots + \beta_n X_n \tag{3}$$

Logit(Y) approaches negative infinity as the odds decrease from one to zero, and positive infinity as the odds become increasingly larger than one. Although the probability, the odds, and the logit are three ways of expressing the same thing, the logits have no constraints that would otherwise make it impossible to use regression in a predictive model (Ohlmacher and Davis, 2003).

By converting logit(Y) back to the odds and then the odds back to P($Y = 1$), I derive the logistic regression equation: $P(Y = 1) = \exp(\alpha + \beta_1 X_1 + \beta_2 X_2 + \ldots + \beta_n x_n)/[1 +$

$\exp(\alpha + \beta_1 X_1 + \beta_2 X_2 + \ldots + \beta_n x_n)]$. Further simplification produces a succinct expression from which moraine-dammed lake outburst probability can be estimated in terms of the variables $X_1, X_2, \ldots, X_n$:

$$P(Y = 1) = \{1 + \exp[-(\alpha + \beta_1 X_1 + \beta_2 X_2 + \ldots + \beta_n X_n)]\}^{-1} \quad (4)$$

Linear regression coefficients are estimated using ordinary least squares, whereas logistic regression coefficients are estimated using the maximum likelihood method. Maximum likelihood estimation, in a general sense, yields values for the unknown coefficients that maximize the probability of obtaining the observed set of data (Hosmer and Lemeshow, 2000). Because the relation between the independent predictor variables and outburst probability is non-linear, logistic regression software uses iterative methods to estimate coefficients.

The relative performance of different logistic regression models can be evaluated using a test statistic called the negative log-likelihood, which has approximately a chi-square distribution (Ohlmacher and Davis, 2003). The negative log-likelihood of the reduced (intercept-only) model is compared to that of the fitted model. If the difference between the negative log-likelihood of each model passes a chi-square test of significance, the fitted model better describes the data than the reduced model. The output from logistic regression software closely resembles analysis of variance tables used to test linear regression coefficients, except that the test statistic follows a chi-square distribution rather than an F distribution (Ohlmacher and Davis, 2003).

I performed logistic regression with the software JMP v. 5 (SAS Institute Inc., 2003). Variables were selected using a forward stepwise procedure to ensure that the most parsimonious model was generated and to reduce the chance that two strongly correlated variables were entered into the model (Quinn and Keough, 2002). In a forward stepwise procedure, variables are entered into the model one at a time, beginning with the statistically most important. After each step, the model is re-evaluated to determine whether additional variables should be entered. The re-evaluation is done by comparing the negative log-likelihood of the model before and after the addition of each variable (Dai and Lee, 2003). For this study, a variable under consideration was only entered into the model if the significance was less than a "probability to enter" of 0.05. The process continued until further addition of variables did not significantly improve the model's predictive capability.

2.8 Modelling results

According to the forward stepwise logistic regression, moraine-dammed lake outburst probability in southwestern British Columbia is best predicted by four variables (Tables 2-3 and 2-4). In order of their entry into the model, the variables are moraine height-to-width ratio (*Mhw*), presence/absence of an ice core in the moraine (*IceC*), lake area (*Area*), and main rock type forming the moraine (*Geol*). Continuous predictor variables with positive and negative coefficients have, respectively, independent positive and negative correlations with outburst probability (Table 2-4). All predictor variables are statistically significant at the 0.05 level, but *Mhw* is highly significant ($p<0.0001$) (Table 2-3).

Table 2-3. Wald tests of the significance of predictor variables in the outburst probability model.

Variable	Order of stepwise entry	Degrees of freedom	Wald Chi-square	Prob> Chi-square
Mhw	1	1	17.34	<0.0001
IceC	2	1	4.71	0.0300
Area	3	1	4.70	0.0302
Geol	4	3	9.25	0.0261

Table 2-4. Regression coefficients estimated for the outburst probability model.

Variable	Category	Coefficient
Intercept	-	-7.11 (α)
Mhw	-	9.46 (β_1)
$IceC_j$:	Ice-free	1.23 ($\beta_{Ice\text{-}free}$)
	Ice-cored	-1.23 ($\beta_{Ice\text{-}cored}$)
Area	-	0.016 (β_2)
$Geol_k$:	Granitic	1.58 ($\beta_{Granitic}$)
	Volcanic	3.15 ($\beta_{Volcanic}$)
	Sedimentary	3.77 ($\beta_{Sedimentary}$)
	Metamorphic	-8.50 ($\beta_{Metamorphic}$)

The formula for estimating outburst probability can be expressed, using equation (4), as:

$$P(Y=1) = \{1 + \exp\text{-}[\alpha + \beta_1(Mhw) + \sum \beta_j(IceC_j) + \beta_2(Area) + \sum \beta_k(Geol_k)]\}^{-1}, \quad (5)$$

where α is the intercept, and β_1, β_2, β_j, and β_k are regression coefficients for *Mhw*, *Area*, *IceC*, and *Geol*, respectively (Table 2-4). The measured values of continuous variables *Mhw* and *Area* can be entered directly into the equation. In contrast, indicator variables must be used for the nominal variables *IceC* and *Geol*. $IceC_j$ equals 1 if the moraine dam is ice-cored and 0 if the moraine dam is ice-free, and $Geol_k$ equals 1 if the main rock type forming the moraine dam is *k* and 0 otherwise (Table 2-4). The significance of the fitted logistic regression model was tested by comparing the negative log-likelihood of the full model to that of the reduced (intercept-only) model. The result is highly significant ($p<0.0001$, Table 2-5). Application of the formula to all lakes in the study area generated a distribution of probability estimates ranging from 6.1×10^{-6} to 77% (Fig. 2-5). Only lakes with moraine dams composed of metamorphic rock material, however, have outburst probability estimates less than 0.2%.

Table 2-5. Maximum negative log-likelihood values for testing the significance of probability models.

Whole model test				
Model	-Log-likelihood	Degrees of freedom	Chi-square	Prob> Chi-square
Difference	19.65	6	39.31	<0.0001
Fitted	43.83			
Reduced (intercept-only)	63.48			

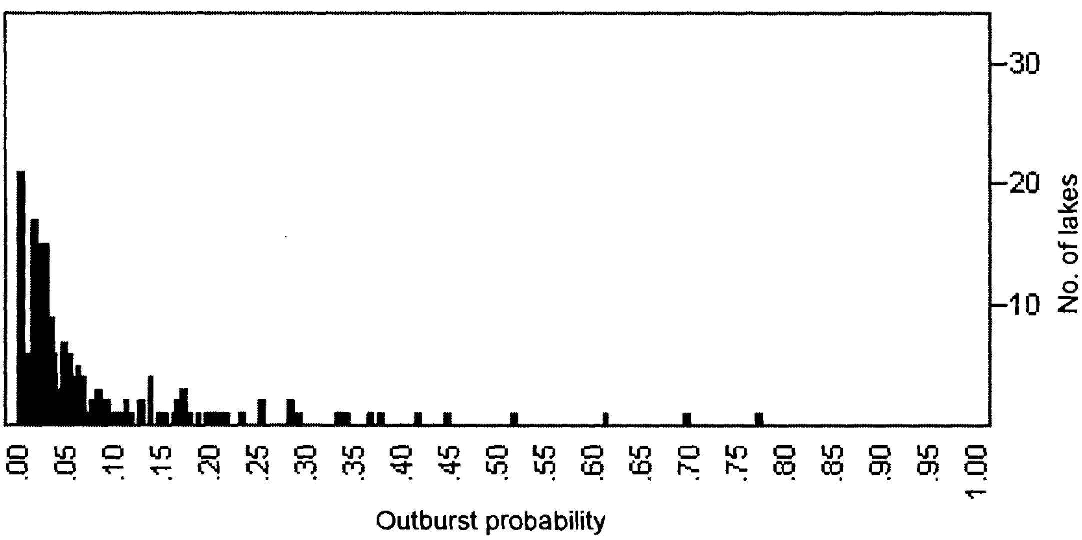

Fig. 2-5. Histogram showing the distribution of outburst probability estimates derived from the logistic regression model.

2.9 Predictive capability of the model

A statistical model's predictive capability must be evaluated before it can be used in hazard assessments. Ideally, predictive success is assessed by applying the model to an independent data set in the study area from which the training sample was taken. Unfortunately, too few drained lakes exist in the study area to set aside a portion for subsequent model validation. If data are limited, it is preferable to base a statistical model on all the data than to generate a model from a portion of the available data and set aside the remainder for validation (I. Bercovitz, personal communication, 2005). My model's predictions were therefore cross-validated with the observations on which the model was based.

In order to determine the proportion of successful predictions, I initially used an outburst probability cut-off value of 50%, above which lakes are classified as drained and below which lakes are classified as undrained. A 50% cut-off value is the default in most statistical programs (e.g., JMP, SAS Institute Inc., 2003) and commonly used in the literature (e.g., Dai and Lee, 2003). Based on this cut-off, the logistic regression model correctly predicts 99% of the undrained lakes, but only 40% of the drained lakes; the overall predictive accuracy is 92% (Table 2-6). Begueria and Lorente (2002) state that an overall accuracy greater than 70% is good in most classification applications.

The proportion of true positives (40%) is referred to as the model's sensitivity; the proportion of true negatives (99%) is the model's specificity. The trade-off between a model's sensitivity and specificity is illustrated in the receiver operating characteristic (ROC) curve (Fig. 2-6). An ROC curve is a plot of a predictive model's sensitivity versus its false positive (i.e., 1 – specificity) rate, according to all possible classification

Table 2-6. Cross-validation of logistic regression model based on (a) a default 50% probability cut-off and (b) a 19% probability cut-off.

(a) 50% probability cut-off		Observations		Total
		0 (*undrained*)	1 (*drained*)	
Predictions	0 (*undrained*)	164 99%	12 60%	176
	1 (*drained*)	2 1%	8 40%	10
Total		166	20	186

(b) 19% probability cut-off		Observations		Total
		0 (*undrained*)	1 (*drained*)	
Predictions	0 (*undrained*)	150 90%	6 30%	156
	1 (*drained*)	16 10%	14 70%	30
Total		166	20	186

Notes: Probability cut-off is the threshold above which lakes are classified as *drained* and below which lakes are classified as *undrained*. Model specificity and sensitivity are 99% and 40%, respectively, for (a) and 90% and 70%, respectively, for (b).

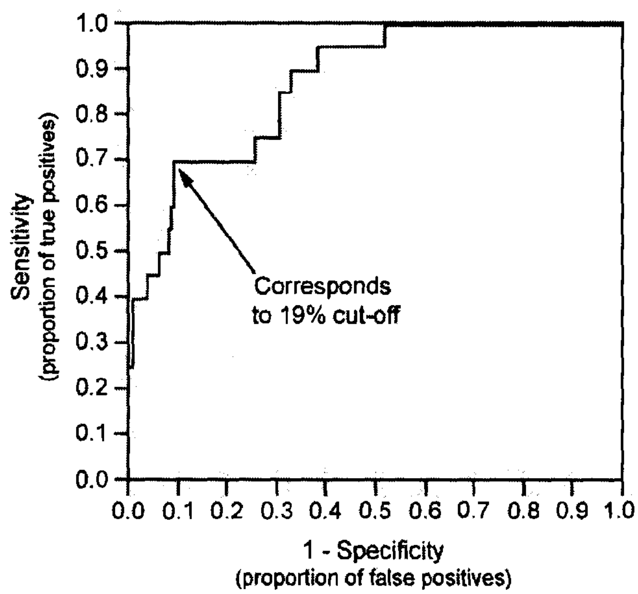

Fig. 2-6. ROC curve for logistic regression model (see text for explanation). The point closest to the upper-left corner of the diagram corresponds to a probability threshold of 19%. The area under the ROC curve is 0.869.

cut-off values (Austin and Tu, 2004). The area under the ROC curve provides a measure of the model's diagnostic ability (Hanley and McNeil, 1982). A straight line with a 45° slope represents a model with no predictive capability (area under the curve is 0.5). In contrast, a vertical line coincident with the sensitivity axis represents a model that correctly predicts all cases (area under the curve is 1.0). The area under this model's ROC curve is 0.869, which is comparable to values reported for successful predictive models in other disciplines (Austin and Tu, 2004).

The arbitrary probability cut-off threshold can be decreased to increase the sensitivity, or conservativeness, of a model for use in hazard assessments. A more sensitive model, however, will generate more false positives. Pagano and Gauvreau (2000) recommend decreasing the threshold to the point on the ROC curve closest to the upper-left corner, which corresponds to the probability threshold that simultaneously maximizes sensitivity and specificity, 19% in this study.

Both the specificity and sensitivity of the model change if a probability threshold of 19% instead of the default 50% is used to evaluate the model's predictive success. The specificity decreases slightly to 90%, which corresponds to an increase in the number of false positives, but the sensitivity improves substantially to 70% (Table 2-6). With a 19% cut-off, the logistic regression model now correctly classifies 14 of the 20 drained moraine-dammed lakes in the study area (Fig. 2-7).

Given the number of possible trigger mechanisms for moraine dam failures and the relatively small sample size on which the predictive model is based, I recommend categorizing probability estimates. Using probability ranges or intervals instead of discrete values ensures that estimates do not convey more precision than is warranted.

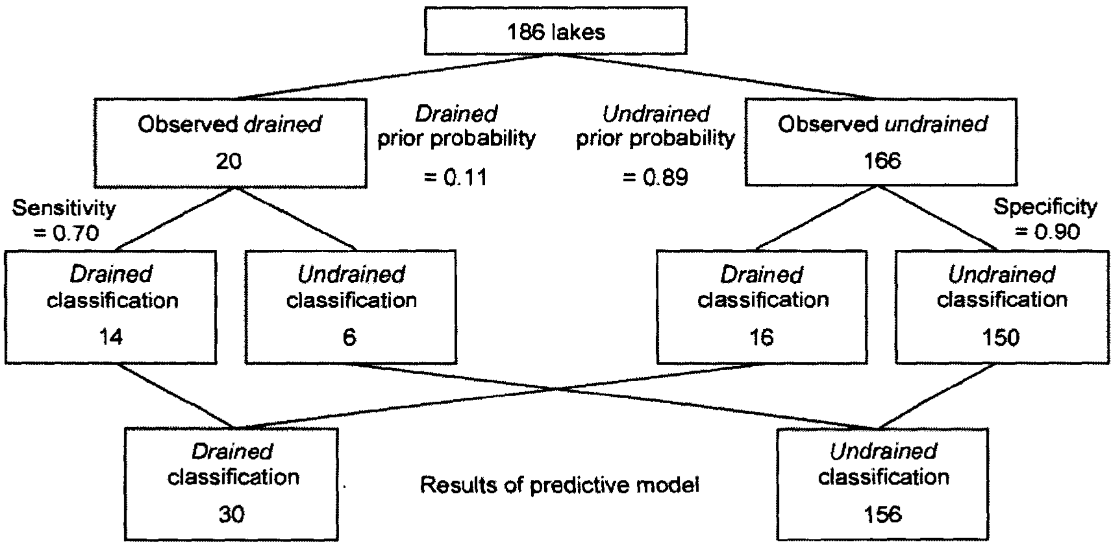

Fig. 2-7. Schematic representation of the performance of the logistic regression model as a predictor of outburst probability, based on a 19% probability cut-off value (based on Pagano and Gauvreau, 2000, Fig. 6.3).

Numerous researchers arbitrarily categorize probabilities, particularly for display purposes (e.g., Dai and Lee, 2003), but a curve showing the cumulative percentage of drained lakes versus probability provides a more objective basis for defining probability thresholds. Outburst probabilities are best classified as very low (<6%), low (6-12%), medium (12-18%), high (18-24%), and very high (>24%), based on the probabilities of the breaks in slope in Fig. 2-8. The few drained lakes that have "low" or "very low" outburst probability estimates (Fig. 2-8, Appendices A and D), based on pre-outburst conditions, have no unusual characteristics that lead to the erroneous probabilities. Their low estimates are simply attributed to their relatively broad moraine dams, a characteristic that is heavily weighted by the logistic regression model (Table 2-4).

I demonstrate the application of the model retrospectively by presenting the four relevant measurements and resulting probability equation for an unnamed lake above the Gilbert Glacier in the southern Coast Mountains that partially breached its moraine dam

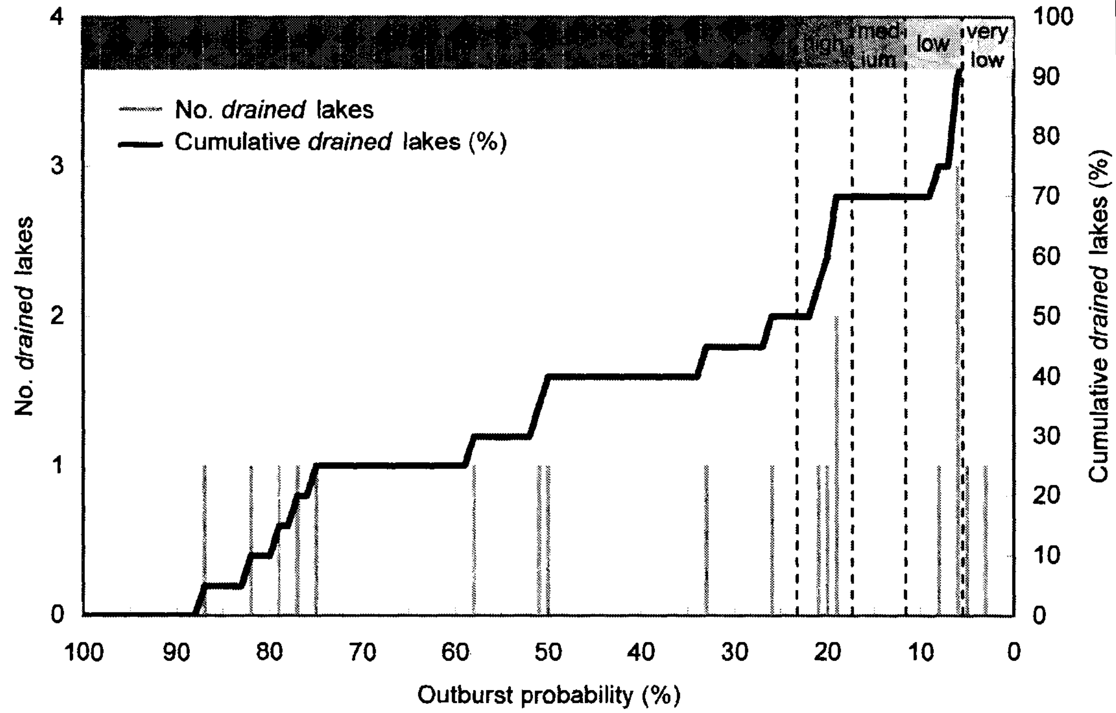

Fig. 2-8. Distribution of outburst probability estimates for drained lakes in the statistical database. The black curve is the cumulative percentage of drained lakes based on outburst probability estimates. Breaks in the slope of this curve, for example at 6%, provide an objective basis for defining probability categories (top of graph).

sometime between July 29, 1965 and September 11, 1977 (Fig. 2-9; see Fig. 1-1 for location). A conspicuous strandline visible in aerial photographs taken on September 3, 2003 (Fig. 2-9) indicates that the lake had an *area* of 4.0 ha prior to its outburst. Its *ice-free* moraine dam is composed of *volcanic* rock and had a *height-to-width ratio* of about 0.3. Substituting the continuous variable pre-outburst values and appropriate nominal variable indicator values into equation (5), $P(\text{outburst}) = \{1 + \exp\text{-}[-7.11 + (9.46)*(0.3) + (1.23)*(1) + (0.016)*(4.0) + (3.15)*(1)]\}^{-1}$, yields a "very high" outburst probability of 52%.

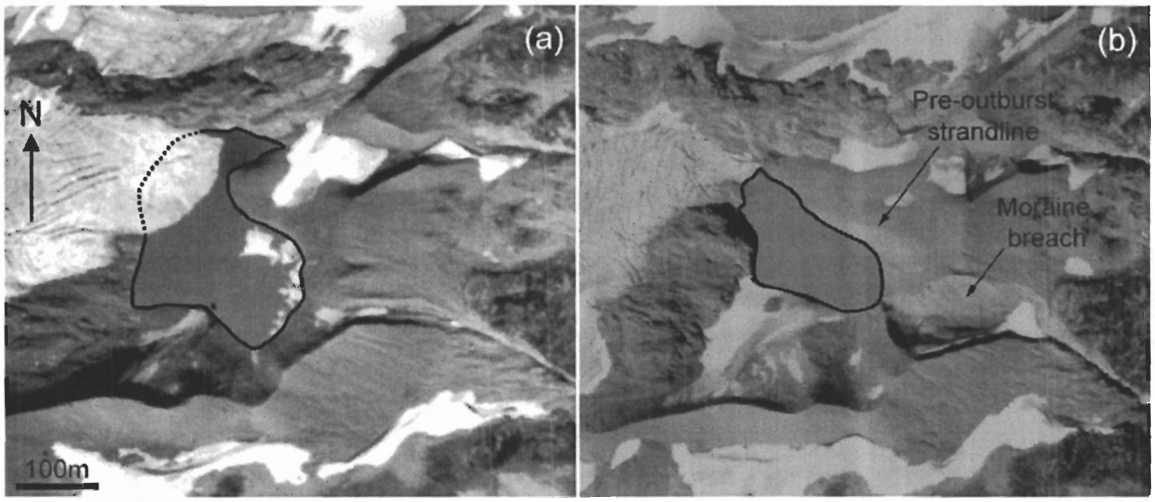

Fig. 2-9. Unnamed moraine-dammed lake above the Gilbert Glacier in the southern Coast Mountains (black star in Fig. 1-1) (a) before and (b) after a partial outburst. Aerial photographs (a - BC1218-22; July 17, 1950; b - 30BCC03025-54; September 3, 2003) reproduced with permission of the Province of British Columbia. Other aerial photographs constrain the date of the outburst to between July 1965 and September 1977.

2.10 Discussion

2.10.1 Implications of the four-predictor-variable logistic regression model

The entry of only four predictor variables into the logistic regression model has important implications. According to the model, the outburst probability of a given lake in my study area depends most on *Mhw* (Table 2-3). The implication of the positive regression coefficient, that outburst probability increases as moraine dams become higher and narrower, supports qualitative assessments of conditions that predispose a moraine dam to fail (Chen et al., 1999; Clague and Evans, 2000; Richardson and Reynolds, 2000; Huggel et al., 2004). Water flowing over a narrow moraine dam need erode only a small volume of sediment from the distal flank and crest before incision reaches the lakeshore and catastrophic failure begins.

Area, another variable in the logistic regression model, also has a positive regression coefficient. Thus, all other things being equal, outburst probability in the study area increases with increasing lake area. Although the surface area of a lake, in itself, does not affect outburst probability, *Area* was included because it is proportional to lake volume (O'Connor et al., 2001; Huggel et al., 2002) and, probably, lake depth at the moraine dam. I interpret the significance of *Area* in the model as an indication that a lake with a relatively large surface area and, therefore, greater depth and volume is more susceptible to catastrophic drainage due to high hydrostatic pressure on the moraine dam. Furthermore, the rate at which lake outflow discharge decreases over time during the breaching process is slower for lakes with large areas (Walder and O'Connor, 1997). Therefore, large lakes have an increased likelihood of self-enhancing breach growth.

The entry of *Geol* into the final model implies the composition of the moraine dam may influence outburst probability. Clague and Evans (2000) imply that moraine dams with a large proportion of boulders will better resist catastrophic incision of their outlet channels than dams composed mainly of sand and pebble-cobble gravel. Therefore, bedrock that is prone to intense glacial comminution may form especially erodible moraine dams. In my study area, moraine dams composed dominantly of sedimentary rock debris have a higher likelihood of failure than dams composed of more competent or resistant rock debris. An observation that supports the inclusion of *Geol* in the model is that some drained lakes are surrounded by numerous slope failures originating in morainal debris of the same bedrock type as their breached moraine dams. This finding suggests that a moraine's composition may predispose it to fail. The dependence of the outburst probability model on *Geol* highlights the need for field investigations in addition to remote hazard assessments. Through on-site and subsequent laboratory analysis, one could determine whether any significant differences exist between the grain size distributions of breached and intact moraine dams. The proportion of boulders in a moraine dam, for example, may be a significant predictor of a lake's outburst probability.

Several implications of the four-predictor-variable model described above seem counterintuitive. The model suggests, all other things being equal, that ice-cored moraine dams are less likely to fail than ice-free moraine dams (Table 2-4). This result indicates that the model does not capture the temporally related increase in moraine dam failure potential as a moraine is downwasting due to ice core melting (Richardson and Reynolds, 2000). Reynolds et al. (1998), Richardson and Reynolds (2000), and Yesenov and Degovets (1979) have shown, however, that increased permeability and subsidence of ice-cored moraine dams due to melting can increase a dam's susceptibility to catastrophic failure. Three possible explanations for the model's contradictory implication are suggested. First, ice-cored moraine dams in the study area are smaller than those that have failed in the Himalayas (Watanabe et al., 1994) and, therefore, undergo only minor subsidence through melting. Second, most ice-cored moraine dams are broader and more rounded than ice-free dams (Østrem and Arnold, 1970) and thus are more slowly eroded by overflowing water. Third, a moraine dam containing a solid ice core may better resist incision during anomalous overflow events than a moraine dam comprising only unconsolidated sediment because the rate of mechanical erosion through unconsolidated sediment exceeds the rate of thermally induced incision through ice in subaerial environments.

The absence in the model of all six candidate predictor variables associated with glaciers (Tables 2-1 and 2-3) implies that a lake's susceptibility to ice avalanches is, in itself, not a good indicator of its outburst probability. Exclusion of all glacier-related predictor variables was unexpected, given that ice avalanche impact waves triggered at least 53% of the catastrophic moraine dam failures in the Himalayas in the twentieth century (Richardson and Reynolds, 2000) and at least four of the nine documented failures in British Columbia (Clague and Evans, 2000). One possible explanation is that the proportion of drained moraine-dammed lakes situated beneath glaciers is not significantly different from the proportion of undrained lakes situated beneath glaciers.

Many authors have emphasized the contribution of topographic setting to a moraine-dammed lake's likelihood of draining catastrophically (Lu et al., 1987; Richardson and Reynolds, 2000; O'Connor et al., 2001). O'Connor et al. (2001) schematically illustrate three different "topographic-setting criteria" for evaluating the potential for a moraine dam to fail. My model suggests, however, that the moraine dam itself may contribute most to outburst probability. Not only is *Mhw* entered first in the stepwise procedure (Table 2-3), but the three other predictor variables in the final logistic regression model relate to the moraine dam. *Mhw*, *IceC*, and *Geol* are descriptive characteristics of the moraine, established during its formation. *Area* depends on moraine height (O'Connor et al., 2001). The significance of this finding is that on-site hazard assessments of moraine-dammed lakes may overemphasize the importance of the topographic setting and underemphasize the importance of the moraine dam itself.

The four predictor variables that were entered into the final logistic regression model best classify the lakes in my study area as undrained or drained according to their observed status. One cannot say with certainty, however, that these variables are, in fact, true independent predictors of outburst probability in the study area without first performing bootstrap resampling (Austin and Tu, 2004). The premise of bootstrap resampling, in this application, is that only those predictor variables that are consistently entered into models generated from hundreds to thousands of randomly selected subsamples of the original data set are true independent predictors of outburst probability. Although bootstrap resampling could indicate that variables that were unexpectedly entered into the model such as *IceC* or *Geol* should be removed from the model, the observed set of data in this study is best explained with their inclusion.

2.10.2 Implications of a drained lake classification

The main goal of this research was to identify moraine-dammed lakes in southwestern British Columbia that have a high probability of catastrophic drainage. Therefore, the classification of an undrained lake as drained does not represent a flaw in the predictive model. According to Begueria and Lorente (2002), false positives can be considered cases where a high probability of outburst exists, "but no events have been observed within the sample period, due to the rarity of the process" (p. 19). If a lake's outburst probability estimate is high or very high (>18%), the lake is simply more similar to the drained lakes than to the undrained lakes on which the statistical model was based. In other words, the lake's moraine dam is more likely to fail catastrophically than it is to erode gradually over time.

Land-use planners require an estimate of the period within which a moraine dam is likely or unlikely to fail. A common approach for estimating the probability of occurrence *P* of a debris flow in a particular channel or region, during a period of *n* years, uses the binomial formula (e.g., Jakob, 2005b), $P(\text{debris flow}) = 1 - (1 - 1/T)^n$, where *T* is the return period of debris flows. This approach cannot be used to estimate the timing of a lake outburst, however, because moraine dam failures are generally non-recurrent. An alternative method that is appropriate for isolated events is needed.

Initially, one may hypothesize that lakes with relatively high outburst probabilities will drain sooner than lakes with relatively low outburst probabilities. For instance, one may assume that a lake with an outburst probability estimate of 40% will breach its moraine dam before a lake with a probability estimate of 20%. If a correlation between outburst probability estimates and the time since lake formation for lakes to drain catastrophically could be established, periods within which moraine dam failure is or is not likely could be specified. The probability estimates for drained lakes were plotted against their approximate longevities to determine whether a relation exists between the outburst probability estimates and the time to failure. Lakes were assumed to form with the abandonment of Little Ice Age terminal moraines (~1900 A.D. in the study area; Ryder and Thomson, 1986). The data revealed no statistically significant trend, but more accurate knowledge of lake longevities is clearly needed to provide a fair analysis. Until demonstrated otherwise, I conclude that the approach generates estimates of outburst probability, based on certain moraine dam characteristics, without implying a period within which moraine dam failure is or is not likely to happen.

Although the period to which my probability estimates apply cannot be specified, I can provide land-use planners and decision makers with the probability that moraine-dammed lakes classified by the model as drained will actually drain catastrophically (positive test). According to Bayes' theorem, this conditional probability can be expressed as:

$$P(D \mid T^{+}) = [P(D) * P(T^{+} \mid D)] / \{[P(D) * P(T^{+} \mid D)] + [P(U) * P(T^{+} \mid U)]\}, \qquad (6)$$

where $P(D)$ is the prior probability that a moraine-dammed lake will drain catastrophically, $P(U)$ is the prior probability that a moraine dam will not drain catastrophically, $P(T^+ \mid D)$ is the sensitivity, and $P(T^+ \mid U)$ is 1 minus the specificity (Pagano and Gauvreau, 2000). After substituting appropriate values (Fig. 2-7) into equation (6), I determine $P(D \mid T^+)$ is about 0.44. The probability that existing moraine-dammed lakes that have been classified as drained using logistic regression analysis will actually drain catastrophically is thus 44%.

2.10.3 Changes to outburst probability over time

The outburst probability of a moraine-dammed lake may change over time. Three of the four factors that best explain a lake's outburst probability may vary after the lake forms: (1) moraine dam height-to-width ratio, which, as defined in Fig. 2-4, changes as lake level fluctuates; (2) lake area, which changes as the glacier retreats or advances, or due to delta progradation; and (3) presence/absence of an ice core in the moraine. Hazard assessments thus must be revised as conditions change.

The most sudden change occurs when a lake partially breaches its moraine dam, achieving a new, lower level, with a new dam height-to-width ratio. The outburst probability of the lake perched above the Gilbert Glacier (Figs. 1-1 and 2-9), prior to the outburst that occurred between July 1965 and September 1977, was about 52%; after the outburst, however, the probability of a second outburst dropped to 29%. A partially breached moraine dam may actually be more stable than a dam that has never breached for two reasons. First, the bouldery lag that develops in the outlet channel during catastrophic incision and commonly prematurely terminates the first breach (Clague and Evans, 1992) may resist erosion during subsequent anomalous outflow events. Second, the gradient of the outlet channel through the breach is generally lower after the first breach than before it, thus outflowing water will have lower erosional competence. Outburst probability will change most after a drop in water level in lakes with narrow moraine dams, because the change in the ratio of moraine height (referenced to lake level) to width, will be large.

Recognizing the time-dependent nature of outburst probability is an important aspect of using my assessment procedure. My method is based on data acquired through remote sensing and thus, strictly speaking, applies only to the instant the aerial photograph or satellite image was taken. Even relatively minor fluctuations in lake level caused by high runoff or prolonged drought can change the moraine height-to-width ratio and thus outburst probability.

2.10.4 Potential sources of error

The reliability and robustness of a statistical model depends, in part, on the quality of the data on which it is based. Erroneous predictions can arise from several possible aerial photograph interpretation errors. First, the type of dam impounding a lake may be misinterpreted due to snow cover, cloud cover, shadows, distortion due to high relief terrain, or the presence of a morainal veneer over bedrock. Second, photogrammetric measurements may be inaccurate due to limitations imposed by aerial photograph scale, object clarity, object size, and the skill of the interpreter (Avery and Berlin, 1985). In this study, percentage errors for vertical and horizontal distance measurements were evaluated by comparing aerial photograph and ground measurements. Vertical measurement error was particularly sensitive to object height. Percentage errors for objects more than 50 m high were consistently less than 10%, whereas errors for objects less than 10 m high reached 60% (Table 2-2). Features were plotted in their correct planimetric positions using Lillesand and Kiefer's (2000) approach for correcting for relief displacement on a point-by-point basis. Thus, percentage errors for horizontal distance measurements were generally less than 5% and never exceeded 10% (Table 2-2). Third, measurements of moraine width and, therefore, height-to-width ratio can be imprecise. Because the toe of the proximal flank of the moraine dam is commonly below the lake surface, moraine width was measured from the lakeshore to the toe of the distal flank of the moraine (Fig. 2-4). Identification of a moraine's distal toe was only difficult in rare cases where the break-in-slope at its base is gradual or subtle. As a result, height-to-width ratios of moraine dams with gentle proximal flanks, in particular, may be too large. Fourth, basing the classification of moraine type solely on aerial photograph interpretation is imperfect. Whereas almost all moraines interpreted by Østrem (1964) to be ice-cored did indeed contain ice cores, ground truthing revealed ice cores in a few of the moraines that he had classified as ice-free. Fifth, and perhaps most important, lake status can be equivocal. The criteria for classifying a lake as drained include a distinct V-notch in the moraine dam, a coherent, disproportionately large debris fan directly below the dam, and evidence of catastrophic flooding in the valley below. In a few cases, normal erosional and depositional processes and vegetative establishment make lake classification difficult. Lake misclassification may have a significant impact on the predictive model.

Sample size, in a strict sense, is not a source of error, but it has an effect on model reliability. It is not unreasonable to base a statistical model on a data set of 186 lakes, but the results are more reliable where the proportion of *ones* (events) is similar to the proportion of *zeros* (non-events) (King and Zeng, 2001; Dai and Lee, 2003). In my study, only 20 out of 186 lakes produced outburst floods. Because statistical models such as logistic regression tend to underpredict the probability of rare events (King and Zeng, 2001), it is not surprising that three-quarters of my outburst probability estimates are less than about 13% (Fig. 2-5).

The distribution of observed values of a particular categorical predictor variable also can have a substantial effect on probability estimates. In my study, for example, none of the 11 lakes impounded by dams derived from metamorphic rocks has produced an outburst flood. As a result, the coefficient associated with metamorphic moraine dams is negative and, compared to the coefficients associated with other moraine dams, is large (Table 2-4). Outburst probability estimates for granitic, volcanic, or sedimentary moraine dams range from 0.2 to 77%, whereas estimates for metamorphic moraine dams range from 6.1×10^{-6} to only 1.5%. Thus, my model yields low estimates of outburst probability for metamorphic moraine dams, regardless of the values of other predictor variables. A future expansion of my study area and database would facilitate development of an outburst probability model that is less biased by small sample size.

Although error sources have been described separately, the errors themselves may compound. In some cases, for example, errors may compound such that the derived outburst probability is under- or overestimated. In other instances, errors may offset each other, thereby yielding a reasonable estimate of outburst probability. The diversity of error sources, degrees of uncertainty with which each is associated, and enhancing versus offsetting effect of multiple errors make quantifying compound errors difficult and beyond the scope of this study.

2.10.5 Applicability of results

In spite of the possible errors, the statistical model provides an objective and quantitative estimate of outburst probability. According to the model, Klattasine Lake, which drained catastrophically between June 1971 and September 1973 (Clague et al., 1985), indeed had a "high" outburst probability of 20% prior to the sudden failure of its moraine dam. The predictive model should not be incorporated into hazard assessments, however, without first acknowledging the issues that may limit its applicability. For example, incorporating drained lakes from outside the study area to increase the number of ones violates the otherwise random, or in this case complete, sampling scheme. The effect on the predictive model of supplementing the sample of drained lakes with foreign, although morphologically similar, drained lakes is uncertain.

An approach based on remote sensing limits the use of my methodology to regions with similar data sources. Large-scale aerial photograph stereopairs or overlapping, very high resolution satellite images, from which moraine height can be accurately measured, are the minimum imagery needed for this approach. In regions such as the Alps, where access to moraine-dammed lakes is not difficult, field measurements can provide an alternative basis for statistical analysis.

The empirical model for estimating outburst probability is applicable to the population from which the statistical sample was taken, that is lakes between Fraser and Klinaklini rivers in the southern Coast Mountains. The model must still be tested in neighbouring watersheds and regions with similar physiography and moraine dam morphologies to evaluate its applicability to other glacierized areas. I suspect, however, that application of the model to mountain ranges such as the Andes or Himalayas is inappropriate. Andean and Himalayan moraine-dammed lakes differ from those in my study area. They are commonly shadowed by steep slopes with local relief of thousands of metres, which influences the rate and magnitude of rockfalls and ice avalanches into the lakes. Second, Andean and Himalayan moraine dams are generally larger and more bulky than moraine dams in southern British Columbia (Richardson and Reynolds, 2000). Third, Andean and Himalayan lakes commonly form through coalescence of supraglacial ponds on stagnant, downwasting debris-covered glaciers (Watanabe et al., 1994; Richardson and Reynolds, 2000). Different mechanisms may control the catastrophic drainage of these ice-contact moraine-dammed lakes. In general, the reliability of the model is expected to decrease with increasing disparity in moraine-dammed lake characteristics. It is more appropriate to use the proposed methodology to develop a region-specific model for estimating outburst probability.

Even within southwestern British Columbia, the model should only be used for preliminary assessments of outburst probability. The model has not been independently validated due to the rarity of outburst floods in the study area. Furthermore, follow-up field investigations may be necessary to identify unique, potentially hazardous conditions that cannot be documented through aerial photograph interpretation alone. The model does not eliminate the need for on-site measurements. Rather, it is designed to provide a method for objectively prioritizing the order in which detailed field investigations of potentially hazardous moraine-dammed lakes are carried out.

2.11 Conclusion

Few outburst floods from moraine-dammed lakes in British Columbia have caused significant damage to infrastructure or urban development, which can be attributed to the low development density in the Coast Mountains. However, as development advances into mountain valleys, the likelihood of economic losses and loss of life from outbreak events will increase if the hazard remains unmitigated. Accordingly, professional engineers and geoscientists will be required to complete assessments of hazards posed by moraine-dammed lakes.

An objective method, based on measurements derived from aerial photographs and maps in combination with logistic regression analysis, is proposed for making preliminary assessments of the probability of catastrophic draining of moraine-dammed lakes. The method is quick, inexpensive, and yields reproducible results. The method selects variables that discriminate best between drained and undrained lakes. Logistic regression allows the conservativeness of predictions to be adjusted to suit different applications.

The results of the statistical analysis suggest that large lakes impounded by narrow, ice-free moraine dams composed of debris derived from sedimentary rock have the highest outburst probabilities. Because a lake's outburst probability may change over time, especially with fluctuating lake levels, assessments of moraine dam failure potential must be revised as conditions change. Engineers and geoscientists could use the method as a screening tool for making preliminary assessments of outburst probability, but would need to follow the remote assessments with detailed field investigations and dam stability analysis.

CHAPTER 3:

A PROCEDURE FOR MAKING OBJECTIVE PRELIMINARY ASSESSMENTS OF OUTBURST FLOOD HAZARD FROM MORAINE-DAMMED LAKES IN SOUTHWESTERN BRITISH COLUMBIA

3.1 Abstract

Existing methods of evaluating the hazard posed by moraine-dammed lakes are unsystematic, subjective, and depend on the expertise and bias of the engineer or geoscientist. In this paper, a framework is proposed for making objective preliminary assessments of outburst flood hazard in southwestern British Columbia. The procedure relies on remote sensing methods and requires only limited knowledge of glacial, dam breach, and flood processes so that evaluations of outburst flood hazard can be incorporated into hazard assessments of glacierized regions. Objective approaches, which incorporate existing empirical relations applicable to the study region, are described for estimating outburst peak discharge, maximum volume, maximum travel distance, maximum area of inundation, and probability. Outburst flood hazard is greatest for large lakes that are impounded by large, narrow, ice-free moraine dams composed of sedimentary rock debris and drain into steep, sediment-filled gullies above major river valleys. Application of the procedure is demonstrated using three case studies, and outbreak flood hazard is shown to vary, especially with major changes in lake level. The

assessment scheme yields reproducible results and enables engineers and geoscientists to prioritize potentially hazardous lakes for more detailed field investigation.

3.2 Introduction

Sudden large floods have resulted from the catastrophic failure of moraine dams in glacierized mountains throughout the world (Costa and Schuster, 1988), including the Cordillera Blanca, Peru (Lliboutry et al., 1977), Himalayas (Richardson and Reynolds, 2000), and the Cordillera of western North America (Clague and Evans, 2000; O'Connor et al., 2001). Outburst floods from moraine-dammed lakes can be particularly destructive because large volumes of water are released over a short period, downstream valleys are commonly steep and locally V-shaped, large volumes of sediment are available for entrainment from, and downstream of, the dam, and most failures occur with little or no warning and thus are unexpected.

Moraine dam failures in British Columbia have caused only minor damage (e.g., Blown and Church, 1985), but the likelihood that people will be affected by these events will increase as glacierized regions in the province are further developed and settled. Mining and forestry operations, for example, commonly involve networks of access roads, which may be damaged by outburst floods. Numerous run-of-the-river hydroelectric facilities have recently been constructed on glacier-fed streams in British Columbia, in some cases with only cursory hazard assessments. Outdoor tourism companies are expanding their operations in British Columbia's rugged mountain landscapes.

Outburst flood hazard can be reduced and even eliminated through mitigation measures. Engineers and geoscientists have successfully stabilized moraine dams in the Himalayas (Richardson and Reynolds, 2000), Andes (Lliboutry et al., 1977), and Swiss Alps (Haeberli et al., 2001) by armouring their surfaces with concrete and blocky fill, by constructing concrete trenches across the crest of the moraine dams, and by draining water out of lakes to increase freeboard, thus decreasing the possibility that displacement waves will overtop and incise the dams. Mitigation, however, is time-consuming, costly, and sometimes unsafe (Lliboutry et al., 1977), and it is not possible to prevent the sudden failure of all moraine dams. Safe development of mountainous regions, therefore, must rely on the ability of engineers and geoscientists to identify moraine-dammed lakes that pose a hazard.

Methods used in British Columbia to assess outburst flood hazard, which can be defined as the product of outburst magnitude and probability (Fell, 1994), are currently unsystematic, inconsistent, and depend, to a large extent, on the background of the analyst. Assessments are generally either done subjectively and qualitatively, in which case the results are difficult to incorporate into the design of downstream engineering works, or they are done in such rigorous detail, even during preliminary investigations, that they are unnecessarily time-consuming and expensive. Without a geoscience background, the person doing the assessment may even be unaware of the potential hazard posed by moraine-dammed lakes. Sophisticated procedures, such as flow route modelling (Fread, 1996), may be used during later stages of hazard investigations, but preliminary hazard assessments generally rely on simple empirical relations. Huggel et al. (2004) provide the most comprehensive published procedure for assessing outburst flood hazard from moraine-dammed lakes, but it is partly subjective and based mainly on observations from outburst floods in the Swiss Alps.

The purpose of this paper is to provide engineers and geoscientists with a procedure for making objective preliminary assessments of outburst flood hazard from moraine-dammed lakes in southwestern British Columbia. I describe methods that require only aerial photographs or satellite images for estimating outburst probability and four measures of outburst magnitude – peak discharge, maximum volume, maximum travel distance, and maximum area of inundation. Wherever possible, I incorporate existing published methods, after evaluating their applicability to my study area. I apply my procedure to 175 moraine-dammed lakes larger than one hectare in the southern Coast Mountains of British Columbia (Fig. 3-1) and demonstrate its application with three case studies.

3.3 Flow characteristics of outburst floods

To this point, I have used the term "outburst flood" loosely to refer to any mixture of sediment and water that flows down a channel during and immediately after the catastrophic draining of a moraine-dammed lake. Eyewitness accounts of outburst floods (Vuichard and Zimmermann, 1987) and observations of outburst deposits (O'Connor et al., 2001; Kershaw et al., 2005) indicate, however, that there is a continuum of flow characteristics of outbursts from moraine-dammed lakes. At one end of the continuum are outburst floods that are water floods, exhibiting turbulence and having no shear strength (Costa, 1988). Outbursts that occur in relatively low-gradient and broad valleys (e.g., Nostetuko Lake, Blown and Church, 1985; Queen Bess Lake, Kershaw et al., 2005), or in areas with little sediment available for entrainment, generate outburst

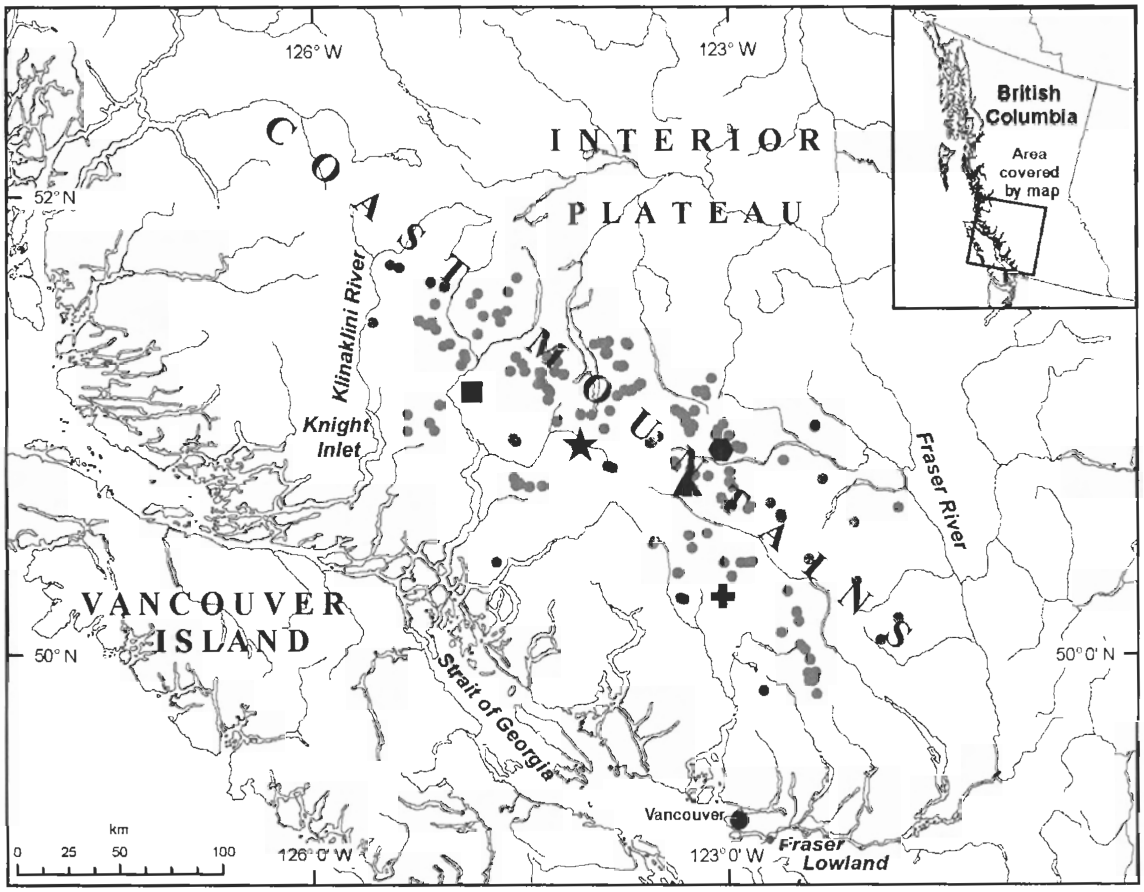

Fig. 3-1. Study area showing locations of 175 moraine-dammed lakes larger than 1 ha. Lakes discussed in text are represented by unique symbols: Klattasine Lake (square), Scherle Lake (hexagon), Salal Lake (triangle), unnamed lake above Gilbert Glacier (star), and unnamed lake in upper Soo River watershed (cross). Map projection is BC Albers. Map data provided by, and reproduced with permission of, the Province of British Columbia.

floods or "debris floods" (Hungr et al., 2001). If the channel gradient downstream of the moraine dam is sufficiently steep and if sediment is readily available for entrainment, however, lake outbursts may transform into debris flows, which exhibit visco-plastic behaviour and are more than 50% sediment by volume (e.g., Klattasine Lake, Clague et al., 1985; Tats Lake, Clague and Evans, 1992). Debris flows are multiphase events that can transform their flow rheology several times during the event and increase and decrease their volume and peak discharge.

The flow behaviour of outbursts has implications for hazard assessment. Whereas peak discharge is perhaps the most important measure of magnitude of an outburst flood, the most important measure of an outburst-generated debris flow depends more on the downstream elements at risk. Outburst-generated debris flow peak discharge is required in bridge design, for example, but the volume of debris delivered to the runout zone is crucial in the design of debris retention basins. Most empirical relations for predicting outburst flood peak discharge assume that the peak is achieved within the moraine breach. Outburst floods that transform into debris flows, however, may increase their peak discharge as they travel downstream (e.g., Broken Top, O'Connor et al., 2001; Tats Lake, Clague and Evans, 1992; Lake Weingarten, Huggel et al., 2003). Debris flows generally travel at higher velocities than outburst floods and are capable of transporting large boulders over greater distances (Pierson, 2005). However, the erosive capacity of outburst floods, especially those with sediment concentrations approaching the threshold of hyperconcentrated flow, may exceed that of outburst-generated debris flows (Pierson, 2005).

The question of whether an outburst will remain a flood or will generate a debris flow has serious hazard implications. For example, channels constructed on downstream fans may safely convey outburst floods with low sediment concentrations, but may become blocked by debris flows, sending subsequent surges of debris into developed areas (Costa, 1988). On the other hand, overly conservative mitigation structures are unnecessarily costly.

Differences in the behaviour and potential consequences of outburst floods and outburst-generated debris flows require that evaluations of the hazard posed by moraine-dammed lakes acknowledge the possibility that an outburst flood will transform into a debris flow. To maintain procedure objectivity, I assume that an outburst flood will generate a debris flow in a channel downstream from a moraine-dammed lake that has sediment available for entrainment and at least one reach steeper than 10^o. The 10^o threshold is based on (1) the observation of Hungr et al. (1984) that erosion is dominant in debris-flow channels in southwestern British Columbia where the channel gradient exceeds about 10^o (Hungr et al., 1984) and (2) data on historic outburst-triggered debris flows in western Canada (Clague and Evans, 1994) and the Alps (Huggel, 2002). Wherever possible, I provide separate methods for assessing hazards of outburst floods and outburst-generated debris flows.

3.4 Assessment procedure

My outburst hazard assessment procedure can be summarized in a series of steps (Fig. 3-2). For all lakes, the procedure begins with estimation of outburst peak discharge, assuming a complete drainage scenario. If the gradient downstream of the lake does not exceed 10^o, which means a debris flow is unlikely to form due to catastrophic lake drainage, then the assessment is complete once outburst probability is estimated. If the downstream valley gradient exceeds 10^o, however, I assume the outburst will generate a debris flow, thus requiring estimation of maximum debris flow volume, travel distance, and area of inundation. The assessment concludes, as before, with the estimation of outburst probability.

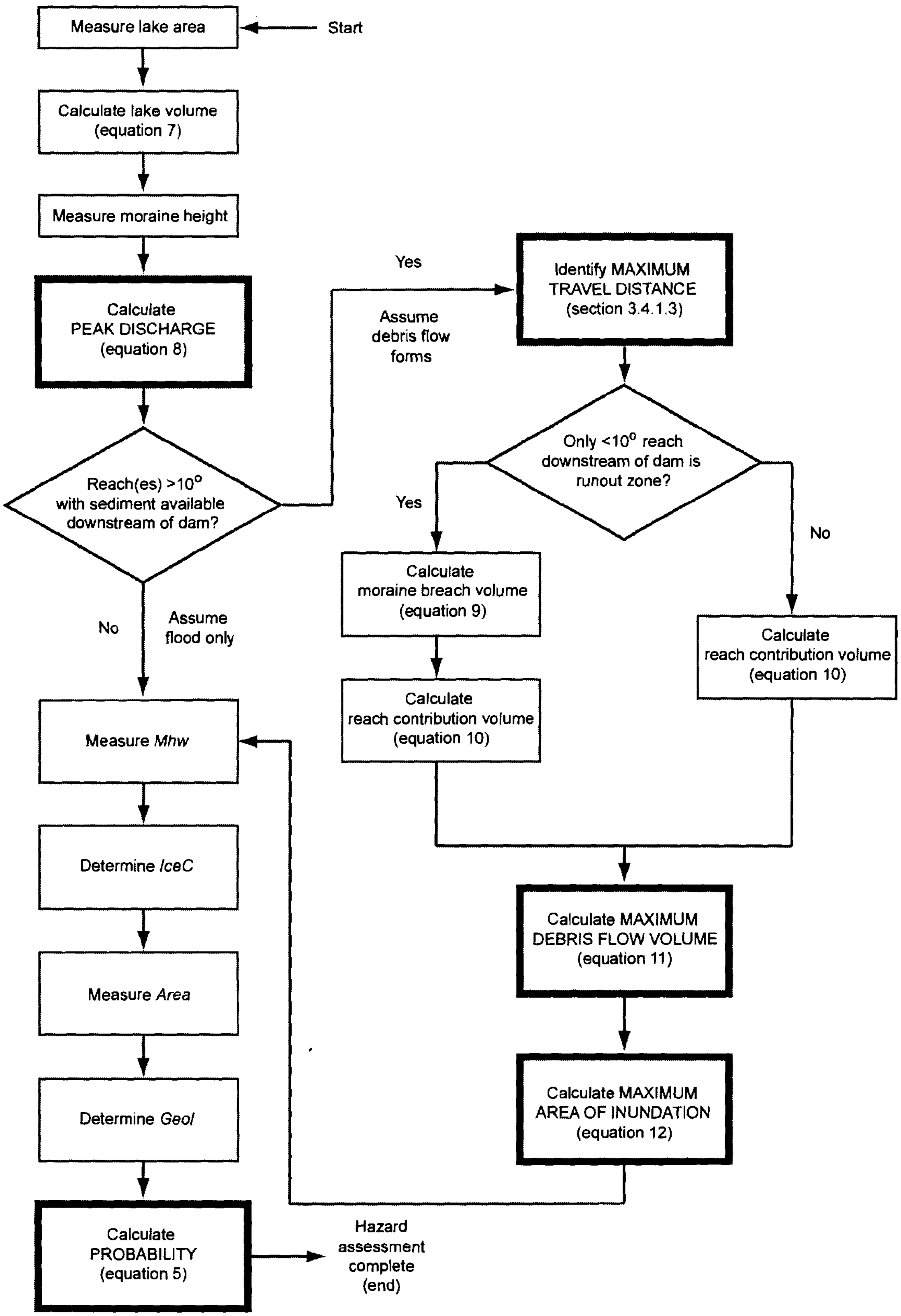

Fig. 3-2. Summary flow chart of outburst flood hazard assessment procedure. See Chapter 2 for definition of variables used in the calculation of outburst probability.

3.4.1 Outburst magnitude

3.4.1.1 Peak discharge

Outburst flood peak discharge is the maximum instantaneous volume of water and sediment that passes a particular point in a channel. An estimate of peak discharge is required for the design of bridges, culverts, and channelization works (Jakob, 2005a). Outburst floods generally attenuate as they travel downstream unless they travel through a confined canyon, thus the peak discharge is generally achieved just downstream of the moraine dam.

Outburst flood peak discharge depends on a variety of factors, including the volume of available water, the outburst-initiating event or breach mechanism, and, perhaps most importantly, the rate at which the breach develops (Blown and Church, 1985; Walder and O'Connor, 1997). Breach erosion is controlled by the size and shape of the dam; the size, stratigraphy, and cohesion of the dam material; and the existence and size of pipes (MacDonald and Langridge-Monopolis, 1984). Because moraine dams have substantially different morphologies and material properties, a wide range of failure behaviours can be expected (Blown and Church, 1985).

The geotechnical properties of moraine dams cannot be determined by remote sensing, thus researchers generally rely on morphological parameters to estimate peak discharge. The most widely used empirical relations are those that relate peak discharge to lake volume and moraine dam height (Hagen, 1982; Haeberli, 1983; MacDonald and Langridge-Monopolis, 1984; Costa and Schuster, 1988; Huggel et al., 2002). Huggel et al. (2002) found that by doubling the numerator in Haeberli's (1983) simple peak discharge formula, they could define an upper discharge limit on a log-log plot of peak discharge against lake volume.

One of the key parameters in most empirical equations is lake volume, which cannot be directly determined using remote sensing methods (Huggel et al., 2002). Fortunately, moraine-dammed lake volume correlates reasonably well with lake area (O'Connor et al., 2001; Huggel et al., 2002), which can be measured remotely. I compared lake volume, estimated using the relations developed by O'Connor et al. (2001) and Huggel et al. (2002), with outburst volumes from documented drainings of moraine-dammed lakes in southwestern British Columbia (Table 3-1). In cases of partial lake drainage, the empirically derived estimates should exceed the outburst volumes.

I recommend the following relation, developed by O'Connor et al. (2001), to estimate moraine-dammed lake volume in southwestern British Columbia:

$$V = 3.1A + 0.0002A^2 \tag{7}$$

where V is lake volume (m^3) and A is lake area (m^2). This equation is preferred over that of Huggel et al. (2002) for several reasons. First, it is based only on moraine-dammed lakes, whereas Huggel et al.'s relation is partially based on ice-dammed lakes, which may have different hypsometries. Whereas the maximum depth of ice-dammed lakes is typically located at the lake-glacier interface, moraine-dammed lakes are more commonly deepest a considerable distance from the dam (e.g., Kershaw et al., 2005). Second, the seven moraine-dammed lakes in the data set of O'Connor et al. (2001) are more similar to moraine-dammed lakes in southwestern British Columbia than several of the Himalayan and Andean lakes included in Huggel et al.'s data set. Third, unlike Huggel et al.'s relation, equation (7) yields conservative estimates of lake volume for several analyzed

Table 3-1. Lake volume estimates and observed outburst volumes for documented moraine-dammed lake drainings in southwestern British Columbia.

Lake	Outburst date	Outburst volume (m^3)	Reference	Lake area (m^2)	Lake volume estimate (m^3) O'Connor et al. (2001)[a]	Huggel et al. (2002)[b]
Bridge	1964-1970	1-2 x 10^6	Ryder (1991)	0.8 x 10^5	1.3 x 10^6	**9.5 x 10^5**
Klattasine	1971-1973	1.7 x 10^6	Clague et al. (1985)	1.6 x 10^5	4.5 x 10^6	2.4 x 10^6
Nostetuko	July 19, 1983	6.5 x 10^6	Blown and Church (1985)	2.3 x 10^5	9.6 x 10^6	**4.3 x 10^6**
Queen Bess	August 12, 1997	6.5 x 10^6	Kershaw et al. (2005)	6.5 x 10^5	7.4 x 10^7	1.9 x 10^7

Notes:

Bold value = underestimate, compared to observed outburst volume.

[a] $V = 3.1A + 0.0002A^2$ (equation 1), where V = lake volume (m^3) and A = lake area (m^2).

[b] $V = 0.104A^{1.42}$, where V = lake volume (m^3) and A = lake area (m^2).

lakes in my study area (Table 3-1). I acknowledge, however, that equation (7) is based mainly on lakes with small areas and relatively large volumes due to emplacement of moraine dams on steep slopes (O'Connor et al., 2001). Lakes impounded by moraines on gentle slopes will tend to have smaller volumes relative to their area than the lakes in O'Connor et al.'s data set. As a result, equation (7) can be expected to increasingly overestimate lake volumes as lake area increases, but no other lake area-volume relation more appropriate for lakes with large areas has been published for moraine-dammed lakes. Even for relatively large, 20 ha lakes, however, the relation yields volumes only two times larger than those predicted by Huggel et al.'s relation.

Using estimates of lake volume derived from equation (7), I applied the empirical relations of Hagen (1982), Costa and Schuster (1988), Walder and O'Connor (1997), and Huggel et al. (2002) to drained lakes in southwestern British Columbia to assess how well each predicts peak discharge in my study area. I assume that the published estimates of peak discharge for the events are reasonable order-of-magnitude approximations, even though none was reportedly directly measured. If this assumption is correct, the relations of Costa and Schuster (1988) and Huggel et al. (2002) provide the best estimates of peak discharge. Huggel et al.'s relation is the simplest, but its application to lakes in British Columbia may be inappropriate for several reasons. First, I expect peak discharge estimates, which are based on a complete drainage scenario, to be conservative, but Huggel et al.'s relation overestimates the peak discharge of the outburst flood from Queen Bess Lake (Kershaw et al., 2005) by almost two orders of magnitude because of its heavy weighting of lake volume. Second, Walder and O'Connor (1997) argue against using envelope relations such as Huggel et al.'s, because they have no physical meaning. Third, Huggel et al.'s relation assumes an outburst duration of about 15 to 30 minutes, based on observations of four jökulhlaups in the Swiss Alps. However, Nostetuko and Queen Bess Lakes, in my study area, drained in five hours and eight hours, respectively (Blown and Church, 1985; Kershaw et al., 2005).

I recommend using the relation developed by Costa and Schuster (1988), which has a coefficient of determination (r^2) of 0.78 and a standard error of 92%, to predict peak flood discharge from moraine dam failures in southwestern British Columbia:

$$Qp = 0.00013(PE)^{0.60} \tag{8}$$

where Qp is peak discharge (m^3/s), and PE is the potential energy of the lake water, which is the product of dam height to the lake surface (m), lake volume (m^3) (from equation (7)), and the specific weight of water (9800 N/m^3). Equation (8) is based on only eight moraine-dammed lake outburst events, but it yields estimates of peak discharge for several small outbursts in Oregon that agree well with O'Connor et al.'s (2001) indirect measurements of peak discharge. Retrospective predictions using equation (8) are conservative, but less extreme than those made using Huggel et al.'s (2002) relation.

3.4.1.2 Maximum volume

Hazard assessments of moraine-dammed lakes that may generate a debris flow during an outburst must include estimates of the maximum volume of debris that will be delivered to the runout zone. Estimates of maximum debris flow volume are used in the design of debris retention basins and deflection structures, which are constructed to prevent debris from reaching developed areas (Jakob, 2005a). The volume of water released during an outburst is generally excluded from debris flow volume estimates (M. Jakob, personal communication, 2005) because engineers assume it will pass through retention structures. Furthermore, the proportion of water is difficult to estimate after the event, because the pore water in the deposited debris usually has partially drained by the time researchers appear at the scene. Debris volume also affects the travel distance and area of inundation of a debris flow (e.g., Scheidegger, 1973; Corominas, 1996).

Moraine dams may contribute a large proportion of the debris transported by outburst-generated debris flows. Therefore, a realistic estimate of debris flow volume requires estimation of the volume of sediment likely to be eroded from the moraine dam. Huggel et al. (2004) recommend multiplying the maximum observed breach cross-sectional area (750 m^2, Huggel et al., 2002) by the width of the moraine dam to conservatively estimate breach volume. Because the maximum breach cross-section is restricted to the crest of the dam, however, application of the 750 m^2 value can lead to order-of-magnitude overestimates of breach volume (e.g., Lake Weingarten outburst, Huggel et al., 2004).

An alternative approach is to use Hagen's (1982) empirical relation between breach volume, moraine dam height, and lake volume, which is based on data collected from constructed concrete and earth-fill dams. This relation, however, underestimates by nearly 50% the surveyed Nostetuko Lake breach volume of 1.2 x 10^6 m^3 (Blown and Church, 1985) and underestimates the breach volumes of two moraine dam failures in Oregon by an order-of-magnitude (O'Connor et al., 2001). Furthermore, it overestimates the breach volume of Klattasine Lake (4000 m^3; Clague et al., 1985) by more than an order-of-magnitude. A more accurate relation for making preliminary estimates of breach volume would employ moraine width, rather than lake volume, in addition to moraine height.

I estimate breach volume from remotely measured moraine dam dimensions and the expected cross-sectional area of the breach (Fig. 3-3). Based on simple geometrical analysis, I derive the following expression:

$$V_b = W(H_d^2/\tan\theta) \quad (9)$$

where V_b is breach volume (m^3), W is moraine width from the lakeshore to the distal toe of the moraine dam (m), H_d is moraine height to lake surface (m), and θ is the steepness of breach sidewalls ($^\circ$). Identification of a moraine's distal toe is only difficult in rare cases where the break-in-slope at its base is gradual or subtle. Dam height is measured to the lake surface, rather than to the crest of the moraine, because the edges of a breach are generally closer in elevation to the lake surface than to the moraine crest. I assume a repose angle of 35° for breach sidewalls, which is a typical value for natural dams (Waythomas et al., 1996), and is consistent with values at Klattasine Lake (Clague et al., 1985), Nostetuko Lake (Blown and Church, 1985), and Queen Bess Lake (Kershaw et al.,

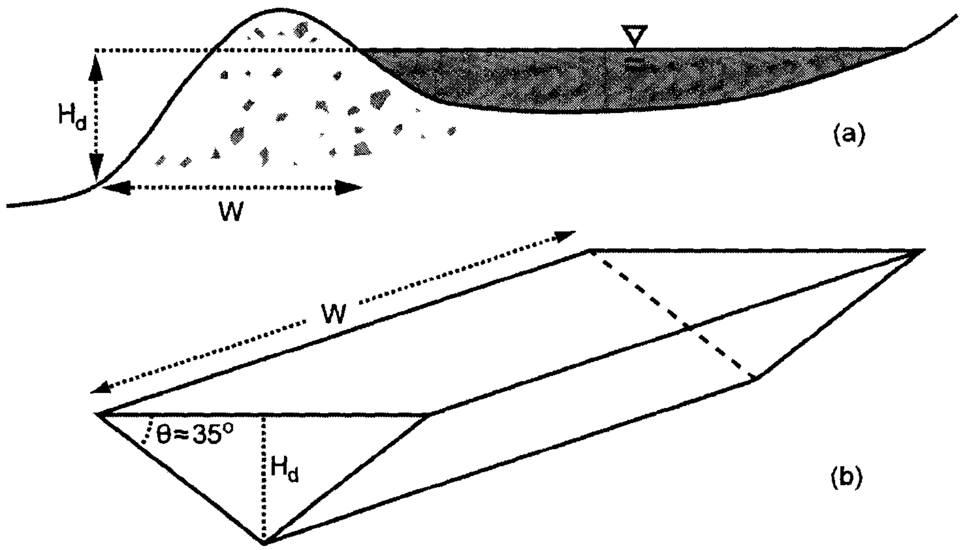

Fig. 3-3. Schematic diagram of moraine dam measurements used in the estimation of breach volume, where W is moraine width, H_d is moraine dam height to lake surface, and θ is steepness of breach sidewalls. (a) Cross-section through moraine dam. (b) Idealized moraine dam breach volume (triangular prism).

2005). Equation (9) yields conservative estimates because it is based on the assumption that a breach is a perfect triangular prism. The estimates will be especially conservative for sharp-crested moraine dams whose heights greatly exceed lake depth. Nevertheless, equation (9) overestimates the Klattasine breach volume (Clague et al., 1985) by only a factor of two, only slightly underestimates the Queen Bess breach volume (Clague and Evans, 2000), and yields an estimate of the Nostetuko breach that is almost identical to the surveyed value (Blown and Church, 1985).

Entrainment of bed and bank material into a debris flow as it travels downstream can lead to a two order-of-magnitude increase in debris volume (King, 1996; Jakob et al., 1997; O'Connor et al., 2001). Channel banks that collapse due to undercutting during the passage of a debris flow, for example, can introduce large amounts of sediment to the flow, sometimes even temporarily blocking the flow before liquefying and generating a new surge. The efficiency of debris entrainment depends on channel gradient, channel width and depth, vegetation, bed and bank material, and debris flow discharge (Hungr et al., 2005).

Hungr et al. (1984) developed the yield rate approach to quantify the rate of debris entrainment during debris flows. They proposed several "channel debris yield rates," based on channel gradient and bed and bank material for five debris flows in the mountains of southwestern British Columbia. One of the problems with this approach is defining the threshold channel gradient below which deposition dominates and above which erosion dominates. This gradient depends on debris flow volume, confinement, sedimentology, and the water content of the surge front (Hungr et al., 2005). Ikeya (1981) and Hungr et al. (1984) propose a threshold deposition angle of 10°, although in rare cases debris flows may deposit sediment on slopes exceeding 40° (Wong et al., 1997) and may erode on slopes as gentle as 1° (Pierson, 1995). I have modified the table of channel debris yield rates in Hungr et al. (1984) slightly to make their approach suitable for analysis based on remote sensing (Table 3-2). For simplicity, I assume that debris is entrained if the local channel gradient is greater than 10° and deposited if the channel gradient is less than 10°.

Table 3-2. Channel debris yield rates used in assessment procedure (modified from Hungr et al., 1984, Table 2, with permission from National Research Council of Canada).

Channel type	Average gradient ($^{\circ}$)	Bed material	Side slopes	Channel erodibility coefficient, e_i (m^3/(m km))
A	<10	N/A	N/A	0
B	>10	Non-erodible[a]	Non-erodible	0-5
C	>10	Thin debris[b]	Mainly non-erodible	5-10
D	>10	Thick sediments[c]	<5 m high	10-15
E	>10	Thick sediments	>5 m high	15-30[d]

[a] Bedrock or basal till.

[b] Discontiguous veneer of till, colluvium, alluvium, or lacustrine deposits (bedrock locally visible).

[c] Contiguous blanket of till, colluvium, alluvium, or lacustrine deposits (no bedrock visible).

[d] Channel erodibility coefficients for deeply incised channels can be up to 100 m^3/(m km) in special cases, e.g., an incision through a fresh slump.

Outburst-generated debris flow volume can be estimated by following seven steps, based on Hungr et al.'s (1984) yield rate approach:

1. Estimate the volume of the moraine dam breach V_b (m^3) using equation (9);
2. Identify the expected point of termination of the debris flow, based on Huggel et al. (2002, 2004) and section 3.4.1.3 in this paper;
3. Divide the channel between the moraine dam and the point of maximum runout into homogeneous reaches (minimum 400 m long) with respect to the characteristics that affect channel debris yield rate (Table 3-2);
4. Measure the length (L_i) and drainage area (A_i) of each reach (Fig. 3-4) [drainage area, which is easily measured remotely, is related by its square root to channel width (Kellerhals, 1970)];
5. Assign a channel erodibility coefficient e_i ($m^3m^{-1}km^{-1}$) to each reach, according to Table 3-2;
6. Calculate the total volume of sediment entrained within the reaches downstream of the moraine dam using the yield rate equation (Hungr et al., 1984):

   $$V_r = \sum [A_i^{1/2} L_i e_i] \qquad (10)$$

   where V_r is the volume of sediment entrained within the reaches (m^3), A_i is the drainage area (km^2) bordering a reach i, L_i is the length of reach i (m), and e_i is the "channel erodibility coefficient" ($m^3m^{-1}km^{-1}$) for reach i (based on my simplifying assumptions, all debris entrained to a particular point is to be deposited in depositional (<10°) reaches; therefore, only the debris contributions from erosional (>10°) reaches upstream of the runout zone (i.e., the most downstream depositional reach), but not upstream of any other depositional reach, are entered into this equation); and
7. Calculate the probable maximum outburst-generated debris flow volume using the following simplified equation:

   $$V_m = V_b + V_r \qquad (11)$$

   where V_m is the maximum debris flow volume (m^3), V_b is the breach volume (m^3), and V_r is the volume entrained within the reaches (m^3) [note that breach volume is excluded from the equation if a depositional reach other than the runout zone exists in the flow path (Fig. 3-2)].

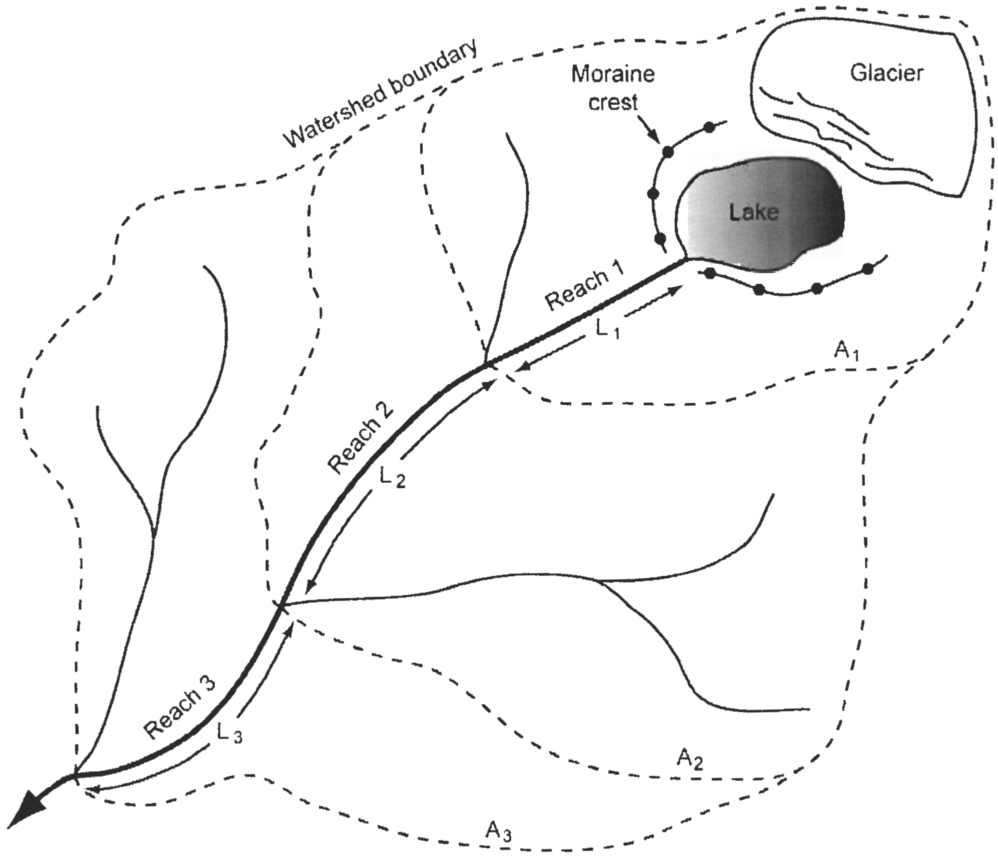

Fig. 3-4. Schematic diagram showing definitions of reach length and drainage area, both of which are used to estimate maximum debris flow volume. Drainage area is related by its square root to channel width (Kellerhals, 1970). Note that the drainage area for reach 3, for example, is the total drainage area above the downstream end of the reach, not just the additional contribution downstream of reach 2.

3.4.1.3 Maximum travel distance

One of the hazardous characteristics of outburst-generated debris flows is their ability to travel long distances downstream from their source. Most moraine-dammed lakes in southwestern British Columbia are located in the remote headwaters of glacierized watersheds, but they may pose a risk to development on stream fans many kilometres downstream. Numerous topographic and hydraulic factors may affect how far a particular debris flow travels. Momentum can be lost in channel bends (Lancaster et al., 2003); obstacles in the runout zone, such as large trees, can rapidly decelerate flowing debris (Corominas, 1996); and large woody debris and coarse boulders in debris flow fronts can increase frictional resistance to flow (Lancaster et al., 2003). Complex flow-routing software is available for modelling outburst flood attenuation (e.g., Fread, 1996), and Huggel et al. (2003) have successfully used GIS software to model the paths of outburst-generated debris flows, but such detailed analyses are beyond the scope of preliminary hazard assessments. Simple empirical observations of debris flow travel distance can, however, be used in their place.

Huggel et al. (2002) measured the horizontal and vertical travel distances of at least six outburst-generated debris flows in the Swiss Alps to determine the angle between the lake outlet and the downstream limit of debris. The minimum average slope is 11°. The same angle applies to several hundred, coarse debris flows in the Swiss Alps unrelated to lake outbursts (Rickenmann and Zimmermann, 1993). All documented outburst-generated debris flows in British Columbia stopped before achieving an average slope of 11°, with the exception of the debris flow generated by the catastrophic drainage of Klattasine Lake (Table 3-3). It travelled over 8 km on an average slope of 10° to

Table 3-3. Average runout slopes for outburst-generated debris flows in British Columbia.

No.	Lake	Average runout slope (°) [a]
15	Gilbert	14
31	Klattasine	10[b]
103	East Grouty	30
189	Soo Lower	18
302	Leckie South	18
-	Patience Mountain	19
-	South Macoun	18
-	North Macoun	20
-	Tats	15

[a] Average runout slope is the average angle with the horizontal between the lake outlet and the terminal debris lobe.
[b] Less than the 11° minimum average runout slope observed for outburst-generated debris flows in the Swiss Alps.

Homathko River, where it formed a temporary dam (Clague et al., 1985).

One might be tempted to use the more conservative value of 10° to define the probable maximum travel distance of outburst-generated debris flows in southwestern British Columbia. In some cases, however, use of an average slope of 10° might greatly overestimate the travel distance of a debris flow. A debris flow cannot be sustained for long distances in low-gradient, unconfined channels, which may be present within the runout zone defined by an overall average slope of 10°. In addition, debris flows commonly change to debris floods upon entering higher-order rivers (Jakob, 2005a). To maintain the objectivity of the assessment procedure and to more realistically estimate the maximum travel distance of debris flows, I specify a limit of runout upstream of the point defined by the 10° average slope, if at least one of Ikeya's (1979) two conditions for premature termination is met: (1) the slope angle in the runout zone is reduced by at least a factor of two; or (2) the flow width increases at least two-fold. I note, however, that the termination point I define does not necessarily delineate the downstream limit of potential damage. A destructive debris flood may continue tens of kilometres downstream before attenuating to background levels (Richardson and Reynolds, 2000).

Estimating the maximum travel distance of outburst floods that do not transform into debris flows is more subjective because outburst floods do not generally have discrete termination points. Unlike debris flows, which deposit lobes of debris at their termini, debris floods attenuate slower, gradually depositing sediment as flow competence decreases. Flood routing is best left to the detailed stage of a hazard assessment.

3.4.1.4 Maximum area of inundation

Hazard zoning studies commonly require, in addition to the maximum travel distance of debris flows, estimates of the area likely to be inundated by debris. Delineation of detailed debris flow inundation areas is beyond the scope of preliminary assessments, but empirical equations facilitate rapid assessment of the general area likely to be covered by debris. The area in the runout zone likely to be covered for bouldery (i.e., non-volcanic) debris flows can be predicted using the following equation (Griswold, 2004):

$$B_m = 20V^{2/3} \qquad (12)$$

where B_m is maximum area of inundation (m^2), and V is debris flow volume (m^3), which can be estimated using the methods described in section 3.4.1.2. This equation, however, is based on observations of debris flows originating from localized slope failures. Therefore, it may underestimate areas inundated by outburst-generated debris flows, which contain larger volumes of water and thus may have greater mobility.

Outburst floods that do not transform into debris flows may also deposit large volumes of sediment in lower gradient and unconfined channel reaches. Floodplains that historically have never been flooded may be inundated by sediment-laden floodwater. Estimation of expected areas of inundation by floodwater, however, is beyond the scope of preliminary hazard assessments.

3.4.2 Outburst probability

Outburst probability is defined here as the likelihood that a lake will drain, or partially drain, catastrophically within an unspecified period. Outburst probability is difficult to determine for three reasons: (1) lakes generally drain catastrophically only once, thus no recurrence interval can be used to estimate mean annual probability; (2) the rarity of outburst floods limits understanding of failure processes; and (3) the numerous possible trigger mechanisms (Clague and Evans, 2000; Richardson and Reynolds, 2000) and diversity of moraine dam form and structure preclude deterministic analysis.

Fell (1994) argues, however, that geoscientists should estimate event probabilities, even if approximate and subjective, and several authors propose subjective approaches for estimating the probability of outburst floods from moraine-dammed lakes (Lu et al., 1987; Richardson and Reynolds, 2000; O'Connor et al., 2001). Most recently, Huggel et al. (2004) have proposed a list of five indicators for deriving a qualitative probability of outbursts from moraine-dammed lakes in the Swiss Alps. The subjectivity of this approach, however, can result in assessments that are inconsistent and depend on the expertise of the geoscientist.

I propose using a statistical model for making preliminary estimates of outburst probability. The outburst probability of a moraine-dammed lake in southwestern British Columbia is calculated using equation (5), derived from logistic regression analysis. To avoid conveying unrealistic precision in the probability estimates, I recommend classifying outburst probabilities as very low (<6%), low (6-12%), medium (12-18%), high (18-24%), and very high (>24%) (Fig. 2-8).

3.5 Application of procedure

I applied the outburst flood hazard assessment procedure to 175 moraine-dammed lakes larger than one hectare in the southern Coast Mountains of British Columbia. Here, I illustrate its application with three case studies (Table 3-4). Application of the assessment procedure to Klattasine Lake, which drained catastrophically in the early 1970s (Clague et al., 1985), shows retrospectively that the procedure predicts reasonably well the known probability and magnitude of the event. The outburst-generated debris flow from Klattasine Lake had a higher observed volume, travel distance, and area of inundation than I predict for the 174 other analyzed moraine-dammed lakes in southwestern British Columbia, suggesting that this event represents an approximate upper limit of outburst-generated debris flow magnitude in the region. I present the results of my assessment of Scherle Lake because the lake is small but has a high outburst probability and a high predicted magnitude. Salal Lake is included as an example of a large lake with a relatively high, predicted outburst magnitude but low outburst probability.

Table 3-4. Hazard assessment input parameters and results for three case studies.

Variable	Data source	Klattasine Lake		Scherle Lake	Salal Lake
		Observed	Predicted	Predicted	Predicted
Lake area (m^2)	TRIM[a]	1.6×10^5 [e]	1.6×10^5	2.0×10^4	7.0×10^4
Lake volume (m^3)	Equation (7)	N/A	4.5×10^6	1.3×10^5	1.0×10^6
Peak discharge (m^3/s)	**Equation (8)**	**>1000**[f]	**1500**	**310**	**1400**
Breach volume (m^3)	Equation (9)	4000[f]	11 000	1×10^5	N/A[i]
Sum of reach contributions (m^3)	Table 3-2, Equation (10)	~9×10^5 [g]	$3 - 6 \times 10^5$	$1 - 2 \times 10^5$	N/A
Maximum debris flow volume (m^3)	**Equation (11)**	**~9×10^5** [g]	**$3 - 6 \times 10^5$**	**$1 - 2 \times 10^5$** [h]	**N/A**
Vertical drop (m) corresponding to 10°	TRIM	1500	1500	1400	N/A
Maximum travel distance (m)	**TRIM**	**8800**[f]	**8800**	**5800**	**N/A**
Maximum area of inundation (m^2)	**Equation (12)**	**~1.6×10^5** [e]	**$1.0 - 1.5 \times 10^5$**	**$4.3 - 6.6 \times 10^4$**	**N/A**
Moraine height-to-width ratio (-) (*Mhw*)	AP[b]	N/A	0.3	0.5	0.1
Ice-cored moraine (*IceC*)	AP, M[c]	N/A	ice-free (0)	ice-free (0)	ice-free (0)
Lake area (ha) (*Area*)	TRIM	N/A	15.5	2.0	7.0
Main rock type forming moraine (*Geol*)	BCGS[d]	N/A	granitic (1)	granitic (1)	granitic (1)
Probability (%)	**Equation (5)**	**drained**	**20 (high)**	**61 (very high)**	**5 (very low)**

Notes:
[a] TRIM = 1:20 000-scale Terrain Resource Information Management topographic map (Province of British Columbia, 2001).
[b] AP = ~1:15 000-scale aerial photographs (Appendix B).
[c] M = 1:2 000 000-scale moraine type map (Østrem and Arnold, 1970).
[d] BCGS = online 1:250 000-scale British Columbia Geological Survey geological map (Massey et al., 2005).
[e] Pre-outburst estimate.
[f] Clague et al. (1985).
[g] Blown and Church (1985).
[h] Estimate excludes breach volume because morainal debris would be deposited in meadow downstream of lake and not be delivered to the runout zone.
[i] N/A = not applicable; debris flow could not be sustained downstream of dam.

3.5.1 Klattasine Lake

Klattasine Lake is located at an elevation of about 1650 m at the west edge of the Homathko Icefield in the southern Coast Mountains of British Columbia (Fig. 3-1). It was impounded by a narrow, sharp-crested moraine perched at the edge of a bedrock sill above steep bluffs (Fig. 3-5). Sometime between June 1971 and September 1973, Klattasine Lake breached its moraine dam (Clague et al., 1985). Less than 4000 m^3 of sediment were eroded from the moraine dam, but the floodwaters quickly transformed into a debris flow as they cascaded over the bluffs below the lake (Fig. 3-5) (Clague et al., 1985). The debris flow had sufficient momentum to traverse two small meadows, before descending steeply through a sediment-choked canyon, where it entrained large volumes of debris (Fig. 3-6). It travelled over 8 km to the mouth of Klattasine Creek, where it deposited about 9×10^5 m^3 of debris (Blown and Church, 1985).

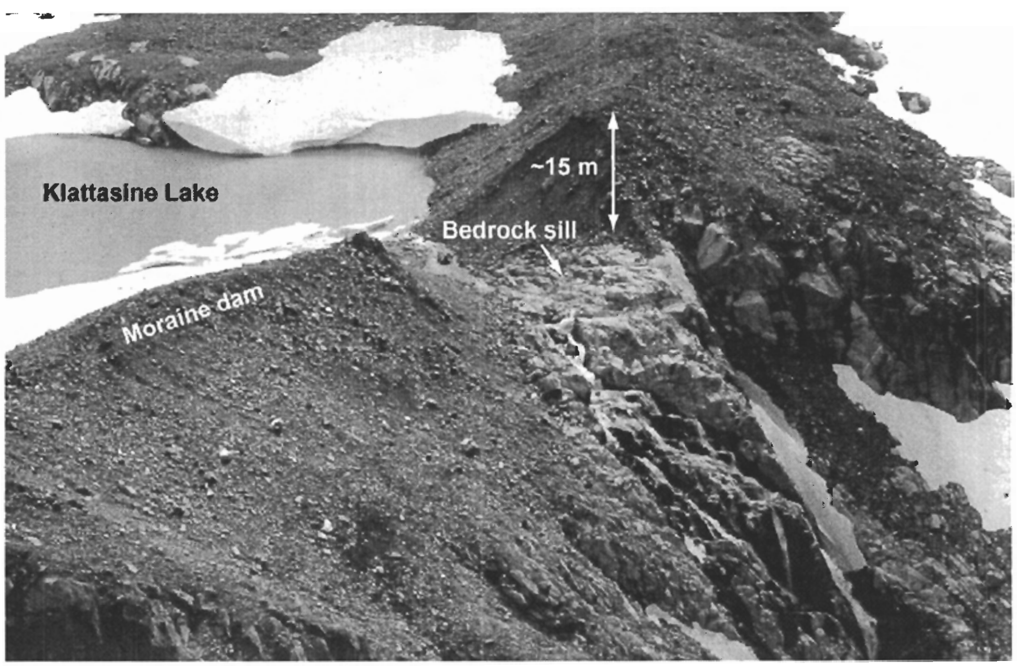

Fig. 3-5. Low-level oblique aerial photograph of Klattasine Lake and its moraine dam after the early 1970s outburst (photograph by Steve Evans).

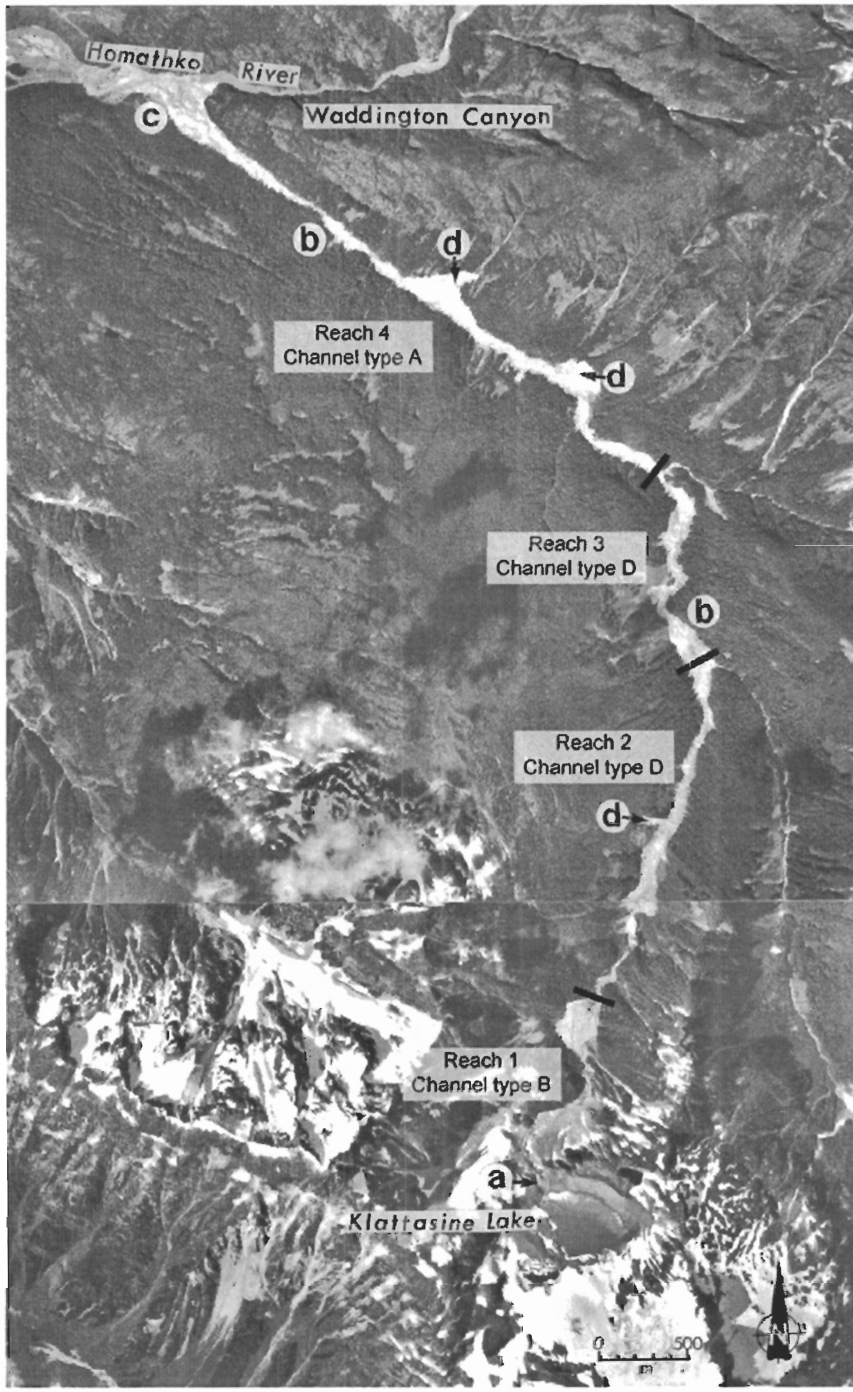

Fig. 3-6. Post-outburst aerial photograph mosaic of Klattasine Lake's outburst-generated debris flow path, showing (a) breached moraine, (b) unvegetated strip delineating the path of the flow, (c) debris fan at the confluence with the Homathko River, and (d) secondary slope failures (modified from Clague et al., 1985, Fig. 2, and reproduced with permission of National Research Council of Canada). Aerial photographs BC79069-235 and BC79074-041 (July 14-15, 1979) reproduced with permission of the Province of British Columbia. Thick black lines define reach breaks, and "Channel types" are defined in Table 3-2. Note that the procedure, which assumes erosion does not occur in reaches with average gradients less than 10°, requires Reach 4 to be classified as "Channel type A." An evaluation of this event, however, indicates that the debris flow may have had sufficient energy to entrain material in at least the upper half of Reach 4.

The input parameters for, and results of, my retrospective hazard assessment of Klattasine Lake are provided in Table 3-4. Although they made no direct or indirect measurements, Clague et al. (1985) used empirical relations to conclude that the outburst peak discharge exceeded 1000 m^3/s, which is consistent with my estimate of about 1500 m^3/s. My estimate of 6.5×10^5 m^3 for the maximum volume of the debris flow is slightly less than Blown and Church's (1985) estimate of the amount of debris deposited by the initial debris flow, probably because my approach assumes erosion does not occur in the main stem of Klattasine Creek (reach 4, Fig. 3-6), which has an average gradient less than 10°. The Klattasine debris flow descended about 1500 m over a horizontal distance of about 8800 m, which corresponds to an average slope of 10° (Fig. 3-7). My estimate of 15 ha as the maximum expected area of debris inundation is similar to the observed area (Clague et al., 1985, their Fig. 7). Equation 5 yields a "high" outburst probability. Compared with other empirical relations for assessing outburst hazard, my assessment procedure provides a reasonable evaluation of the hazard posed by Klattasine Lake. While my method consistently yields estimates that are within about two times the observed values (Table 3-4), other methods, such as Huggel et al.'s (2002) and Hagen's (1982), produce estimates that are an order-of-magnitude too high.

3.5.2 Scherle Lake

Scherle Lake (informal name) is a small (2.0 ha) moraine-dammed lake located at an elevation of 2180 m in the Dickson Range, 2.5 km west of Scherle Peak (Fig. 3-1). The dam is narrow and has a steep distal flank (Fig. 3-8). The stream flowing from the lake descends more than 1400 m over talus cones, through a steep V-shaped valley with unstable slopes, and across a small fan to its confluence with Bridge River (Fig. 3-9).

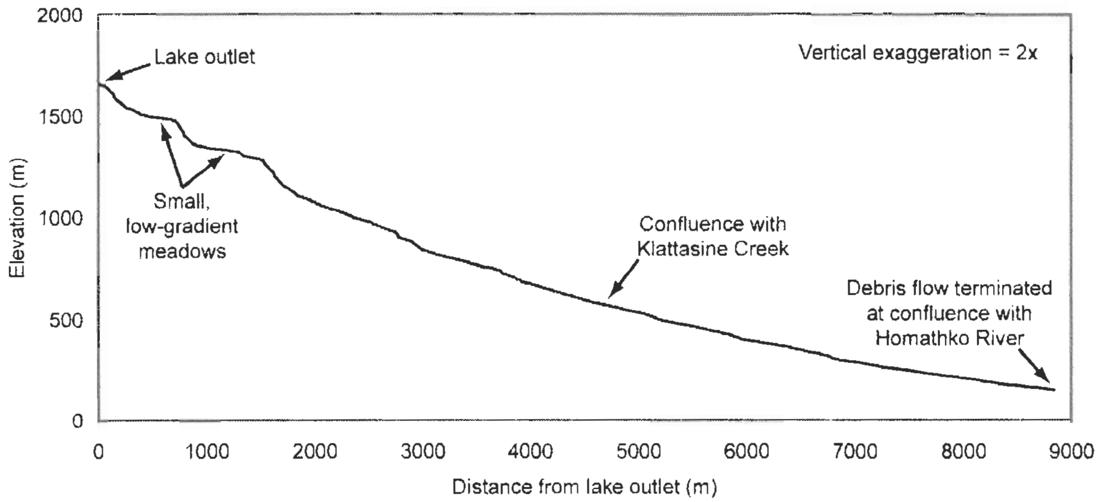

Fig. 3-7. Longitudinal profile of Klattasine Lake's outburst-generated debris flow path.

Fig. 3-8. Scherle Lake and its steeply-flanked lobate moraine dam. Note person standing at outlet for scale.

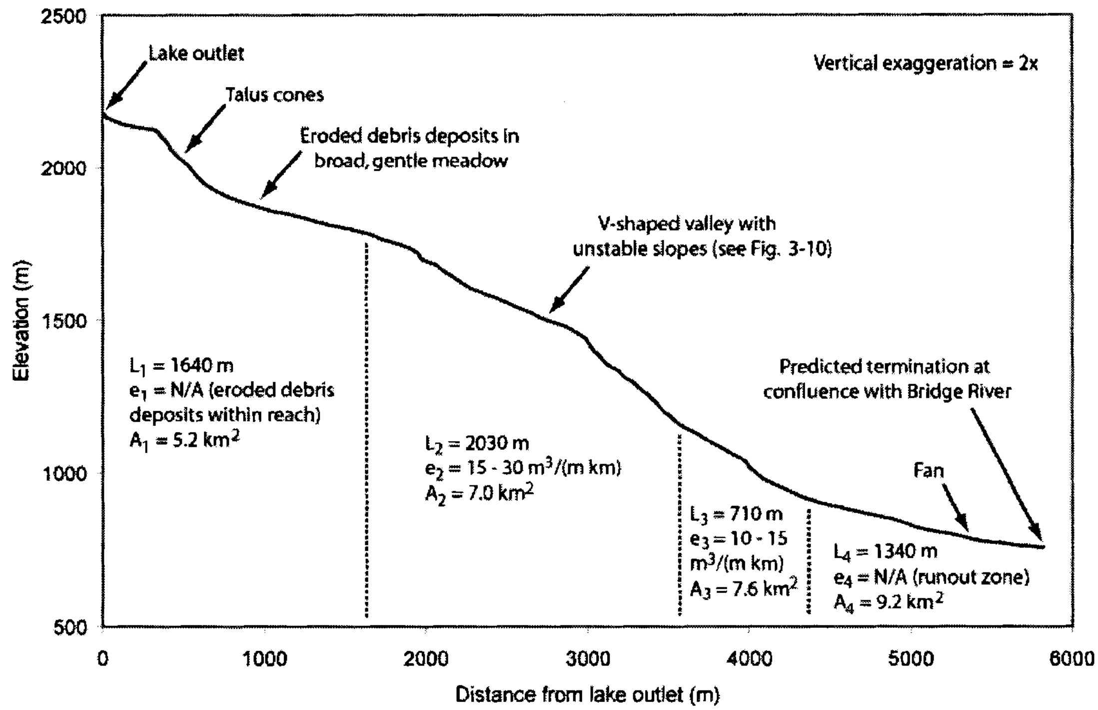

Fig. 3-9. Longitudinal profile of hypothetical outburst-generated debris flow path from Scherle Lake. Reach breaks are shown with dotted vertical lines, and input parameters for equation (10) – reach length (L_i), channel erodibility coefficient (e_i), and tributary drainage area (A_i) – are located beneath the curve. Vertical exaggeration = 2x.

The input values and results of my hazard assessment of Scherle Lake are summarized in Table 3-4. According to equation (5), Scherle Lake has a "very high" outburst probability of 61%, one of the highest estimates in the study area. Only about 1.3 x 10^5 m^3 of water would be released if the lake completely drained, but that would probably be sufficient to generate a debris flow in the steep, debris-choked valley downstream. Debris eroded from the moraine dam and talus slopes below the lake would deposit in a small meadow about 1 km downstream of the lake, but steep, 100-m-high talus aprons on the valley sides above the middle reach (Fig. 3-10) would likely contribute large volumes of sediment to a debris flow. Given the likelihood of substantial bulking of the debris flow through debris entrainment, I caution that my estimate of peak discharge, which I assume would be achieved in the moraine breach, may be too low.

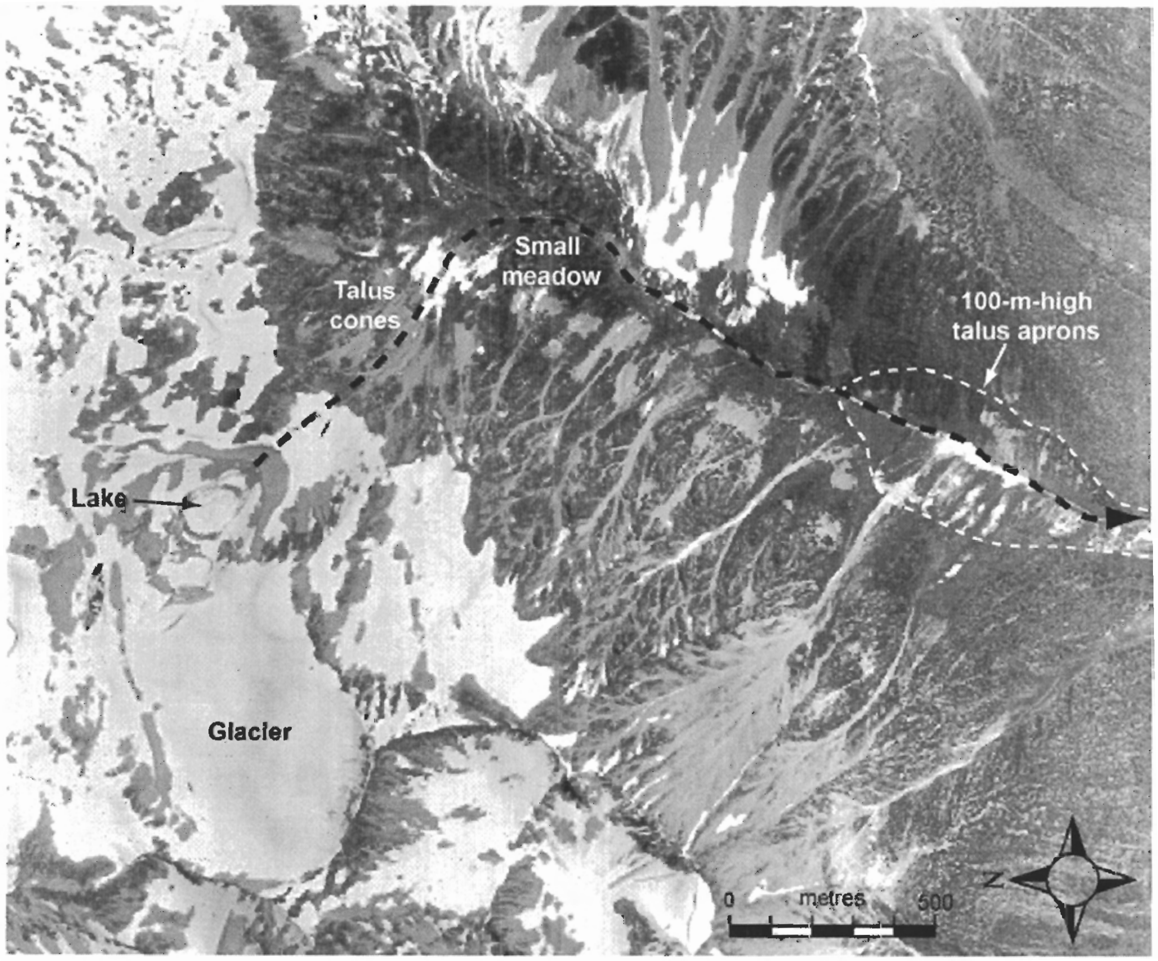

Fig. 3-10. Unstable valleysides that would likely contribute a large volume of debris to an outburst flood originating from Scherle Lake (aerial photograph 30BCC97087-036 (July 20, 1997) reproduced with permission of the Province of British Columbia). Dashed black line delineates upper part of hypothetical debris flow path. Confluence with Bridge River is not shown.

Deposition might begin about 1.5 km upstream of the Bridge River confluence due to the lower, more variable channel gradient there. I assume, however, that the debris flow would have sufficient momentum and local confinement to reach Bridge River (average slope of about 14^{o} from Scherle Lake), at which point all remaining coarse debris would be deposited. Even if the debris flow temporarily dammed Bridge River, any subsequent outburst flood from the landslide dam would terminate upon entering Downton Lake reservoir, a few kilometres downstream.

3.5.3 Salal Lake

Salal Lake (informal name) is located at an elevation of about 1600 m in the headwaters of Salal Creek, in the upper Lillooet River watershed (Fig. 3-1). The oval-shaped, 7.0 ha lake is dammed by a broad, 50-m-high, multi-crested moraine (Fig. 3-11). A retreating glacier with a crevassed snout terminates above the lake on a moderately steep slope, but no evidence of ice avalanches reaching the lake has been observed in historical aerial photographs or during several field visits over the past three years. The outlet stream flows down the distal flank of the moraine dam, which slopes up to 15° (Fig. 3-12), and enters Salal Creek, which has an average local gradient of about 5° and a broad floodplain.

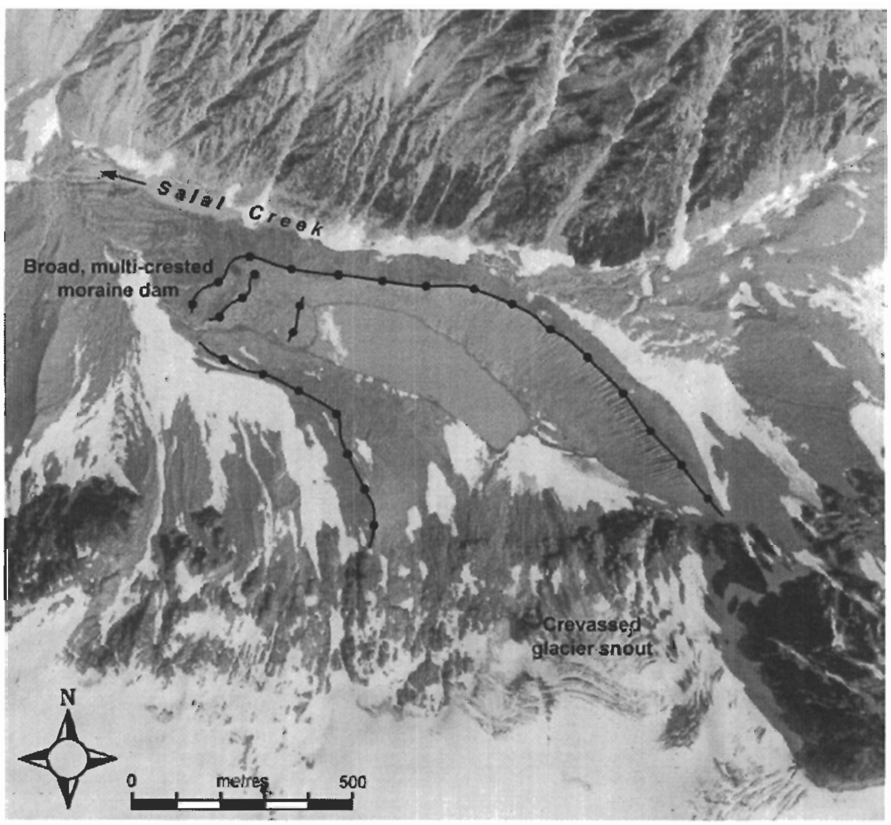

Fig. 3-11. Salal Lake and its broad, multi-crested moraine dam (aerial photograph 30BCC97086-089 (July 20, 1997) reproduced with permission of the Province of British Columbia). Black lines with dots delineate the crests of moraines.

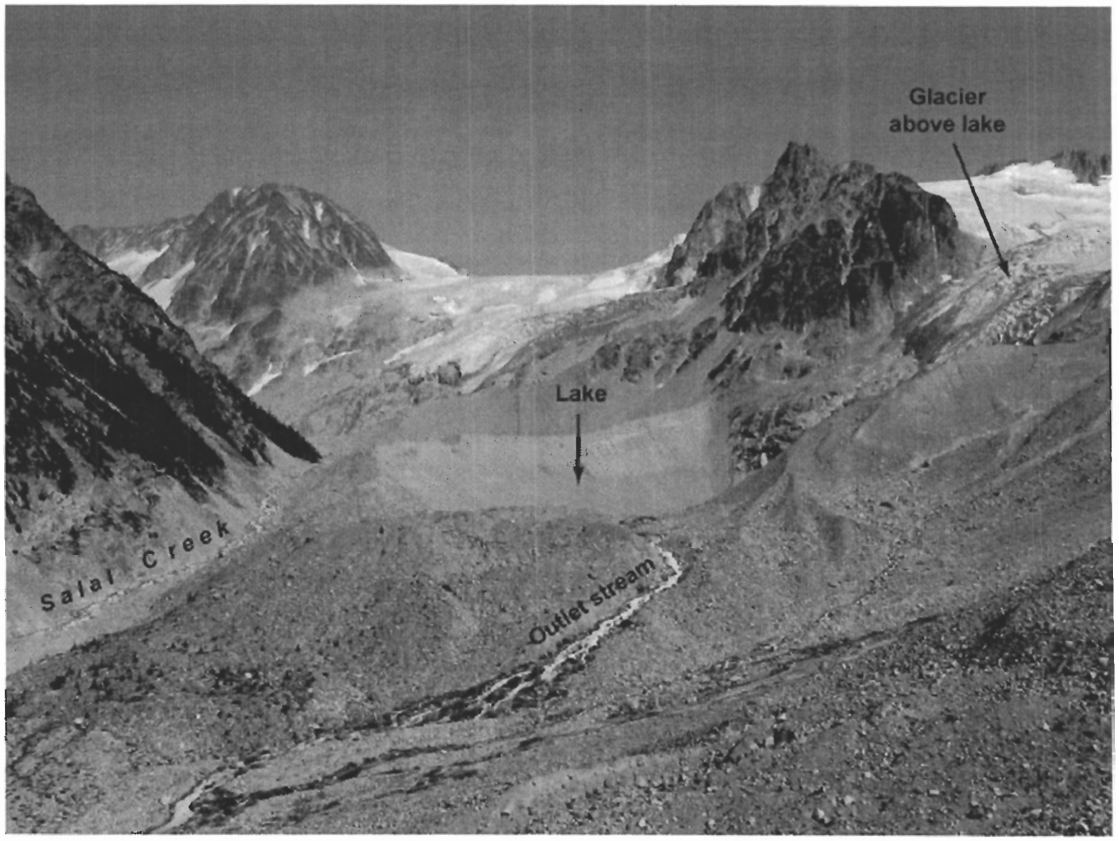

Fig. 3-12. View upstream toward Salal Lake. Note the locally steep distal flank of its moraine dam and the glacier hanging above the lake.

Although escaping floodwaters might generate a debris flow on the distal flank of the dam, my assessment procedure predicts that a debris flow would not be sustained on the broad, gentle floodplain of Salal Creek. Thick outwash deposits along the south side of Salal Creek show no evidence of debris flows, even though debris flow gullies on the north side of Salal Creek deliver large volumes of sediment to the channel.

Data relevant to the outburst flood hazard assessment of Salal Lake are provided in Table 3-4. My estimate of lake volume is 1 x 10^6 m^3. The height of the moraine dam (to the lake surface) is 50 m. From these values, I estimate that peak discharge through the moraine dam would be about 1400 m^3/s. I would expect an outburst to generate a debris flood because of the instability of Salal Creek's alluvial and colluvial banks, as seen in historical aerial photographs. According to equation (5), however, Salal Lake has a very low probability of draining catastrophically. My evaluation of outburst probability is consistent with Jordan's (1987) subjective classification of the lake as "stable," due to the large width and relatively low gradient of its moraine dam and to the infrequency of ice avalanches from the hanging glacier.

3.6 Discussion

3.6.1 Characteristics of lakes with high outburst flood hazard

One of the main goals of my research is to identify the hazardous characteristics of moraine-dammed lakes in southwestern British Columbia. Not surprisingly, peak discharge estimates are highest for large lakes with tall moraine dams. A less obvious finding, however, is that these lakes are unlikely to generate debris flows during outbursts because most are located in valleys with relatively low gradients. Large lakes rarely form behind moraine dams emplaced on steep slopes because the possible lake basin area, which is partially controlled by moraine dam height, decreases with increasing valley side steepness. Outburst floods from moraine-dammed lakes in cirques or hanging valleys high above major river valleys are most likely to generate debris flows capable of travelling long distances and depositing large volumes of sediment and woody material over extensive areas. Outburst-generated debris flows that travel down steep, confined channels with unstable banks may entrain large volumes of debris, but enough sediment can be eroded from the moraine dam during the breaching process to form a debris flow with no downstream contribution of debris. The largest predicted debris flow volumes, however, are from lakes with outlet streams that flow down the steep distal flank of a high, incised moraine dam and then for a considerable distance along confined steep channels with high banks composed of loose sediment.

According to the results of the statistical analysis (section 2.8), outburst probability is positively correlated with lake area and moraine height-to-width ratio. Furthermore, a moraine dam is most likely to fail catastrophically if it is ice-free and composed mainly of debris derived from sedimentary rock.

3.6.2 Changes to outburst flood hazard over time

The hazard posed by moraine-dammed lakes changes over time through variations in outburst probability and magnitude. Three of the four variables that influence outburst probability are dynamic: lake area, moraine dam height-to-width ratio, and the presence/absence of an ice core in the moraine dam. Outburst probability is especially sensitive to fluctuations in lake level. Thus, probability estimates apply to the particular time at which the measurements were taken and must be revised as conditions change. Hazard assessments should always state the date to which they apply.

Outburst magnitude may also change with changes in lake level. I retrospectively estimate an outburst peak discharge of about 800 m^3/s for the partial outburst between July 1965 and September 1977 from the moraine-dammed lake above Gilbert Glacier. I predict a peak discharge of only 360 m^3/s, however, for a second outburst, because the lake is 10 m lower than before the first outburst and only half its original area.

The maximum volume and inundation area of a future outburst-generated debris flow may either increase or decrease following a partial outburst. When the small lake in the cirque north of Patience Mountain, in southeastern British Columbia, partially drained between 1951 and 1966, the outflowing waters removed vegetation and surficial deposits in a swath up to 50 m wide over a distance of nearly 2 km below the lake, in the process generating a debris flow (Evans, 1987). A pre-outburst hazard assessment, using my method, would have predicted a moderately large debris flow during an outburst, whereas a post-outburst assessment would assume that too little sediment is now available to generate a debris flow. In contrast, an outburst flood that undercuts and destabilizes talus slopes may increase the rate of debris entrainment during subsequent outburst floods.

Not only can the outburst hazard posed by a lake change within days or even hours, new lakes can form rapidly and without warning. For example, a dangerous lake formed in the Cordillera Blanca in Peru in only five years (Richardson and Reynolds, 2000). My comprehensive aerial photographic inventory of moraine-dammed lakes in southwestern British Columbia revealed that several lakes formed during the 1990s because of glacier retreat. In the next century, however, numerous moraine-dammed lakes that presently have a high outburst flood potential may drain gradually through slow downcutting of the dam or may fill in with sediment.

3.6.3 Limitations of assessment procedure

My hazard assessment procedure should not be applied without an acknowledgement of its limitations. My estimates of peak discharge may be exceeded in at least four circumstances. First, waves that overtop a moraine dam may have higher peak discharges than those predicted by equation (8), which applies only to flow through a rapidly eroding breach. The massive displacement wave that overtopped the broad moraine dam impounding Queen Bess Lake, for example, had a peak discharge two to four times larger than the peak discharge of the subsequent dam breach phase of the outburst flood (Kershaw et al., 2005). The peak discharge of a large overtopping wave, however, depends on a variety of factors, including lake bathymetry and the momentum of the displacing mass (Singerland and Voight, 1982), and thus is beyond the scope of preliminary hazard assessments. Second, process interactions and chain reactions can lead to higher peak discharges than equation (8) predicts. For example, I do not take into account the potential peak discharge that could result from a secondary failure of a dam created by an outburst-generated debris flow, nor do I address what effect sequential outbursts of paternoster moraine-dammed lakes can have on peak discharge. Recognizing such process interactions is important because an outburst flood, rather than gradually attenuating downstream, may undergo rapid, short-lived increases in peak discharge. Third, peak discharge may be higher than indicated by equation (8) if the outburst occurs during a time of high runoff, when streams are near bankfull level and high pore water pressures in the channel bed and banks ease sediment entrainment. For ungauged streams, a routine regional hydrologic analysis can provide an estimate of storm-induced flood discharge to which outburst peak discharge can be added. Fourth, the peak discharge of an outburst flood that transforms into a debris flow through sediment entrainment may exceed my estimates, which are based on lake and dam characteristics, but do not take into account downstream erosion potential.

Estimates of the maximum debris flow volume and area of inundation are highly dependent on the selection of a minimum channel gradient below which erosion is assumed not to occur. In this study, an erosion threshold of 10° is used, based on Hungr et al.'s (1984) observations of debris flows in southwestern British Columbia. To illustrate the effect that changing this threshold can have on predicted magnitudes, I repeated the analysis of expected debris flow volume and area of inundation using a lower threshold of 8^{0}, which applies to outburst-generated debris flows in Oregon (O'Connor et al., 2001). Even such a small change can substantially increase estimates of debris flow volume and area of inundation. An 8^{0} threshold increases the predicted maximum debris flow volume from the hypothetical outburst of Scherle Lake (Figs. 3-7 to 3-9) from 2×10^{5} m^{3} (Table 3-4) to 4×10^{5} m^{3}. The reason for the increase is that, based on an 8^{0} threshold, debris eroded from the moraine dam and talus slopes immediately downstream of the dam is no longer deposited in the hanging valley meadow (Figs. 3-8 and 3-9), which has an average gradient of about 9^{o}. All entrained debris is delivered to the runout zone. The probable maximum area of inundation increases, correspondingly, by about 50% from 6.6×10^{4} m^{2} (Table 3-4) to 10.1×10^{4} m^{2}. This simple analysis reinforces the importance of erosion threshold selection and highlights how such a minor change in the assessment procedure can have a significant effect on the predicted outcomes.

In order to ensure the consistency and objectivity of my assessment procedure, I have made simplifying assumptions about outburst-generated debris flow behaviour that may affect the accuracy of my estimates of the volume and area of debris inundation. For example, I assume, based on channel gradient, that debris flows either erode or deposit debris rather than achieve an equilibrium in any given channel section. Realistic application of Hungr et al.'s (1984) yield rate approach to all outlet channels in the study area required a minimum reach length to be established. Otherwise, according to the gradient-based reach definition used in this study, a reach break would have to be defined at every location where channel gradient crossed the 10^{o} threshold. I used a minimum reach length of 400 m, based on Blown and Church's (1985) observation that the Klattasine Lake outburst-generated debris flow had sufficient momentum to traverse meadows up to 400 m long. Of course, channel gradient and thus yield rate may change over shorter channel lengths. Smaller debris flows, in particular, may deposit debris in short, low-gradient or wide reaches.

My procedure does not address possible secondary hazards resulting from catastrophic drainage of moraine-dammed lakes, but hazard analysts should be familiar with them. For example, outburst floods may destabilize valley walls by eroding talus aprons and alluvial sediments. In the years following the Klattasine Lake outburst, landslides on the valley sides above the channel enlarged through retrogressive slumping (Fig. 3-6). Analysis of tilted and impact-scarred trees revealed that debris flows occurred at Klattasine Creek for years following the outburst (Clague et al., 1985), probably due to secondary landslides on valley sides. Breached moraines can themselves pose a hazard to downstream areas. Several debris flows have originated in the steep sidewalls of a breached moraine in the upper Soo River watershed (Fig. 3-13; see Fig. 3-1 for location) (Jordan, 1987). The largest of these debris flows travelled over 2 km from the breached dam.

3.6.4 Potential sources of error

High-resolution, remote sensing imagery permits preliminary hazard assessments to be made without field investigations, but the assessments have several possible sources

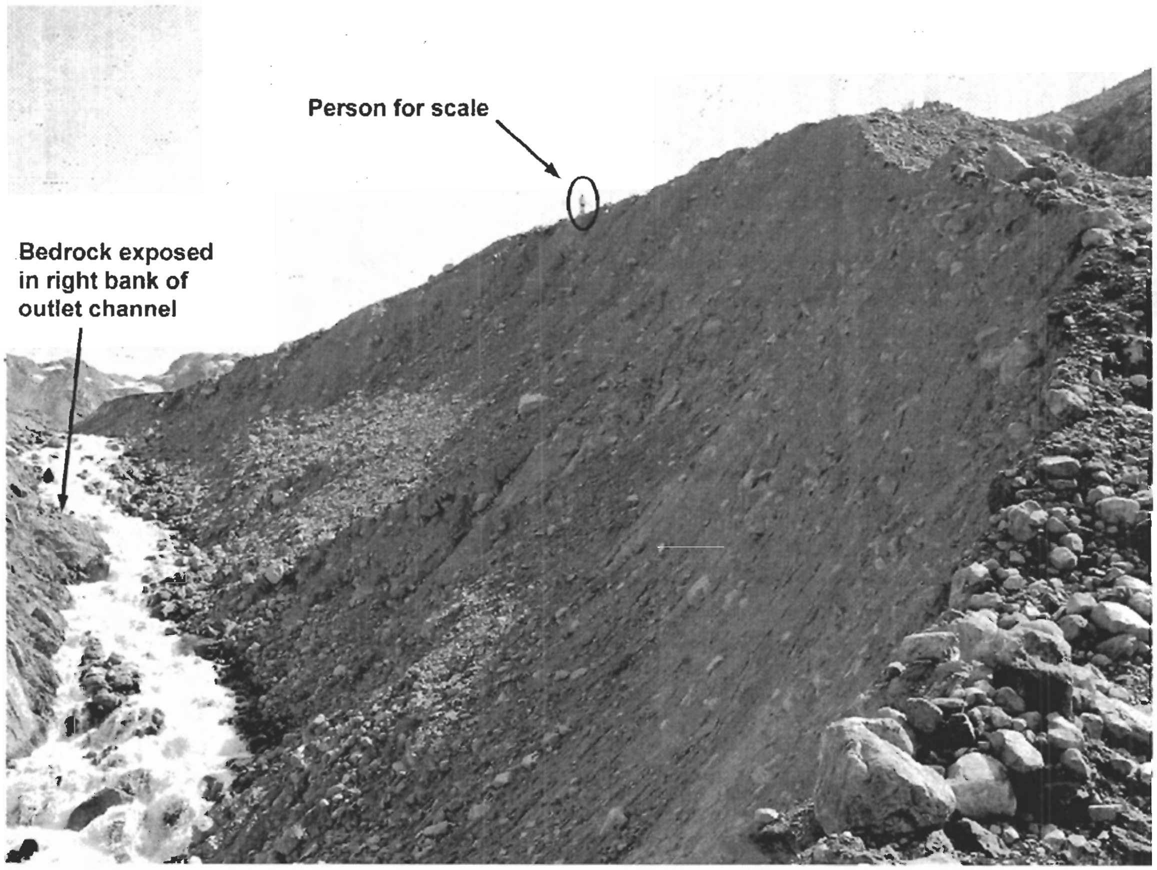

Fig. 3-13. Sidewall of breach through moraine dam in the upper Soo River watershed. Historical aerial photographs indicate several debris flows, unrelated to the outburst, have originated from this sidewall, which is nearly 50° steep at the top.

of error. For example, lake volumes estimated using empirical relations rather than bathymetric surveys may be inaccurate, particularly for lakes with unusual bathymetries. Substitution of empirically derived lake volumes into equation (8) may then lead to inaccurate peak discharge estimates. Prediction of maximum debris flow volume from aerial photographs is difficult without a detailed complementary field survey of the channel. Determining moraine breach volume solely on the height and width of the dam, rather than on a detailed field survey, may result in substantial overestimates, especially in the case of dams that are relatively high relative to lake depth. Debris yield rates are especially difficult to estimate for channels that have no shallow, firm substrate (Hungr et al., 2005).

Several possible sources of error are associated with remotely evaluating moraine-dammed lake outburst probability. Possible errors include misinterpretation of dam type, misinterpretation of rate of draining of lake (i.e., gradual vs. catastrophic), inaccuracies associated with photogrammetric measurements, and inconsistencies in defining moraine width. Erroneous estimates of outburst probability may also stem from the relatively small sample size on which the outburst probability formula is based.

3.6.5 Applicability of procedure

Assessments of moraine-dammed lake outburst hazard will always have considerable uncertainty due to the variety of possible trigger mechanisms, the numerous factors that affect the rate at which the breach enlarges, complex topographic and hydraulic controls on downstream flow processes, and the limited understanding of bulking processes. Examples provided by Huggel et al. (2004) and those in this paper demonstrate, however, that outburst flood hazard assessments based on remote sensing can provide reasonable preliminary evaluations of outburst probability and magnitude. In addition to being systematic and practical, my assessment procedure is objective and thus yields reproducible results.

My motivation for developing a hazard assessment method for moraine-dammed lakes is to facilitate prioritization of potentially hazardous lakes for subsequent field investigation. Currently, analysts address outburst flood hazard in one of two ways during preliminary hazard assessments: (1) they assume that all moraine-dammed lakes are equally hazardous, thereby requiring expensive, time-consuming, and unnecessary field investigations at a later stage in the project; or (2) they recognize and report that certain moraine-dammed lakes are more hazardous than others, but, depending on the expertise of the analyst, are unsure how to assess the hazard so that the findings can be incorporated into engineering designs. Engineers and geoscientists without training in glacier hazard analysis may even be unaware that moraine dams can fail catastrophically. Using my assessment procedure, analysts with only basic skills in aerial photograph interpretation and geomorphology can rapidly estimate regional outburst flood hazard.

My assessment procedure is based on observations of drained and undrained moraine-dammed lakes in the southern Coast Mountains of British Columbia (Fig. 3-1). Strictly speaking, it should only be applied to lakes within this region, although follow-up studies may justify its use in neighbouring watersheds or in regions with similar physiography and moraine dam morphologies. Direct application of the outburst probability formula to the Himalayas and Andes is inappropriate. The Himalayas, unlike the Coast Mountains, have local relief greater than 4000 m; its moraine dams are extraordinarily large; and its lakes commonly originate through coalescence of supraglacial ponds (Richardson and Reynolds, 2000). Different mechanisms may be responsible for the catastrophic failure of such moraine dams. The methodologies used in this study can be used to generate a region-specific model for evaluating outburst probability. The channel debris yield rates of Hungr et al. (1984) (Table 3-2) are based only on observations from debris flows in southwestern British Columbia, thus their applicability to other mountainous regions with different climates, geology, and vegetation is uncertain and may be scale-dependent.

3.7 Conclusion

Outburst floods from moraine-dammed lakes pose a significant hazard, necessitating at least a preliminary hazard assessment. Greater development downslope of glacierized mountains in British Columbia will increase the likelihood of economic losses and loss of life from outburst events. Engineers and geoscientists may be required to complete regional hazard assessments and feasibility studies in remote areas where this hazard exists.

Existing methods for assessing outburst flood hazard are inconsistent, subjective, and may require expensive field investigations. To estimate outburst magnitude, analysts must currently choose, sometimes arbitrarily, from a large selection of empirical relations, which may or may not be applicable to their project areas. Further, until recently, only qualitative and subjective methods existed for evaluating outburst flood probability.

Appropriate methods for making rapid preliminary assessments of outburst flood hazard must be objective, practical, and comprehensive. I propose a stepwise procedure based on observations acquired from remote sensing imagery to estimate outburst peak discharge, maximum volume, maximum travel distance, maximum area of debris inundation, and outburst probability. My assessment scheme, which yields reproducible results, is designed specifically for moraine-dammed lakes in southwestern British Columbia. It allows engineers and geoscientists to remotely prioritize lakes for further field-based study.

CHAPTER 4:

CONCLUSION

Outburst floods from moraine-dammed lakes are rare, but their destructive potential is so great that systematic methods for assessing downstream flood hazard are needed for the safe development of glacierized regions. Engineers and geoscientists are faced with the challenge of predicting the likelihood of catastrophic lake drainage and the size of the resulting flood without objective guidelines and data required for a reliable assessment. This chapter summarizes proposed hazard assessment methods that will help make evaluations of outburst flood hazard in southwestern British Columbia more objective, consistent, and less expensive. It also highlights the significance and limitations of this research and makes recommendations for further research.

4.1 Estimating outburst probability

Data were collected from 175 moraine-dammed lakes in the southern Coast Mountains of British Columbia to facilitate statistical analysis of differences between *drained* and *undrained* lakes. Using logistic regression, I generated an expression with four remotely measured predictor variables, from which the outburst probability of a particular lake can be estimated. Drained moraine-dammed lakes are best discriminated from undrained lakes by their moraine height-to-width ratio, presence/absence of an ice core in the moraine, lake area, and main rock type forming the moraine. The model is based on a relatively small sample, but its overall predictive accuracy is 88%. It enables analysts with basic knowledge of geomorphology and photogrammetry to complete hazard assessments of moraine-dammed lakes in southwestern British Columbia.

4.2 Completing outburst flood hazard assessments

Existing approaches for outburst flood hazard assessments are unsystematic and subjective. I provide an objective procedure for making comprehensive preliminary assessments of the hazard posed by moraine-dammed lakes in southwestern British Columbia. The procedure is based on analysis of aerial photographs and yields order-of-magnitude estimates of outburst peak discharge, maximum volume, maximum travel distance, maximum area of inundation, and probability. I incorporate existing empirical relations that are applicable to the study area and demonstrate the application of the procedure with three case studies. The reasonable retrospective evaluation of the outburst flood from Klattasine Lake indicates that the likelihood and potential magnitude of future outburst events in the southern Coast Mountains can be predicted.

4.3 Significance and limitations

Identification of 175 moraine-dammed lakes in the southern Coast Mountains of British Columbia highlights the need to assess the hazard posed by lakes whose catastrophic drainage could impact humans. The inventory of moraine-dammed lakes includes their location (Appendix A), aerial photograph coverage (Appendix B), characteristics (Appendix C), and outburst flood hazard (Appendix D). A significant finding is that the outburst-generated debris flow from Klattasine Lake in the early 1970s had a larger volume, travel distance, and area of inundation than predicted for all other analyzed moraine-dammed lakes in southwestern British Columbia. This result suggests that the Klattasine event may be an approximate upper limit of outburst-generated debris flow magnitude in the region. No other lake comparable in size to Klattasine Lake is perched so high on a valley side and drains through such a long, steep, V-shaped canyon, confined on both sides by talus slopes.

The frequency of catastrophic moraine dam failures at a mountain range scale is important in regional hazard assessments. Based on historical records of 33 outburst floods from moraine-dammed lakes, Richardson and Reynolds (2000) demonstrate that the frequency of events since the 1930s has been increasing in the Himalayas. The frequency of outburst flooding from moraine-dammed lakes in the southern Coast Mountains of British Columbia, however, has been relatively constant. Based on interpretation of aerial photographs, which have been available for the study area since the late 1940s, one to two outburst floods have occurred each decade. Interestingly, the magnitudes of these events exhibit an upward trend. The two most recent outburst floods, from Nostetuko Lake in 1983 (Blown and Church, 1985) and Queen Bess Lake in 1997 (Kershaw et al., 2005), had peak discharges several times higher than all previously documented outbursts in the study area.

The absence of all glacier-related candidate predictor variables in the outburst probability model and presence of the main rock type forming the moraine dam suggest that current hazard assessments may be placing too much emphasis on a lake's topographic setting and not enough on the moraine dam itself. The physical properties of a moraine dam, including sedimentology and morphology, strongly influence its potential for catastrophic failure. Therefore, field investigations will always be required during more detailed stages of hazard assessment.

The proposed hazard assessment procedure provides engineers and geoscientists with a practical tool for making preliminary assessments of outburst flood hazard from moraine-dammed lakes in southwestern British Columbia. Unlike existing methods, my statistical approach makes estimation objective, enables analysts with basic geomorphology and photogrammetry skills to perform assessments, yields reproducible and comparable results, and can be adjusted to suit different applications. Because the entire assessment scheme may be completed using aerial photographs, users will be able to incorporate evaluation of outburst flood hazard into routine hazard assessments of glacierized regions.

The dependency of the assessment procedure on aerial photographs means that it can only be used in regions with large-scale (~1:15 000) photograph coverage. In addition, qualitative and quantitative measurements made on aerial photographs have several possible sources of error, the most serious of which is misinterpretation of whether a particular moraine dam failed catastrophically or eroded gradually.

The applicability of the proposed assessment procedure is limited by the small sample on which it is based. The absence of moraine dams composed of metamorphic rock, for example, leads to erroneous estimates of outburst probability for moraine dams formed of metamorphic rock debris. Once its limitations have been acknowledged, the procedure should only be applied to lakes within the population from which the sample was taken, in this case southwestern British Columbia. Furthermore, it should only be used in preliminary assessments because the empirical relations are based on relatively few events. While the approach recommended in this study is unlikely to change, specific thresholds and coefficient values may be revised as more data become available.

4.4 Recommendations for further research

Development of the statistical model for discriminating drained from undrained lakes, based on lake, dam, glacier, and basin variables, is a first step towards quantifying outburst probability. However, the model's predictive capability and spatial applicability could be increased by expanding the statistical database. Bootstrap resampling (Austin and Tu, 2004) should be performed to determine whether the predictor variables in the final expression are actually true independent predictors of outburst probability.

Additional new candidate predictor variables may also improve the model. Glacier aspect, which was removed from a preliminary list of candidate predictor variables because other variables better quantified glacier instability and thus a lake's susceptibility to ice avalanches (Table 2-1), has been reconsidered as a candidate predictor variable. South-facing glaciers may be more readily destabilized than north-facing glaciers due to more extreme diurnal temperature variations and higher subglacial meltwater flows. Subsequent attempts to improve the model by adding new candidate predictor variables and redoing the statistical analysis have been left for follow-up studies.

The outburst probability model has not been tested on an independent sample of lakes. Because the entire population of moraine-dammed lakes larger than one hectare in the study area was used to generate the statistical model, the model should be tested on neighbouring watersheds with similar physiography and moraine dam morphologies.

Evaluating the applicability of the model to other glacierized mountain ranges, such as the Swiss Alps, is also recommended.

The large number of factors that influence flow in steep channels inhibits understanding of, and the ability to predict, sediment entrainment rates. Detailed studies of debris yield rates in channels in southwestern British Columbia could improve estimates of outburst-generated debris flow volume.

The data summarized in Appendices A-D provide an opportunity for a variety of research projects. One could evaluate spatial relations or trends of moraine-dammed lake characteristics that might aid regional hazard assessments. Identifying any features that are common to all drained lakes in a particular area, for example, could provide further insight into failure mechanisms. The identification of watersheds in which hazardous lakes are concentrated may be useful in the preliminary planning stages of linear infrastructure projects. A study of how moraine-dammed lakes and their outburst flood hazard evolve could provide additional insight into the factors that control moraine dam failure.

The outburst probability model indicates whether a moraine dam is likely or unlikely to fail catastrophically, but it provides no indication of the period within which failure may occur. With enough data on lake longevity, it might be possible to generate a statistical expression for predicting, within broad bounds, the time of the failure of a dam of known age.

REFERENCES

Alean, J., 1985. Ice avalanches: some empirical information about their formation and reach. Journal of Glaciology 31, 324-333.

Anglin, F.M., Wetmiller, R.J., Horner, R.B., Rogers, G.C., Drysdale, J.A., 1990. Seismicity Map of Canada. Geological Survey of Canada. Canadian Geophysical Atlas, Map 15, scale 1:10 000 000.

Austin, P.C., Tu, J.V., 2004. Bootstrap methods for developing predictive models. The American Statistician 58, 131-137.

Avery, T.E, Berlin, G.L., 1985. Interpretation of Aerial Photographs. Burgess Publishing Company, Minneapolis, MN, 554 pp.

Begueria, S., Lorente, A., 2002. Landslide hazard mapping by multivariate statistics: comparison of methods and case study in the Spanish Pyrenees. Debrisfall Assessment in Mountain Catchments for Local End-users. http://damocles.irpi.cnr.it/docs/reports/df_modelling.pdf (last visit May 26, 2005).

Blachut, S.P., Ballantyne, C.K., 1976. Ice-dammed lakes: a critical review of their nature and behaviour. Discussion Paper 6, Hamilton, Ontario, Department of Geography, McMaster University.

Blown, I., Church, M., 1985. Catastrophic lake drainage within the Homathko River basin, British Columbia. Canadian Geotechnical Journal 22, 551-563.

Bovis, M.J., Jakob, M. 1999. The role of debris supply to determine debris flow activity in southwestern B.C. Earth Surface Processes and Landforms 24, 1039-1054.

Canadian National Committee for the International Hydrological Decade, 1978. Hydrological Atlas of Canada. Fisheries and Environment Canada, Ottawa, ON, 7 pp.

Chen, C., Wang, T., Zhang, Z., Liu, Z., 1999. Glacial lake outburst floods in upper Nainchu River Basin, Tibet. Journal of Cold Regions Engineering 13, 199-212.

Clague, J.J., Evans, S.G., 1992. A self-arresting moraine dam failure, St. Elias Mountains, British Columbia. In: Current Research, Part A. Geological Survey of Canada Paper 92-1A, 185-188.

Clague, J.J., Evans, S.G., 1994. Formation and failure of natural dams in the Canadian Cordillera. Geological Survey of Canada Bulletin 464, 35 pp.

Clague, J.J., Evans, S.G., 2000. A review of catastrophic drainage of moraine-dammed lakes in British Columbia. Quaternary Science Reviews 19, 1763-1783.

Clague, J.J., Mathews, W.H., 1992. The sedimentary record and Neoglacial history of Tide Lake, northwestern British Columbia. Canadian Journal of Earth Sciences 29, 2383-2396.

Clague, J.J., Evans, S.G., Blown, I.G., 1985. A debris flow triggered by the breaching of a moraine-dammed lake, Klattasine Creek, British Columbia. Canadian Journal of Earth Sciences 22, 1492-1502.

Corominas, J., 1996. The angle of reach as a mobility index for small and large landslides. Canadian Geotechnical Journal 33, 260-271.

Costa, J.E., 1988. Rheologic, geomorphic, and sedimentologic differentiation of water floods, hyperconcentrated flows, and debris flows. In: Baker, V.R., Kochel, R.C., and Patton, P.C. (Eds.), Flood Geomorphology, John Wiley & Sons, Inc., New York, 113-122.

Costa, J.E., Schuster, R.L., 1988. The formation and failure of natural dams. Geological Society of America Bulletin 100, 1054-1068.

Dai, F.C., Lee, C.F., 2003. A spatiotemporal probabilistic modelling of storm-induced shallow landsliding using aerial photographs and logistic regression. Earth Surface Processes and Landforms 28, 527-545.

Dillon, W.R., Goldstein, M. 1984. Multivariate Analysis: Methods and Applications. John Wiley & Sons, New York, 587 pp.

Ding, Y., Liu, J., 1992. Glacier lake outburst flood disasters in China. Annals of Glaciology 16, 180-184.

Evans, S.G., 1987. The breaching of moraine-dammed lakes in the southern Canadian Cordillera. Proceedings, International Symposium on Engineering Geological Environment in Mountainous Areas, Beijing, 2, 141-150.

Fell, R., 1994. Landslide risk assessment and acceptable risk. Canadian Geotechnical Journal 31, 261-272.

Fread, D.L., 1996. Dam-breach floods. In: Singh, V.P. (Ed.), Hydrology of Disasters, Water Science and Technology Library, Volume 24, Dordrecht, Kluwer Academic Publishing, 85-126.

Goldsmith, W. 1998. Soil reinforcement by river plants: progress results. Proceedings of the Wetland Engineering and River Restoration Conference 1998, American Society of Civil Engineers. Washington DC, 7 pp.

Griswold, J.P., 2004. Mobility Statistics and Hazard Mapping for Non-Volcanic Debris Flows and Rock Avalanches. Unpublished Masters thesis. Portland State University, Portland.

Grove, J.M., 1988. Little Ice Age. Methuen, London, 498 pp.

Haeberli, W., 1983. Frequency and characteristics of glacier floods in the Swiss Alps. Annals of Glaciology 4, 85-90.

Haeberli, W., Kääb, A., Vonder Mühll, D., Teysseire, P., 2001. Prevention of outburst floods from periglacial lakes at Gruben Glacier, Valais, Swiss Alps. Journal of Glaciology 47, 111-122.

Hagen, V.K., 1982. Re-evaluation of design floods and dam safety. Transactions, 14th International Congress on Large Dams, Rio de Janeiro 1, 475-491.

Hanley, J.A., McNeil, B.J., 1982. The meaning and use of the area under a receiver operating characteristic (ROC) curve. Radiology 143, 29-36.

Hosmer, D.W., Lemeshow, S., 2000. Applied Logistic Regression. John Wiley & Sons, New York, 375 pp.

Huggel, C., Haeberli, W., Kaab, A., Bieri, D., Richardson, S., 2004. An assessment procedure for glacial hazards in the Swiss Alps. Canadian Geotechnical Journal 41, 1068-1083.

Huggel, C., Kaab, A., Haeberli, W., Krummenacher, B., 2003. Regional-scale GIS-models for assessment of hazards from glacier lake outbursts: evaluation and application in the Swiss Alps. Natural Hazards and Earth System Sciences 3, 1-16.

Huggel, C., Kaab, A., Haeberli, W., Teysseire, P., Paul, F., 2002. Remote sensing based assessment of hazards from glacier lake outbursts: A case study in the Swiss Alps. Canadian Geotechnical Journal 39, 316-330.

Hungr, O., Evans, S.G., Bovis, M.J., Hutchinson, J.N., 2001. A review of the classification of landslides of the flow type. Environmental and Engineering Geoscience 7, 221-238.

Hungr, O., McDougall, S., Bovis, M.J., 2005. Entrainment of material by debris flows. In: Jakob, M., Hungr, O. (Eds.), Debris-flow Hazards and Related Phenomena, Praxis, Springer Verlag, Berlin, Heidelberg, 135-158.

Hungr, O., Morgan, G.C., Kellerhals, R., 1984. Quantitative analysis of debris torrent hazards for design of remedial measures. Canadian Geotechnical Journal 21, 663-677.

Ikeya, H., 1979. Introduction to Sabo Works: The Preservation of Land against Sediment Disaster (first English edition), The Japan Sabo Association, Tokyo, 168 pp.

Ikeya, H., 1981. A method of designation for area in danger of debris flow. Erosion and Sediment Transport in Pacific Rim Steeplands (IAHS Publication No. 132), International Association of Hydrological Sciences, Wallingford, UK, 576-588.

Jakob, M., 2005a. A size classification for debris flows. Engineering Geology 79, 151-161.

Jakob, M., 2005b. Debris-flow hazard analysis. In: Jakob, M., Hungr, O. (Eds.), Debris-flow Hazards and Related Phenomena, Praxis, Springer Verlag, Berlin, Heidelberg, 411-443.

Jakob, M., Hungr, O., Thomson, B., 1997. Two debris flows with anomalously high magnitude. In: Chen, C-L. (Ed.), Debris-flow Hazards Mitigation: Mechanics, Prediction and Assessment: Proceedings of the 1st International Conference, American Society of Civil Engineers, American Society of Civil Engineers, New York, 382-394.

Jordan, P., 1987. Terrain Hazards and River Channel Impacts in the Squamish and Lillooet Watersheds, British Columbia. Unpublished report, prepared for the Geological Survey of Canada.

Kattelmann, R., 2003. Glacial lake outburst floods in the Nepal Himalaya: A manageable hazard? Natural Hazards 28, 145-154.

Kellerhals, R., 1970. Runoff routing through steep channels. ASCE Journal of the Hydraulics Division 96, 2201-2217.

Kershaw, J.A., Clague, J.J., Evans, S.G., 2005. Geomorphic and sedimentological signature of a two-phase outburst flood from moraine-dammed Queen Bess Lake, British Columbia, Canada. Earth Surface Processes and Landforms 30, 1-25.

King, G., Zeng, L., 2001. Logistic regression in rare events data. Political Analysis 9, 137-163.

King, J., 1996. Tsing Shan Debris Flow (Special Project Report SPR 6/96). Geotechnical Engineering Office, Hong Kong Government, 133 pp.

Laenen, A., Scott, K.M., Costa, J.E., Orzol, L.L., 1987. Hydrologic hazards along Squaw Creek from a hypothetical failure of the glacial moraine impounding Carver Lake near Sisters, Oregon. U.S. Geological Survey Open-File Report 87-41, 48 pp.

Lancaster, S.T., Hayes, S.K., Grant, G.E., 2003. Effects of wood on debris flow runout in small mountain watersheds. Water Resources Research 39, 1168, doi:10.1029/2001WR001227, 21 pp.

Lillesand, T.M., Kiefer, R.W., 2000. Remote Sensing and Image Interpretation. John Wiley & Sons, New York, 724 pp.

Lliboutry, L., Morales Arno, B., Pautre, A., Schneider, B., 1977. Glaciological problems set by the control of dangerous lakes in Cordillera Blanca, Peru. I. Historical failures of morainic dams, their causes and prevention. Journal of Glaciology 18, 239-254.

Lu, R., Tang, B., Li, D., 1987. Debris flow of the outbursts of the terminal moraine lakes in Tibet. World of Mountains 7, 2-9.

MacDonald, T.C., Langridge-Monopolis, J., 1984. Breaching characteristics of dam failures. ASCE Journal of Hydraulic Engineering 110, 567-586.

Massey, N.W.D., MacIntyre, D.G., Desjardins, P.J., Cooney, R.T., 2005. Digital Map of British Columbia: Tile NM10 Southwest B.C., B.C. Ministry of Energy and Mines, GeoFile 2005-3, http://webmap.em.gov.bc.ca/mapplace/minpot/bcgs.cfm.

Mathews, W.H. 1989. Development of Cordilleran landscape during the Quaternary. In: Chapter 1 of Quaternary Geology of Canada and Greenland, R.J. Fulton (Ed.). Geological Survey of Canada, Geology of Canada, 1, 32-34.

Matthes, F.E., 1939. Report of Committee on Glaciers. American Geophysical Union Transactions 20, 518-523.

Monger, J.W.H., Journeay, J.M., 1994. Guide to the geology and tectonic evolution of the southern Coast Mountains. Geological Survey of Canada Open File 2490, 77 pp.

O'Connor, J.E., Hardison, J.H., Costa, J.E., 2001. Debris flows from failures of neoglacial-age moraine dams in the Three Sisters and Mount Jefferson wilderness areas, Oregon. US Geological Survey Professional Paper 1606, 93 pp.

Ohlmacher, G.C., Davis, J.C., 2003. Using multiple logistic regression and GIS technology to predict landslide hazard in northeast Kansas, USA. Engineering Geology 69, 331-343.

Østrem, G., Arnold, K., 1970. Ice-cored moraines in southern British Columbia and Alberta. Geografiska Annaler 52A, 120-128.

Pagano, M., Gauvreau, K., 2000. Principles of Biostatistics. Duxbury, California, 525 pp.

Parrish, R.R., 1983. Cenozoic thermal evolution and tectonics of the Coast Mountains of British Columbia; 1. Fission track dating, apparent uplift rates, and patterns of uplift. Tectonics, 2, 601-631.

Pierson, T.C., 1995. Flow characteristics of large eruption-triggered debris flows at snow-clad volcanoes: Constraints for debris flow models. Journal of Volcanology and Geothermal Research 66, 283-294.

Pierson, T.C., 2005. Hyperconcentrated flow – transitional process between water flow and debris flow. In: Jakob, M., Hungr, O. (Eds.), Debris-flow Hazards and Related Phenomena, Praxis, Springer Verlag, Berlin, Heidelberg, 159-202.

Press, S.J., Wilson, S., 1978. Choosing between logistic regression and discriminant analysis. Journal of the American Statistical Association 73, 699-705.

Province of British Columbia, 2001. British Columbia Base Map, Ministry of Sustainable Resource Management, http://maps.gov.bc.ca/.

Quinn, G.P., Keough, M.S., 2002. Experimental Design and Data Analysis for Biologists. Cambridge University Press, Cambridge, 537 pp.

Reynolds, J.M., Dolecki, A., Portocarrero, C., 1998. The construction of a drainage tunnel as part of glacial lake hazard mitigation at Hualan, Cordillera Blanca, Peru. In: Maund, J.G., Eddleston, M. (Eds.), Geohazards in Engineering Geology, Geological Society Engineering Geology Special Publication 15, 41-48.

Richardson, S.D., Reynolds, J.M., 2000. An overview of glacial hazards in the Himalayas. Quaternary International 65/66, 31-47.

Rickenmann, D., Zimmermann, M., 1993. The 1987 debris flows in Switzerland: Documentation and analysis. Geomorphology 8, 175-189.

Ryder, J.M., 1991. Geomorphological processes associated with an ice-marginal lake at Bridge Glacier, British Columbia. Géographie physique et Quaternaire 45, 35-44.

Ryder, J.M., 1998. Geomorphological processes in the alpine areas of Canada: The effects of climate change and their impacts on human activities. Geological Survey of Canada Bulletin 524, 44 pp.

Ryder, J.M., Thomson, B., 1986. Neoglaciation in the southern Coast Mountains of British Columbia: Chronology prior to the late Neoglacial maximum. Canadian Journal of Earth Sciences 23, 273-287.

SAS Institute Inc., 2003. JMP: The Statistical Discovery Software for Windows, Release 5.0.1.2. SAS Institute Inc., JMP Software, Cary, NC.

Scheidegger, A.E., 1973. On the prediction of the reach and velocity of catastrophic landslides. Rock Mechanics 5, 231-236.

Singerland, R., Voight, B., 1982. Evaluating hazard of landslide-induced water waves. Journal of the Waterway, Port, Coastal and Ocean Division 108, 504-512.

USGS, 2002. Pacific Northwest seismic hazard map. United States Geological Survey, http://earthquake.usgs.gov/hazmaps/products_data/2002/2002October/PN/PNpga500v3.pdf.

Vuichard, D., Zimmerman, M., 1987. The catastrophic drainage of a moraine-dammed lake, Khumbu Himal, Nepal: Cause and consequences. Mountain Research and Development 7, 91-110.

Walder, J.S., O'Connor, J.E., 1997. Methods for predicting peak discharges of floods caused by failure of natural and constructed earthen dams. Water Resources Research 33, 2337-2348.

Watanabe, T., Ives, J.D., Hammond, J.E., 1994. Rapid growth of a glacier lake in Khumbu Himal, Nepal: Prospects for a catastrophic flood. Mountain Research and Development 14, 329-340.

Waythomas, C.F., Walder, J.S., McGimsey, R.G., Neal, C.A., 1996. A catastrophic flood caused by drainage of a caldera lake at Aniakchak Volcano, Alaska, and implications for volcanic-hazards assessment. Geological Society of America Bulletin 108, 861-871.

Wong, H.N., Ho, K.K.S., Chan, Y.C., 1997. Assessment of consequences of landslides. In: Fell, R., Cruden, D.M. (Eds.), Proceedings of the Landslide Risk Workshop, A.A. Balkema, Rotterdam, 111-126.

Yamada, T., 1998. Glacier lake and its outburst flood in the Nepal Himalaya. Japanese Society of Snow and Ice, Data Centre for Glacier Research Monograph No. 1, 96 pp.

Yesenov, U.Y., Degovets, A.S., 1979. Catastrophic mudflow on the Bol'shaya Almatinka River in 1977. Soviet Hydrology: Selected Papers 18, 158-160.

APPENDICES

Appendix A. Locations of moraine-dammed lakes in study region

		Longitude[b]			Latitude					Dam	
No.	Lake[a]	Deg	Min	Sec	Deg	Min	Sec	TRIM[c]	Elev. (m)[d]	type[e]	Outburst date
1	"Doran"	124	36	55	51	15	19	092N027	1870	1	N/A
2	"Queen Bess"	124	30	52	51	15	12	092N028	1699	2	Aug. 12, 1997
3	Nostetuko	124	24	38	51	12	23	092N018	1630	1	July 19, 1983
4	"Nostetuko Adjacent"	124	24	50	51	12	9	092N028	1649	1	N/A
5	Frobisher	124	25	21	51	11	40	092N018	1722	3	N/A
6	"East Fork Nostetuko"	124	24	7	51	14	44	092N028	1875	3	N/A
7	"Treadcroft Head"	124	18	35	51	15	1	092N029	2090	2	N/A
8	"Girdwood Head"	124	17	15	51	17	42	092N029	2330	1	N/A
9	"Stikelan"	124	21	33	51	18	57	092N039	2090	2	N/A
10	"Mt. Queen Bess E"	124	32	3	51	17	11	092N028	1818	3	N/A
11	"Stonsayako Head"	124	34	38	51	19	1	092N038	1932	3	N/A
12	"Elliot Creek East"	124	35	27	50	56	23	092K098	1377	3	N/A
13	"Elliot Creek Head"	124	36	50	50	57	9	092K097	756	3	N/A
14	"Gilbert"	124	10	51	50	55	0	092K100	2024	1	July 29, 1965 - Sept. 11, 1977
15	"Ramose"	123	58	43	50	59	35	092J091	1977	1	N/A
16	"Sparks"	124	18	9	51	1	50	092N009	1815	2	N/A
17	"Windscoop Glacier"	124	8	30	51	3	29	092N010	1697	3	N/A
18	"Chilko Glacier"	124	3	51	51	3	17	092N010	1795	3	N/A
19	Altruist	123	56	13	51	4	9	092O001	2154	2	N/A
20	"Landmark"	124	54	10	51	8	36	092N016	1307	2	N/A
21	"Allaire"	124	21	31	51	7	35	092N019	1870	1	N/A
22	"Nine Mile"	124	21	47	51	10	24	092N019	1805	2	N/A
23	"Mount Jewakwa"	124	53	49	51	9	48	092N016	1410	1	N/A
24	"Klattasine"	124	55	7	51	10	39	092N016	1667	1	June 1971 - Sept. 1973
25	"Mount Whitton"	124	16	55	51	20	43	092N039	2187	3	N/A
26	"Tredcroft West"	124	15	12	51	14	11	092N029	2017	2	N/A
27	"Duff Island"	124	1	49	51	22	3	092N040	2215	2	N/A
28	"Robertson East"	123	57	48	51	22	23	092O031	1999	2	N/A
29	"Robertson West"	123	58	59	51	22	23	092O031	1973	1	N/A
30	"Over Robertson Divide"	123	57	1	51	21	42	092O031	2225	1	N/A

Appendix A (continued)

No.	Lake[a]	Longitude[b] Deg	Min	Sec	Latitude Deg	Min	Sec	TRIM[c]	Elev. (m)[d]	Dam type[e]	Outburst date
31	"W Mt. Tatlow"	123	55	28	51	22	43	092O031	2121	2	N/A
32	"Tsoloss West"	123	48	23	51	22	7	092O031	2150	1	N/A
33	"Tsoloss East"	123	47	32	51	21	37	092O032	2257	1	N/A
34	"SW Mt. Tatlow W"	123	57	7	51	19	21	092O031	1977	2	N/A
35	"SW Mt. Tatlow E"	123	56	23	51	19	27	092O031	2060	1	N/A
36	"Olson"	123	51	59	51	16	3	092O021	2038	1	N/A
37	"East Olson Small"	123	50	11	51	16	5	092O021	2187	2	N/A
38	"East Olson Large"	123	49	41	51	16	1	092O021	2268	2	N/A
39	"Dill Dill Plateau"	123	13	10	51	11	51	092O014	2319	1	N/A
40	"West RCAF East"	123	46	41	51	9	30	092O012	2291	2	N/A
41	"RCAF Small"	123	44	1	51	10	30	092O012	2258	2	N/A
42	"RCAF Large"	123	42	46	51	11	3	092O012	2367	2	N/A
43	"Battlement North"	123	19	42	51	8	37	092O014	2123	2	N/A
44	"SW Spectrum Peak"	123	52	55	51	7	55	092O011	2377	1	N/A
45	"West RCAF Middle"	123	47	53	51	9	17	092O012	2136	2	N/A
46	"West RCAF West"	123	49	32	51	9	39	092O011	2231	2	N/A
47	"Powell Head"	123	17	10	51	8	24	092O014	2354	1	N/A
48	"Iron Pass"	123	15	46	51	7	26	092O014	2272	1	N/A
49	"Tosh"	123	16	17	51	8	45	092O014	2265	2	N/A
50	"East Granite"	123	20	49	51	3	30	092O004	2137	1	Before July 2, 1949
51	"W Granite Weird Outlet"	123	26	44	51	2	59	092O003	2335	1	N/A
52	"W Granite Camp"	123	25	56	51	2	39	092O003	2227	2	N/A
53	"S McClure"	123	28	27	51	3	52	092O003	2225	2	N/A
54	"North Griswold Pass"	123	24	44	51	0	31	092O003	1950	2	N/A
55	"South Griswold Pass"	123	23	28	50	59	47	092J094	1990	1	N/A
56	"Griswold E Fork Head"	123	21	27	50	59	30	092J094	2258	1	N/A
57	"Perry"	123	36	26	50	56	44	092J092	2162	1	N/A
58	"Lord Glacier Snout E"	123	39	58	50	55	4	092J092	2070	1	N/A
59	"Tait"	123	39	20	50	55	13	092J092	2153	1	N/A
60	"Bridge Glacier Snout"	123	29	52	50	50	22	092J083	1388	2	N/A

Appendix A (continued)

		Longitude[b]			Latitude					Dam	
No.	Lake[a]	Deg	Min	Sec	Deg	Min	Sec	TRIM[c]	Elev. (m)[d]	type[e]	Outburst date
61	"Scherle"	123	11	29	50	52	3	092J085	2178	1	N/A
62	"South Slim West"	123	4	3	50	53	50	092J085	2158	1	N/A
63	"South Slim Middle"	123	3	9	50	53	28	092J085	2018	3	N/A
64	"South Slim East"	123	1	44	50	53	20	092J085	2162	2	N/A
65	"Bridge"	123	29	28	50	49	27	092J083	1502	1	1964 - 1970
66	"Athelstan"	123	22	49	50	42	49	092J074	1515	2	N/A
67	"Tzela"	124	44	59	50	25	3	092K047	935	1	N/A
68	"Sessel"	123	11	4	50	40	26	092J065	1735	1	N/A
69	"Boomerang"	123	9	10	50	38	42	092J065	1759	2	N/A
70	"Sampson"	123	7	14	50	38	17	092J065	1465	3	N/A
71	"East Grouty"	122	59	25	50	38	0	092J066	1970	1	Before Sept. 28, 1947
72	"West Grouty"	123	0	24	50	37	22	092J065	1998	2	N/A
73	"Noel"	122	51	32	50	38	10	092J066	1965	3	N/A
74	"Overseer"	123	25	23	50	30	53	092J053	1797	2	N/A
75	"South"	123	17	53	50	31	14	092J054	1908	2	N/A
76	"Ryan Head NW"	123	24	7	50	27	38	092J044	1407	2	N/A
77	"Elaho Upper"	123	39	53	50	29	0	092J042	1691	1	N/A
78	"Peterson West"	123	11	11	50	23	23	092J035	1533	2	N/A
79	"NW Wasp"	123	4	14	50	23	15	092J035	1500	3	N/A
80	"N Miller Small"	123	1	16	50	23	15	092J035	1755	2	N/A
81	"N Miller Large"	122	59	51	50	23	16	092J036	1365	3	N/A
82	"Bishop Tributary"	123	57	54	50	49	32	092J081	1252	1	N/A
83	"Bishop Glacier Snout"	123	56	2	50	48	51	092J081	1287	2	N/A
84	"Southgate West"	124	36	19	50	47	13	092K077	1362	1	N/A
85	"Orford Lower"	124	35	37	50	45	17	092K078	1259	2	N/A
86	"Orford Upper"	124	33	55	50	45	39	092K078	1459	2	N/A
87	"Parabola"	124	30	10	50	44	54	092K078	1270	3	N/A
88	Icewall	124	24	55	50	45	2	092K078	918	3	N/A
89	"Pemberton Ice W Large"	123	30	24	50	21	10	092J033	1773	3	N/A
90	"Outlier"	122	41	31	50	1	9	092J007	1923	2	N/A

Appendix A (continued)

		Longitude[b]			Latitude					Dam	
No.	Lake[a]	Deg	Min	Sec	Deg	Min	Sec	TRIM[c]	Elev. (m)[d]	type[e]	Outburst date
91	"Orphan"	122	39	39	49	59	49	092G097	1496	2	N/A
92	"Adieu"	122	37	48	49	57	16	092G097	1578	2	N/A
93	"Tuwasus Upper"	122	39	6	49	53	47	092G087	1710	2	N/A
94	"Tuwasus Lower"	122	38	36	49	53	42	092G087	1560	1	N/A
95	"Greymantle"	122	35	43	49	53	56	092G098	1828	1	N/A
96	Hourglass	122	37	16	49	51	31	092G087	1459	2	N/A
97	Snowcap	122	36	57	49	51	55	092G087	1455	1	N/A
98	Lower Snowcap	122	38	35	49	51	50	092G087	1454	2	N/A
99	"Misty Upper"	122	35	37	49	48	7	092G088	1692	2	N/A
100	"Appa"	123	8	10	50	19	37	092J035	1400	3	N/A
101	"Exodus"	123	29	54	50	14	21	092J023	1975	1	N/A
102	"Dipper"	123	28	29	50	13	56	092J023	1558	2	N/A
103	"Soo Upper"	123	12	52	50	14	34	092J024	1624	2	N/A
104	"Soo Lower"	123	12	57	50	14	51	092J024	1619	1	Aug. 31, 1987 - Aug. 1, 1994
105	"Currie"	122	45	43	50	15	14	092J027	1652	1	N/A
106	Chaos	122	41	33	50	7	24	092J017	1367	1	N/A
107	"Ure"	122	42	29	50	9	45	092J017	1842	1	N/A
108	"Tremor"	122	48	53	50	4	48	092J006	1798	3	N/A
109	"NW Pantheon W"	125	27	11	51	43	19	092N073	1953	2	N/A
110	"NW Pantheon Et"	125	23	12	51	42	41	092N074	2048	2	N/A
111	"Niut"	124	33	43	51	39	44	092N068	2072	2	N/A
112	"Siva"	125	10	10	51	38	45	092N065	1687	3	N/A
113	"Sand"	125	4	14	51	37	40	092N065	2031	1	N/A
114	"S Tiedemann Large"	124	57	35	51	17	5	092N026	1559	2	N/A
115	"S Tiedemann Small"	124	57	17	51	17	13	092N026	1545	1	N/A
116	"Tiedemann Lateral S"	124	56	1	51	18	50	092N036	834	1	N/A
117	"Hidden"	125	6	55	51	6	38	092N015	1270	2	N/A
118	"Stanton"	125	20	16	51	4	11	092N004	1000	1	N/A
119	"Wahkash"	125	20	23	50	59	49	092K094	809	3	N/A
120	"Brew Head"	125	11	8	51	1	52	092N005	1004	1	N/A

Appendix A (continued)

No.	Lake[a]	Longitude[b] Deg	Min	Sec	Latitude Deg	Min	Sec	TRIM[c]	Elev. (m)[d]	Dam type[e]	Outburst date
121	"Brew South"	125	9	9	50	59	51	092K095	1487	2	N/A
122	"Blackhorn"	124	50	10	51	35	50	092N056	1628	2	N/A
123	"Five Finger"	124	52	47	51	33	12	092N056	2025	1	N/A
124	"Crazy"	125	8	7	51	33	15	092N055	1810	2	N/A
125	"Ottarasko Small"	124	37	56	51	31	4	092N057	2081	1	N/A
126	"Ottarasko Large"	124	41	50	51	30	31	092N057	2091	1	N/A
127	"Nude"	124	47	59	51	29	55	092N047	1603	2	N/A
128	"Oval"	125	15	3	51	28	58	092N044	1289	3	N/A
129	"Ottarasko Tributary"	124	40	35	51	28	20	092N047	1475	3	N/A
130	"Scimitar Snout"	125	9	39	51	28	20	092N045	941	2	N/A
131	"Scimitar Right Lateral"	125	11	43	51	27	52	092N045	1212	1	N/A
132	"Cataract Right Lateral"	125	7	52	51	26	24	092N045	1298	1	N/A
133	"Cataract Snout"	125	8	4	51	26	24	092N045	1175	2	N/A
134	"Success"	124	50	29	51	25	15	092N046	1443	3	N/A
135	"Tellot"	125	4	56	51	22	17	092N035	1656	2	N/A
136	Ephemeron	125	2	8	51	22	44	092N035	1034	3	N/A
137	"Tiedemann Lateral N"	124	56	15	51	20	0	092N036	779	1	N/A
138	"Remote"	125	34	33	51	28	12	092N043	1890	1	N/A
139	"Nahatlatch Head"	122	9	15	50	1	2	092J010	2150	1	N/A
140	"Rutledge Large"	122	1	32	50	6	28	092J020	1608	3	N/A
141	"Van Horlick"	122	17	56	50	16	38	092J029	2053	1	N/A
142	"White North"	122	36	43	50	23	5	092J037	1851	3	N/A
143	White South"	122	36	55	50	22	56	092J037	1861	2	N/A
144	"Sockeye South"	122	47	2	50	34	17	092J057	1870	3	N/A
145	"Downton Head"	122	17	31	50	32	0	092J059	2157	1	N/A
146	"Whitecap"	122	29	28	50	43	51	092J078	1925	2	N/A
147	"Surfusion"	123	7	21	50	44	29	092J075	2165	3	N/A
148	"Salal Large"	123	24	5	50	44	55	092J073	1623	2	N/A
149	"Athelney Pass"	123	21	53	50	46	37	092J074	1839	3	N/A
150	"Ochre"	123	23	16	50	48	14	092J084	2122	3	N/A

Appendix A (continued)

		Longitude[b]			Latitude					Dam	
No.	Lake[a]	Deg	Min	Sec	Deg	Min	Sec	TRIM[c]	Elev. (m)[d]	type[e]	Outburst date
151	"McParlon"	123	16	15	50	46	9	092J074	1516	2	N/A
152	"Vayu"	123	7	17	50	47	10	092J075	2088	3	N/A
153	"Truax Middle"	122	44	40	50	49	41	092J087	2290	2	N/A
154	"Truax West"	122	44	54	50	49	41	092J087	2292	2	N/A
155	"Truax East"	122	44	28	50	49	46	092J087	2261	2	N/A
156	"Enterprise"	121	58	29	50	35	43	092I051	2188	2	N/A
157	"Leckie Tributary"	123	12	29	50	56	58	092J094	2235	2	N/A
158	"Leckie South"	123	6	59	50	56	39	092J095	2353	1	Before July 21, 1949
159	"Copper"	123	11	32	50	58	17	092J095	2265	1	July 21, 1949 - July 25, 1964
160	"Gun Head"	123	9	10	50	59	47	092J095	2298	2	N/A
161	"Nichols"	123	23	12	50	58	2	092J094	1988	2	N/A
162	"Lepton"	123	23	25	50	58	36	092J094	2067	1	N/A
163	"Lord"	122	31	16	50	57	50	092J093	2082	3	N/A
164	"Griswold W Fork Head"	123	22	29	51	0	8	092O004	2158	2	N/A
165	"Granite Head"	123	24	39	51	2	0	092O003	2360	1	N/A
166	"E Fork Nostetuko Upper"	124	24	44	51	14	43	092N028	2018	3	N/A
167	"Deschamps Lower"	124	20	59	51	9	28	092N019	1745	1	N/A
168	"Tredcroft East"	124	15	0	51	14	13	092N029	2025	2	N/A
169	"East Olson Upper"	123	50	26	51	15	42	092O021	2427	2	N/A
170	"Elaho Lower"	123	39	47	50	29	24	092J042	1617	2	N/A
171	"Pemberton Ice W Small"	123	30	2	50	21	5	092J033	1780	3	N/A
172	"Lava Uppermost"	122	57	45	49	49	18	092G086	1521	2	N/A
173	"Sockeye Middle"	122	47	25	50	34	25	092J057	1990	1	N/A
174	"Sockeye North"	122	47	24	50	35	14	092J057	2024	1	N/A
175	"Lone Goat"	123	6	1	50	42	59	092J075	2046	3	N/A

[a] Lake names in quotations are unofficial, according to Terrain Resource Information Management (TRIM) maps (Province of British Columbia, 2001).
[b] West Longitude and North Latitude, in degrees (Deg), minutes (Min), and seconds (Sec).
[c] 1:20 000-scale Terrain Resource Information Management topographic map on which lake outlet is located.
[d] Approximate lake elevation (m), based on pre-outburst level for drained lakes, interpolated between 20 m contours if lake elevation not provided on TRIM map.
[e] 1 = "classic" narrow, sharp-crested moraine; 2 = broad, rounded moraine; 3 = low, indefinite moraine.

Appendix B. Aerial photograph coverage of moraine-dammed lakes in study region

							Frame 1		Frame 2	
No.	Lake[a]	Roll no.	Date	Scale[b]	Focal (mm)[c]	Film[d]	No.	Altitude[e] (m)	No.	Altitude[e] (m)
1	"Doran"	30BCC94083	23-Jul-94	1:15 000	302	colour	7	6549	8	6555
2	"Queen Bess"	30BCC94038	11-Jul-94	1:15 000	304	colour	94	6553	95	6553
3	Nostetuko	15BCC286	26-Jul-81	1:40 000	153	colour	13	8230	12	8230
4	"Nostetuko Adjacent"	30BCC94009	9-Jul-94	1:15 000	304	colour	18	6510	17	6504
5	Frobisher	30BCC94009	9-Jul-94	1:15 000	304	colour	18	6510	17	6504
6	"East Fork Nostetuko"	30BCC94038	11-Jul-94	1:15 000	304	colour	88	6553	89	6553
7	"Treadcroft Head"	30BCC94038	11-Jul-94	1:15 000	304	colour	82	6553	83	6553
8	"Girdwood Head"	30BCC94039	11-Jul-94	1:15 000	304	colour	120	6858	121	6858
9	"Stikelan"	30BCC94039	11-Jul-94	1:15 000	304	colour	207	6858	206	6858
10	"Mt. Queen Bess E"	30BCC94039	11-Jul-94	1:15 000	304	colour	133	6858	134	6858
11	"Stonsayako Head"	30BCC94039	11-Jul-94	1:15 000	304	colour	195	6858	194	6858
12	"Elliot Creek East"	30BCC03025	3-Sep-03	1:15 000	306	colour	16	8019	15	8019
13	"Elliot Creek Head"	30BCC03025	3-Sep-03	1:15 000	306	colour	16	8019	15	8019
14	"Gilbert"	30BCC03025	3-Sep-03	1:15 000	306	colour	53	8101	54	8101
15	"Ramose"	30BCC94031	10-Jul-94	1:15 000	304	colour	87	6925	86	6926
16	"Sparks"	30BCC03024	3-Sep-03	1:15 000	306	colour	157	8177	158	8177
17	"Windscoop Glacier"	30BCC94034	10-Jul-94	1:15 000	304	colour	56	6860	57	6866
18	"Chilko Glacier"	30BCC94034	10-Jul-94	1:15 000	304	colour	52	6859	53	6859
19	Altruist	15BCB01028	8-Sep-03	1:35 000	153	B&W	181	8089	182	8089
20	"Landmark"	30BCC94163	21-Sep-94	1:15 000	306	colour	98	5639	99	5639
21	"Allaire"	30BCC03023	3-Sep-03	1:15 000	306	colour	203	8432	202	8432
22	"Nine Mile"	30BCC94007	9-Jul-94	1:15 000	304	colour	92	6495	91	6497
23	"Mount Jewakwa"	30BCC94163	21-Sep-94	1:15 000	306	colour	96	5639	95	5639
24	"Klattasine"	30BCC94163	21-Sep-94	1:15 000	306	colour	95	5639	94	5639
25	"Mount Whitton"	30BCC94064	20-Jul-94	1:15 000	304	colour	200	6891	199	6893
26	"Tredcroft West"	30BCC94038	11-Jul-94	1:15 000	304	colour	79	6553	80	6553
27	"Duff Island"	30BCC94064	20-Jul-94	1:15 000	304	colour	81	6887	82	6887
28	"Robertson East"	30BCC94008	10-Jul-94	1:15 000	304	colour	51	6873	52	6868
29	"Robertson West"	30BCC94008	10-Jul-94	1:15 000	304	colour	52	6868	53	6858
30	"Over Robertson Divide"	30BCC94064	20-Jul-94	1:15 000	304	colour	77	6889	78	6887

Appendix B (continued)

							Frame 1		Frame 2	
No.	Lake[a]	Roll no.	Date	Scale[b]	Focal (mm)[c]	Film[d]	No.	Altitude[e] (m)	No.	Altitude[e] (m)
31	"W Mt. Tatlow"	30BCC94008	10-Jul-94	1:15 000	304	colour	49	6880	50	6877
32	"Tsoloss West"	30BCC97175	14-Aug-97	1:15 000	305	colour	156	6553	155	6553
33	"Tsoloss East"	30BCC97175	14-Aug-97	1:15 000	305	colour	157	6553	156	6553
34	"SW Mt. Tatlow W"	30BCC94148	21-Sep-94	1:15 000	304	colour	57	6810	58	6811
35	"SW Mt. Tatlow E"	30BCC94148	21-Sep-94	1:15 000	304	colour	57	6810	58	6811
36	"Olson"	30BCC94146	27-Aug-94	1:15 000	302	colour	73	6584	72	6582
37	"East Olson Small"	30BCC97205	20-Sep-97	1:15 000	306	colour	76	6553	77	6553
38	"East Olson Large"	30BCC97205	20-Sep-97	1:15 000	306	colour	76	6553	77	6553
39	"Dill Dill Plateau"	30BCC97193	9-Sep-97	1:15 000	305	colour	147	6553	148	6553
40	"West RCAF East"	30BCC97167	11-Aug-97	1:15 000	305	colour	77	6553	76	6553
41	"RCAF Small"	30BCC97194	9-Sep-97	1:15 000	305	colour	5	6553	6	6553
42	"RCAF Large"	30BCC97194	9-Sep-97	1:15 000	305	colour	4	6553	5	6553
43	"Battlement North"	30BCC97167	11-Aug-97	1:15 000	305	colour	57	6553	58	6553
44	"SW Spectrum Peak"	30BCC94007	9-Jul-94	1:15 000	304	colour	57	6471	58	6474
45	"West RCAF Middle"	30BCC97167	11-Aug-97	1:15 000	305	colour	76	6553	75	6553
46	"West RCAF West"	30BCC97167	11-Aug-97	1:15 000	305	colour	75	6553	74	6553
47	"Powell Head"	30BCC97167	11-Aug-97	1:15 000	305	colour	55	6553	56	6553
48	"Iron Pass"	30BCC97166	11-Aug-97	1:15 000	305	colour	75	6553	74	6553
49	"Tosh"	30BCC97167	11-Aug-97	1:15 000	305	colour	55	6553	56	6553
50	"East Granite"	30BCC97109	9-Aug-97	1:15 000	305	colour	27	6553	26	6553
51	"W Granite Weird Outlet"	30BCC97109	9-Aug-97	1:15 000	305	colour	22	6553	21	6553
52	"W Granite Camp"	30BCC97108	9-Aug-97	1:15 000	305	colour	181	6553	182	6553
53	"S McClure"	30BCC97109	9-Aug-97	1:15 000	305	colour	21	6553	20	6553
54	"North Griswold Pass"	30BCC97107	9-Aug-97	1:15 000	305	colour	176	6553	175	6553
55	"South Griswold Pass"	30BCC97107	9-Aug-97	1:15 000	305	colour	128	6706	127	6706
56	"Griswold E Fork Head"	30BCC97107	9-Aug-97	1:15 000	305	colour	125	6706	126	6706
57	"Perry"	30BCC97107	9-Aug-97	1:15 000	305	colour	70	6706	71	6706
58	"Lord Glacier Snout E"	30BCC97107	9-Aug-97	1:15 000	305	colour	44	7010	43	7010
59	"Tait"	30BCC97107	9-Aug-97	1:15 000	305	colour	44	7010	43	7010
60	"Bridge Glacier Snout"	30BCC97087	20-Jul-97	1:15 000	305	colour	21	6784	20	6788

Appendix B (continued)

No.	Lake[a]	Roll no.	Date	Scale[b]	Focal (mm)[c]	Film[d]	Frame 1 No.	Frame 1 Altitude[e] (m)	Frame 2 No.	Frame 2 Altitude[e] (m)
61	"Scherle"	30BCC97087	20-Jul-97	1:15 000	305	colour	37	6701	36	6712
62	"South Slim West"	30BCC97219	11-Aug-97	1:15 000	305	colour	141	6765	142	6761
63	"South Slim Middle"	30BCC97219	11-Aug-97	1:15 000	305	colour	141	6765	142	6761
64	"South Slim East"	30BCC97087	20-Jul-97	1:15 000	305	colour	82	6795	83	6806
65	"Bridge"	BC4245	24-Jul-64	1:15 000	305	B&W	34	6096	35	6096
66	"Athelstan"	30BCC97125	10-Aug-97	1:15 000	305	colour	191	6715	190	6710
67	"Tzela"	30BCC92083	21-Jun-92	1:10 000	304	colour	65	4726	66	4726
68	"Sessel"	30BCC97125	10-Aug-97	1:15 000	305	colour	39	6736	38	6729
69	"Boomerang"	30BCC97125	10-Aug-97	1:15 000	305	colour	27	6692	26	6692
70	"Sampson"	30BCC97125	10-Aug-97	1:15 000	305	colour	24	6696	25	6694
71	"East Grouty"	30BCC97089	10-Aug-97	1:15 000	305	colour	104	6751	103	6750
72	"West Grouty"	30BCC97089	10-Aug-97	1:15 000	305	colour	104	6751	103	6750
73	"Noel"	30BCC97125	10-Aug-97	1:15 000	305	colour	11	6714	12	6714
74	"Overseer"	30BCC94164	21-Sep-94	1:15 000	306	colour	113	6248	114	6248
75	"South"	30BCC94117	28-Jul-94	1:15 000	306	colour	102	6248	101	6248
76	"Ryan Head NW"	30BCC94118	1-Aug-94	1:15 000	306	colour	85	6248	86	6248
77	"Elaho Upper"	30BCC94164	21-Sep-94	1:15 000	306	colour	94	6248	93	6248
78	"Peterson West"	30BCC94119	1-Aug-94	1:15 000	306	colour	89	6248	90	6248
79	"NW Wasp"	30BCC94119	1-Aug-94	1:15 000	306	colour	83	6248	84	6248
80	"N Miller Small"	30BCC94119	1-Aug-94	1:15 000	306	colour	79	6248	80	6248
81	"N Miller Large"	30BCC94119	1-Aug-94	1:15 000	306	colour	78	6248	79	6248
82	"Bishop Tributary"	30BCC03026	4-Sep-03	1:15 000	306	colour	66	8063	67	8063
83	"Bishop Glacier Snout"	30BCC03026	4-Sep-03	1:15 000	306	colour	66	8063	67	8063
84	"Southgate West"	30BCC92034	23-Jun-92	1:10 000	304	colour	189	4726	190	4726
85	"Orford Lower"	30BCC92034	23-Jun-92	1:10 000	304	colour	178	4726	177	4726
86	"Orford Upper"	30BCC92034	23-Jun-92	1:10 000	304	colour	106	4878	107	4878
87	"Parabola"	30BCC03026	4-Sep-03	1:15 000	306	colour	234	7744	233	7744
88	Icewall	30BCC03026	4-Sep-03	1:15 000	306	colour	239	7744	238	7744
89	"Pemberton Ice W Large"	30BCC94160	18-Sep-94	1:15 000	306	colour	101	6248	100	6248
90	"Outlier"	15BCB96099	27-Sep-96	1:40 000	153	B&W	109	8664	110	8659

Appendix B (continued)

							Frame 1		Frame 2	
No.	Lake[a]	Roll no.	Date	Scale[b]	Focal (mm)[c]	Film[d]	No.	Altitude[e] (m)	No.	Altitude[e] (m)
91	"Orphan"	15BCB96099	27-Sep-96	1:40 000	153	B&W	109	8664	110	8659
92	"Adieu"	15BCB96099	27-Sep-96	1:40 000	153	B&W	105	8643	104	8644
93	"Tuwasus Upper"	15BCB96099	27-Sep-96	1:40 000	153	B&W	79	8665	80	8665
94	"Tuwasus Lower"	15BCB96099	27-Sep-96	1:40 000	153	B&W	79	8665	80	8665
95	"Greymantle"	15BCB96099	27-Sep-96	1:40 000	153	B&W	77	8699	78	8676
96	Hourglass	30BCB93027	2-Aug-93	1:15 000	306	B&W	19	6401	18	6401
97	Snowcap	30BCB93027	2-Aug-93	1:15 000	306	B&W	19	6401	18	6401
98	Lower Snowcap	30BCB93027	2-Aug-93	1:15 000	306	B&W	19	6401	18	6401
99	"Misty Upper"	30BCC96129	25-Aug-96	1:15 000	304	colour	134	6096	133	6096
100	"Appa"	30BCC94135	13-Aug-94	1:15 000	306	colour	166	6248	165	6248
101	"Exodus"	30BCC94159	18-Sep-94	1:15 000	306	colour	54	6248	53	6248
102	"Dipper"	30BCC94159	18-Sep-94	1:15 000	306	colour	55	6248	54	6248
103	"Soo Upper"	30BCC94120	1-Aug-94	1:15 000	306	colour	14	6248	13	6248
104	"Soo Lower"	30BCC94120	1-Aug-94	1:15 000	306	colour	14	6248	13	6248
105	"Currie"	30BCC94120	1-Aug-94	1:15 000	306	colour	37	6248	36	6248
106	Chaos	BC5340	19-Jul-69	1:30 000	153	B&W	234	7315	233	7315
107	"Ure"	BC5340	19-Jul-69	1:30 000	153	B&W	233	7315	232	7315
108	"Tremor"	15BCB91157	9-Sep-91	1:40 000	153	B&W	119	9129	120	9129
109	"NW Pantheon W"	BC79146	10-Aug-79	1:20 000	306	B&W	218	7925	219	7925
110	"NW Pantheon Et"	BC79146	10-Aug-79	1:20 000	306	B&W	215	7925	216	7925
111	"Niut"	30BCC94009	9-Jul-94	1:15 000	304	colour	188	6460	189	6460
112	"Siva"	30BCC94067	19-Jul-94	1:15 000	304	colour	103	6844	104	6845
113	"Sand"	30BCC94067	19-Jul-94	1:15 000	304	colour	124	6903	123	6907
114	"S Tiedemann Large"	30BCC94163	21-Sep-94	1:15 000	306	colour	178	5639	177	5639
115	"S Tiedemann Small"	30BCC94163	21-Sep-94	1:15 000	306	colour	178	5639	177	5639
116	"Tiedemann Lateral S"	30BCC94039	11-Jul-94	1:15 000	304	colour	178	6858	177	6858
117	"Hidden"	30BCC94163	21-Sep-94	1:15 000	306	colour	73	5639	74	5639
118	"Stanton"	15BCB96098	26-Sep-96	1:40 000	531	B&W	138	8584	139	8605
119	"Wahkash"	30BCC99014	2-Sep-99	1:15 000	306	colour	106	6706	107	6706
120	"Brew Head"	30BCC94166	21-Sep-94	1:15 000	305	colour	105	5639	106	5639

Appendix B (continued)

							Frame 1		Frame 2	
No.	Lake[a]	Roll no.	Date	Scale[b]	Focal (mm)[c]	Film[d]	No.	Altitude[e] (m)	No.	Altitude[e] (m)
121	"Brew South"	30BCC94163	21-Sep-94	1:15 000	306	colour	29	5639	30	5639
122	"Blackhorn"	30BCC94059	19-Jul-94	1:15 000	304	colour	17	6857	18	6858
123	"Five Finger"	30BCC94059	19-Jul-94	1:15 000	304	colour	104	6865	105	6872
124	"Crazy"	30BCC94059	19-Jul-94	1:15 000	304	colour	117	6817	118	6809
125	"Ottarasko Small"	30BCC94059	19-Jul-94	1:15 000	304	colour	173	6866	174	6872
126	"Ottarasko Large"	30BCC94059	19-Jul-94	1:15 000	304	colour	177	6895	178	6898
127	"Nude"	30BCC94010	9-Jul-94	1:15 000	304	colour	145	6853	144	6850
128	"Oval"	30BCC94010	9-Jul-94	1:15 000	304	colour	121	6761	120	6770
129	"Ottarasko Tributary"	30BCC94010	9-Jul-94	1:15 000	304	colour	167	6826	168	6829
130	"Scimitar Snout"	30BCC94010	9-Jul-94	1:15 000	304	colour	193	6821	194	6835
131	"Scimitar Right Lateral"	30BCC94010	9-Jul-94	1:15 000	304	colour	194	6835	195	6850
132	"Cataract Right Lateral"	30BCC94010	9-Jul-94	1:15 000	304	colour	220	6876	219	6867
133	"Cataract Snout"	30BCC94010	9-Jul-94	1:15 000	304	colour	220	6876	219	6867
134	"Success"	30BCC94059	19-Jul-94	1:15 000	304	colour	241	6925	240	6928
135	"Tellot"	30BCC94068	20-Jul-94	1:15 000	304	colour	202	6871	201	6870
136	Ephemeron	30BCC94068	20-Jul-94	1:15 000	304	colour	205	6871	204	6872
137	"Tiedemann Lateral N"	30BCC94039	11-Jul-94	1:15 000	304	colour	178	6858	177	6858
138	"Remote"	BC79072	14-Jul-79	1:20 000	306	B&W	70	7925	69	7925
139	"Nahatlatch Head"	30BCC97227	8-Sep-97	1:15 000	303	colour	167	6899	168	6906
140	"Rutledge Large"	30BCC97129	19-Sep-97	1:15 000	303	colour	84	6568	85	6569
141	"Van Horlick"	30BCC97131	20-Sep-97	1:15 000	303	colour	88	6530	87	6520
142	"White North"	30BCC94119	1-Aug-94	1:15 000	306	colour	60	6248	61	6248
143	White South"	30BCC94119	1-Aug-94	1:15 000	306	colour	60	6248	61	6248
144	"Sockeye South"	30BCC94103	28-Jul-94	1:15 000	306	colour	72	6248	71	6248
145	"Downton Head"	30BCC97087	19-Jul-97	1:15 000	305	colour	253	6810	252	6802
146	"Whitecap"	30BCC97218	10-Aug-97	1:15 000	305	colour	82	6746	83	6741
147	"Surfusion"	30BCC97086	20-Jul-97	1:15 000	305	colour	73	6754	74	6759
148	"Salal Large"	30BCC97086	20-Jul-97	1:15 000	305	colour	89	6755	88	6759
149	"Athelney Pass"	30BCC97086	20-Jul-97	1:15 000	305	colour	106	6737	105	6738
150	"Ochre"	30BCC97218	10-Aug-97	1:15 000	305	colour	141	6710	140	6700

Appendix B (continued)

							Frame 1		Frame 2	
No.	Lake[a]	Roll no.	Date	Scale[b]	Focal (mm)[c]	Film[d]	No.	Altitude[e] (m)	No.	Altitude[e] (m)
151	"McParlon"	30BCC97086	20-Jul-97	1:15 000	305	colour	110	6736	109	6734
152	"Vayu"	30BCC97086	20-Jul-97	1:15 000	305	colour	118	6748	117	6749
153	"Truax Middle"	30BCC97128	11-Aug-97	1:15 000	305	colour	144	6745	143	6746
154	"Truax West"	30BCC97128	11-Aug-97	1:15 000	305	colour	144	6745	143	6746
155	"Truax East"	30BCC97128	11-Aug-97	1:15 000	305	colour	144	6745	143	6746
156	"Enterprise"	30BCC97089	10-Aug-97	1:15 000	305	colour	31	6755	32	6759
157	"Leckie Tributary"	30BCC97127	14-Aug-97	1:15 000	305	colour	119	6783	120	6777
158	"Leckie South"	30BCC97127	14-Aug-97	1:15 000	305	colour	113	6810	114	6792
159	"Copper"	30BCC97127	14-Aug-97	1:15 000	305	colour	162	6714	161	6707
160	"Gun Head"	30BCC97220	14-Aug-97	1:15 000	305	colour	96	6721	97	6723
161	"Nichols"	30BCC97127	14-Aug-97	1:15 000	305	colour	152	6735	151	6744
162	"Lepton"	30BCC97127	14-Aug-97	1:15 000	305	colour	152	6735	151	6744
163	"Lord"	30BCC97107	9-Aug-97	1:15 000	305	colour	102	6706	101	6706
164	"Griswold W Fork Head"	30BCC97220	14-Aug-97	1:15 000	305	colour	124	6659	123	6653
165	"Granite Head"	30BCC97108	9-Aug-97	1:15 000	305	colour	179	6553	180	6553
166	"E Fork Nostetuko Upper"	30BCC94038	11-Jul-94	1:15 000	304	colour	88	6553	89	6553
167	"Deschamps Lower"	30BCC03023	3-Sep-03	1:15 000	306	colour	123	8231	122	8231
168	"Tredcroft East"	30BCC94038	11-Jul-94	1:15 000	304	colour	79	6553	80	6553
169	"East Olson Upper"	30BCC97205	20-Sep-97	1:15 000	306	colour	76	6553	77	6553
170	"Elaho Lower"	30BCC94164	21-Sep-94	1:15 000	306	colour	95	6248	94	6248
171	"Pemberton Ice W Small"	30BCC94160	18-Sep-94	1:15 000	306	colour	101	6248	100	6248
172	"Lava Uppermost"	30BCC94121	1-Aug-94	1:15 000	306	colour	140	5791	139	5791
173	"Sockeye Middle"	30BCC94103	28-Jul-94	1:15 000	306	colour	72	6248	71	6248
174	"Sockeye North"	30BCC94103	28-Jul-94	1:15 000	306	colour	72	6248	71	6248
175	"Lone Goat"	30BCC97125	10-Aug-97	1:15 000	305	colour	205	6760	204	6758

[a] Lake names in quotations are unofficial, according to Terrain Resource Information Management (TRIM) maps (Province of British Columbia, 2001).
[b] Nominal.
[c] Camera focal length (mm).
[d] Film emulsion = colour or black & white (B&W)
[e] Flying altitude above mean sea level (m) from which photograph was taken.

Appendix C. Measured values of the 19 candidate predictor variables

No.	Frbd (m)	RlfG (m)	FMht (-)	Mhw (-)	Mdfk (°)	LGpx (m)	LGsp (°)	Calv (m)	Lsld (-)	Snow (-)	IceC (-)	Mveg (-)	UsLk (-)	Crev (-)	SnSt (°)	Area (ha)	Wshd (ha)	Geol (-)	Lk (-)
1	0	0	0.00	0.22	24	0	0	370	0	1	1	1	0	0	9	2.0	700	1	1
2	0	0	0.00	0.06	7	0	0	410	1	1	0	1	0	1	13	65.3	840	1	1
3	0	30	0.00	0.16	12	50	26	0	0	1	0	1	0	1	34	23.0	550	1	1
4	0	-	0.00	0.34	34	-	-	-	0	0	0	1	1	-	-	9.4	540	1	3
5	0	230	0.00	0.10	7	460	27	0	0	0	0	1	0	1	32	8.5	340	1	1
6	0	100	0.00	0.08	10	410	14	0	0	0	0	1	1	1	22	1.2	230	1	1
7	0	0	0.00	0.12	11	0	0	140	0	0	0	1	0	0	17	1.5	150	3	1
8	0	-	0.00	0.38	25	-	-	-	0	0	1	1	0	-	-	1.3	25	2	1
9	0	10	0.00	0.03	3	150	3	0	0	0	0	1	0	0	25	4.3	50	3	2
10	0	0	0.00	0.04	19	0	0	260	0	0	0	1	1	0	9	5.0	540	1	1
11	0	0	0.00	0.01	2	0	0	270	0	0	0	1	0	0	13	3.5	500	1	1
12	0	450	0.00	0.09	7	940	26	0	0	0	0	1	0	1	27	12.3	2000	1	1
13	0	0	0.00	0.03	4	0	0	290	0	0	0	0	0	1	10	24.2	4400	1	1
14	0	0	0.00	0.29	25	0	0	210	0	0	0	1	0	1	17	4.0	100	2	1
15	3	0	0.07	0.28	20	0	0	180	0	1	0	1	0	0	34	7.9	100	1	1
16	0	0	0.00	0.06	5	0	0	110	0	0	0	1	0	1	20	1.5	70	1	1
17	0	0	0.00	0.10	7	0	0	150	0	0	0	1	0	0	19	2.0	480	1	1
18	0	170	0.00	0.08	7	260	33	0	0	0	0	1	0	0	20	1.7	390	1	1
19	0	110	0.00	0.03	8	420	15	0	0	0	1	1	0	0	19	4.1	100	1	1
20	0	0	0.00	0.02	19	0	0	190	0	1	1	1	0	1	10	8.0	470	1	1
21	0	0	0.00	0.27	19	0	0	210	0	0	0	1	0	1	21	3.0	60	1	1
22	0	80	0.00	0.13	11	360	13	0	0	0	0	1	0	0	32	2.3	100	1	1
23	5	-	0.05	0.54	33	-	-	-	0	1	0	1	0	-	-	1.0	45	1	2
24	0	180	0.00	0.28	29	240	36	0	0	1	0	1	1	1	29	15.5	160	1	1
25	0	60	0.00	0.32	24	490	7	0	0	0	1	1	0	0	13	3.9	380	2	1
26	3	0	0.97	0.00	8	0	0	70	0	0	1	1	0	0	25	1.4	12	3	1
27	17	0	0.47	0.07	11	0	0	140	0	0	1	1	0	1	29	1.6	30	3	1
28	0	0	0.00	0.21	15	0	0	160	0	0	0	1	0	0	24	2.5	65	2	1
29	14	0	0.63	0.05	10	0	0	170	0	1	1	1	0	1	43	3.8	40	2	1
30	0	-	0.00	0.25	18	-	-	-	0	0	0	1	0	-	-	1.7	13	2	1

Appendix C (continued)

No.	Frbd (m)	RlfG (m)	FMht (-)	Mhw (-)	Mdfk (°)	LGpx (m)	LGsp (°)	Calv (m)	Lsld (-)	Snow (-)	IceC (-)	Mveg (-)	UsLk (-)	Crev (-)	SnSt (°)	Area (ha)	Wshd (ha)	Geol (-)	Lk (-)
31	0	0	0.00	0.05	5	0	0	150	0	0	1	1	0	0	22	3.7	80	2	1
32	8	0	0.57	0.06	15	0	0	260	0	0	1	1	0	1	41	6.2	55	3	1
33	5	0	0.41	0.13	16	0	0	230	0	0	1	1	0	1	24	3.8	27	3	1
34	3	-	0.25	0.07	6	-	-	-	0	1	1	1	0	-	-	1.4	43	2	1
35	0	40	0.00	0.24	22	180	13	0	0	0	1	1	0	1	25	1.4	43	2	1
36	5	120	0.53	0.05	16	250	26	0	0	0	1	1	1	1	25	7.7	290	2	1
37	0	0	0.00	0.06	4	0	0	190	0	0	1	1	1	0	32	4.8	280	2	2
38	0	0	0.00	0.26	16	0	0	170	0	0	1	1	1	1	15	7.8	160	2	1
39	3	0	0.12	0.20	16	0	0	140	0	1	1	1	0	0	48	4.4	24	2	1
40	0	70	0.00	0.05	4	110	34	0	0	1	1	1	0	0	23	4.4	65	2	1
41	8	20	0.08	0.25	24	100	12	0	0	0	1	1	0	0	22	1.1	110	2	1
42	0	20	0.00	0.17	12	90	11	0	0	0	1	1	0	0	22	1.6	50	2	1
43	0	60	0.00	0.05	7	410	9	0	0	0	0	1	0	0	23	1.0	100	2	1
44	0	-	0.00	0.23	28	-	-	-	0	0	0	1	0	-	-	1.1	45	2	1
45	0	190	0.00	0.14	14	370	27	0	0	1	0	1	0	0	32	1.3	60	2	1
46	0	80	0.00	0.12	9	280	17	0	0	1	0	1	0	0	23	1.3	57	2	1
47	3	-	0.51	0.05	29	-	-	-	0	1	0	1	0	-	-	6.0	47	2	1
48	3	0	0.24	0.23	31	0	0	120	0	0	1	1	0	0	20	4.8	70	2	1
49	0	0	0.00	0.05	9	0	0	60	0	0	0	1	0	0	33	1.6	65	3	1
50	0	90	0.00	0.14	25	480	11	0	0	0	0	1	0	0	27	1.4	130	1	1
51	0	20	0.00	0.09	24	120	10	0	0	0	0	1	0	0	16	1.5	55	1	1
52	1	80	0.05	0.07	11	470	9	0	0	0	0	1	1	0	19	2.5	150	1	1
53	0	50	0.00	0.11	14	350	8	0	0	0	0	1	0	0	20	1.7	220	1	1
54	0	10	0.00	0.01	3	180	3	0	0	0	0	1	1	0	11	16.6	650	1	1
55	1	10	0.25	0.14	20	300	2	0	0	0	0	1	0	0	9	8.2	150	1	1
56	0	60	0.00	0.17	25	240	15	0	0	0	0	1	0	0	17	2.0	63	1	1
57	6	200	0.16	0.43	30	340	30	0	0	1	0	1	0	1	26	1.3	30	1	1
58	0	0	0.00	0.09	17	0	0	150	0	0	1	1	0	0	16	1.7	260	1	1
59	0	0	0.00	0.15	30	0	0	120	0	0	0	1	0	0	24	3.9	80	1	1
60	0	0	0.00	0.02	2	0	0	1100	0	0	0	1	0	1	0	202.3	12500	1	1

Appendix C (continued)

No.	Frbd (m)	RlfG (m)	FMht (-)	Mhw (-)	Mdfk (°)	LGpx (m)	LGsp (°)	Calv (m)	Lsld (-)	Snow (-)	IceC (-)	Mveg (-)	UsLk (-)	Crev (-)	SnSt (°)	Area (ha)	Wshd (ha)	Geol (-)	Lk (-)
61	0	30	0.00	0.50	32	130	12	0	0	0	0	1	1	0	20	2.0	55	1	1
62	1	-	0.04	0.28	25	-	-	-	0	1	1	1	0	-	-	2.7	30	1	1
63	0	70	0.00	0.02	3	460	9	0	0	0	0	1	0	0	26	1.9	210	1	1
64	0	-	0.00	0.03	5	-	-	-	0	0	0	1	0	-	-	1.4	50	1	1
65	0	-	0.00	0.15	19	-	-	-	0	0	0	1	0	-	-	8.0	1700	1	2
66	0	0	0.00	0.03	7	0	0	180	1	1	0	1	0	1	20	3.6	1330	1	1
67	0	0	0.00	0.04	16	0	0	600	0	1	0	1	0	1	26	12.0	180	1	1
68	3	-	0.13	0.13	10	-	-	-	0	1	0	1	0	-	-	2.5	200	1	3
69	1	50	0.08	0.16	22	170	17	0	0	1	0	1	0	0	12	7.4	530	2	1
70	0	340	0.00	0.07	4	680	26	0	0	1	1	1	0	1	33	1.8	300	1	1
71	0	-	0.00	0.35	33	-	-	-	0	1	0	1	0	-	-	1.0	55	3	1
72	0	130	0.00	0.04	5	170	38	0	0	0	0	1	0	0	30	3.6	55	2	1
73	0	0	0.00	0.02	3	0	0	20	0	0	0	1	0	0	23	7.6	180	1	1
74	0	60	0.00	0.03	4	430	8	0	0	0	0	1	0	1	20	3.2	360	1	1
75	3	110	0.46	0.00	9	280	21	0	0	0	0	1	0	1	22	1.3	25	1	1
76	0	0	0.00	0.03	1	40	0	0	0	0	0	1	0	0	14	11.1	1700	1	1
77	0	0	0.00	0.06	25	0	0	150	0	0	0	1	0	1	14	5.2	180	1	1
78	0	60	0.00	0.01	3	180	17	0	0	0	0	1	0	1	14	7.7	1050	1	1
79	0	40	0.00	0.03	3	110	20	0	0	0	0	1	0	0	25	12.2	150	1	1
80	0	0	0.00	0.13	12	20	0	0	0	0	0	1	0	1	16	1.8	70	1	1
81	0	130	0.00	0.05	3	410	18	0	0	0	0	0	1	1	22	14.6	600	1	1
82	0	30	0.00	0.05	10	210	9	0	0	0	0	0	0	1	26	20.4	300	2	1
83	0	0	0.00	0.02	10	0	0	1000	0	0	0	1	0	1	5	190.0	9000	1	1
84	0	170	0.00	0.17	25	300	30	0	0	1	0	1	0	1	31	3.5	400	1	1
85	0	0	0.00	0.01	1	320	0	0	0	0	0	1	1	1	14	8.3	1850	1	1
86	0	370	0.00	0.16	10	660	29	0	0	1	0	1	0	1	33	17.8	610	1	2
87	0	180	0.00	0.03	3	380	25	0	0	0	0	0	0	1	11	12.0	1400	1	1
88	0	40	0.00	0.11	7	140	16	0	0	1	0	0	0	1	21	20.9	1500	1	1
89	0	0	0.00	0.06	5	0	0	230	0	0	0	1	0	1	11	8.2	320	1	1
90	0	100	0.00	0.12	15	250	22	0	0	0	0	1	0	1	26	3.0	90	1	1

Appendix C (continued)

No.	Frbd (m)	RlfG (m)	FMht (-)	Mhw (-)	Mdfk (°)	LGpx (m)	LGsp (°)	Calv (m)	Lsld (-)	Snow (-)	IceC (-)	Mveg (-)	UsLk (-)	Crev (-)	SnSt (°)	Area (ha)	Wshd (ha)	Geol (-)	Lk (-)
91	0	130	0.00	0.10	11	280	24	0	0	0	0	1	0	1	29	1.9	280	1	1
92	0	-	0.00	0.02	5	-	-	-	0	1	0	1	0	-	-	13.4	280	1	1
93	6	0	0.05	0.26	17	0	0	140	0	0	0	1	0	0	18	1.1	75	1	1
94	0	150	0.00	0.19	16	650	13	0	0	0	0	1	1	0	18	1.0	135	1	1
95	0	30	0.00	0.08	5	60	25	0	0	0	0	1	0	0	30	2.8	50	1	1
96	0	50	0.00	0.06	14	210	13	0	0	0	0	1	0	1	29	21.4	470	1	1
97	0	50	0.00	0.05	9	1170	3	0	0	1	0	1	1	1	29	69.1	1350	1	3
98	0	0	0.00	0.07	5	0	0	140	0	0	0	1	1	1	26	58.0	1950	1	1
99	0	-	0.00	0.03	3	-	-	-	0	0	0	1	0	-	-	2.7	350	1	2
100	0	50	0.00	0.07	5	750	4	0	0	0	0	1	1	0	15	16.2	2050	1	1
101	0	20	0.00	0.18	15	160	8	0	0	0	0	1	0	0	17	1.9	30	4	1
102	0	380	0.00	0.01	2	910	23	0	0	0	0	1	1	1	13	2.3	270	1	1
103	0	100	0.00	0.03	5	400	14	0	0	0	0	1	0	0	13	1.4	310	2	1
104	0	90	0.00	0.15	25	620	8	0	0	0	0	1	1	0	13	2.1	325	2	1
105	0	300	0.00	0.15	27	830	20	0	0	1	0	1	0	1	36	4.0	390	1	1
106	0	190	0.00	0.22	15	380	27	0	0	1	0	1	0	1	32	8.4	280	1	1
107	0	-	0.00	0.12	15	-	-	-	0	0	0	1	0	-	-	1.5	45	1	2
108	0	20	0.00	0.03	3	60	21	0	0	0	0	1	0	1	22	2.5	410	2	1
109	0	20	0.00	0.02	3	80	13	0	0	0	0	1	0	1	11	7.2	105	1	1
110	0	0	0.00	0.06	3	0	0	90	0	0	1	1	0	1	23	1.8	90	1	1
111	0	190	0.00	0.06	4	570	18	0	0	1	0	1	0	1	25	5.3	390	1	1
112	0	0	0.00	0.00	1	0	0	370	0	0	0	1	0	1	23	11.0	580	1	1
113	0	0	0.00	0.18	30	0	0	200	0	0	0	1	0	0	35	4.9	43	1	1
114	0	10	0.00	0.04	9	30	14	0	0	0	0	1	0	1	20	13.5	200	1	1
115	0	10	0.00	0.07	27	820	1	0	0	0	0	1	1	1	20	2.6	220	1	1
116	0	-	0.00	0.10	16	-	-	-	0	0	0	0	1	-	-	20.2	740	1	2
117	0	200	0.00	0.06	4	500	22	0	0	1	0	1	0	1	31	3.6	670	1	1
118	0	60	0.00	0.12	18	90	34	0	0	1	1	1	0	1	19	2.5	890	1	1
119	0	640	0.00	0.15	9	1050	31	0	0	0	0	0	0	1	29	11.6	1200	1	1
120	0	820	0.00	0.31	31	1430	30	0	0	1	0	0	0	1	23	10.0	590	1	2

Appendix C (continued)

No.	Frbd (m)	RlfG (m)	FMht (-)	Mhw (-)	Mdfk (°)	LGpx (m)	LGsp (°)	Calv (m)	Lsld (-)	Snow (-)	IceC (-)	Mveg (-)	UsLk (-)	Crev (-)	SnSt (°)	Area (ha)	Wshd (ha)	Geol (-)	Lk (-)
121	0	30	0.00	0.07	5	150	11	0	0	0	0	1	0	1	22	2.6	240	1	1
122	1	60	0.04	0.09	7	1220	3	0	0	1	1	1	0	0	11	9.0	1730	1	3
123	0	0	0.00	0.26	25	60	2	0	0	0	0	1	1	0	9	1.1	150	1	1
124	0	60	0.00	0.26	22	450	8	0	0	0	0	1	0	1	9	1.1	220	1	1
125	0	50	0.00	0.06	20	310	9	0	0	0	0	1	0	0	33	1.7	70	1	1
126	1	140	0.20	0.09	13	200	34	0	0	1	1	1	0	1	22	21.1	150	1	1
127	0	0	0.00	0.09	15	0	0	210	0	0	1	1	0	1	18	2.0	710	4	1
128	0	0	0.00	0.13	8	0	0	280	0	1	0	1	0	0	9	18.0	2850	4	1
129	0	360	0.00	0.04	5	630	30	0	0	1	0	1	0	1	31	5.0	440	3	1
130	0	0	0.00	0.02	5	0	0	470	0	1	1	1	1	1	6	8.0	13000	4	1
131	0	590	0.00	0.59	37	1430	22	0	0	1	0	1	0	0	14	1.0	240	4	2
132	0	230	0.00	0.49	26	1040	12	0	0	1	0	1	1	1	21	2.8	310	4	2
133	0	0	0.00	0.02	5	0	0	360	0	0	1	1	1	1	22	2.0	1450	4	1
134	0	310	0.00	0.11	8	570	29	0	0	0	1	1	1	1	28	6.6	710	4	1
135	0	0	0.00	0.08	7	0	0	140	0	0	0	1	0	1	15	1.4	400	1	1
136	0	20	0.00	0.01	4	430	3	0	0	0	1	0	1	1	17	24.4	4900	1	1
137	0	-	0.00	0.16	15	-	-	-	0	0	0	0	0	-	-	26.9	150	1	2
138	0	50	0.00	0.36	24	300	9	0	0	0	0	1	0	1	25	2.4	80	4	1
139	0	0	0.00	0.15	30	0	0	160	0	0	0	1	0	0	9	1.6	70	1	1
140	0	130	0.00	0.12	6	830	9	0	0	0	0	1	1	1	20	18.1	1500	1	1
141	10	50	0.44	0.11	17	190	15	0	0	0	0	1	0	0	21	1.2	50	1	1
142	0	30	0.00	0.05	5	180	10	0	0	0	0	1	0	0	13	5.7	280	1	1
143	0	80	0.00	0.23	17	190	21	0	0	0	0	1	0	1	25	6.7	130	1	1
144	0	200	0.00	0.21	12	550	20	0	0	1	0	1	0	1	31	3.5	220	1	1
145	2	-	0.16	0.15	16	-	-	-	0	1	0	1	0	-	-	2.0	60	3	1
146	0	10	0.00	0.05	9	240	3	0	0	0	0	1	1	1	22	2.4	290	3	1
147	0	0	0.00	0.15	10	0	0	480	0	0	0	1	0	1	16	8.4	110	1	1
148	0	70	0.00	0.12	9	230	16	0	0	1	0	1	0	1	31	7.0	220	1	1
149	0	-	0.00	0.10	6	-	-	-	0	0	0	1	0	-	-	1.0	5	1	1
150	0	10	0.00	0.10	6	250	3	0	0	0	0	1	0	0	11	2.1	195	1	1

Appendix C (continued)

No.	Frbd (m)	RlfG (m)	FMht (-)	Mhw (-)	Mdfk (°)	LGpx (m)	LGsp (°)	Calv (m)	Lsld (-)	Snow (-)	IceC (-)	Mveg (-)	UsLk (-)	Crev (-)	SnSt (°)	Area (ha)	Wshd (ha)	Geol (-)	Lk (-)
151	0	160	0.00	0.05	5	380	23	0	0	1	0	1	0	1	19	5.6	2040	1	1
152	0	20	0.00	0.07	5	250	3	0	0	0	0	1	0	0	11	2.6	250	1	1
153	3	40	0.11	0.22	17	450	6	0	0	0	1	1	1	0	28	2.5	45	4	1
154	1	40	0.29	0.05	4	180	13	0	0	0	1	1	0	0	28	4.4	75	4	1
155	0	10	0.00	0.35	25	160	3	0	0	0	1	1	1	0	18	2.7	225	2	1
156	0	300	0.00	0.14	17	550	29	0	0	1	1	1	0	0	43	5.0	128	3	1
157	0	40	0.00	0.40	23	160	13	0	0	0	0	1	0	0	23	1.6	33	1	1
158	0	10	0.00	0.38	33	110	4	0	0	0	0	1	0	0	23	1.5	47	1	1
159	0	-	0.00	0.35	22	-	-	-	0	1	1	1	0	-	-	1.1	35	1	1
160	1	10	0.04	0.13	13	70	9	0	0	0	0	1	0	0	21	1.2	28	1	1
161	0	90	0.00	0.06	6	540	9	0	0	0	0	1	0	0	11	1.3	100	1	1
162	0	110	0.00	0.31	37	540	11	0	0	0	0	1	0	0	20	2.1	140	1	1
163	0	30	0.00	0.17	10	240	7	0	0	0	0	1	0	0	15	2.5	80	1	1
164	0	0	0.00	0.15	9	0	0	160	0	0	1	1	0	0	26	1.5	35	1	1
165	2	0	0.11	0.25	29	0	0	250	0	0	0	1	0	0	16	1.3	37	1	1
166	0	70	0.00	0.07	7	140	27	0	0	1	0	1	0	1	24	1.5	220	1	1
167	0	60	0.00	0.10	19	980	4	0	0	0	0	1	1	1	21	2.0	290	1	1
168	0	20	0.00	0.01	16	130	7	0	0	0	1	1	0	0	28	2.1	65	3	1
169	18	0	0.93	0.01	17	0	0	130	0	0	1	1	0	0	17	1.5	46	2	1
170	0	-	0.00	0.01	4	-	-	-	0	0	0	1	0	-	-	8.7	30	1	2
171	0	60	0.00	0.06	4	180	17	0	0	0	0	1	1	1	17	1.2	148	1	1
172	0	30	0.00	0.07	7	370	5	0	0	0	0	1	0	0	9	1.1	70	2	1
173	0	10	0.00	0.29	32	150	5	0	0	0	0	1	0	0	25	5.3	110	1	1
174	0	220	0.00	0.28	17	460	26	0	0	0	0	1	0	0	34	5.6	50	1	1
175	0	30	0.00	0.04	4	210	7	0	0	0	0	1	0	0	23	2.8	320	1	1

Notes:
Data for drained lakes based on pre-outburst conditions.
Predictor variable codes (column headings) and units correspond to those in Table 2-1.
(-) indicates particular variable not applicable to lake because no glacier existed in watershed when aerial photograph was taken.
Mhw reported to two decimal places to avoid numerous rounded values of zero in statistical analysis.

Appendix D. Input parameters for, and results of, outburst flood hazard assessments

	Peak discharge estimation data[a]				Maximum debris flow volume estimation data[b]							
No.	A (m^2)	V (m^3)	Hd (m)	**Qp (m^3/s)**	Dam? (-)	W (m)	Hd (m)	Vb (m^3)	Vr_lower (m^3)	Vr_upper (m^3)	**Vm_lower (m^3)**	**Vm_upper (m^3)**
1	2.0E+04	1.3E+05	7	**120**	No	30	7	0.0E+00	5.0E+04	7.4E+04	**5.0E+04**	**7.4E+04**
2	6.5E+05	7.4E+07	18	**9620**	-	290	18	-	-	-	-	-
3	2.3E+05	9.6E+06	53	**5410**	-	320	53	-	-	-	-	-
4	9.4E+04	1.8E+06	59	**2100**	-	170	59	-	-	-	-	-
5	8.5E+04	1.5E+06	40	**1490**	-	380	40	-	-	-	-	-
6	1.2E+04	6.2E+04	9	**90**	-	110	9	-	-	-	-	-
7	1.5E+04	8.5E+04	17	**160**	Yes	140	17	5.8E+04	1.8E+04	2.7E+04	**7.6E+04**	**8.5E+04**
8	1.3E+04	6.9E+04	34	**210**	Yes	90	34	1.5E+05	1.7E+04	2.5E+04	**1.7E+05**	**1.7E+05**
9	4.3E+04	4.5E+05	4	**180**	-	150	4	-	-	-	-	-
10	5.0E+04	5.8E+05	1	**90**	No	20	1	0.0E+00	2.3E+04	3.7E+04	**2.3E+04**	**3.7E+04**
11	3.5E+04	3.2E+05	3	**120**	No	230	3	0.0E+00	4.1E+04	8.5E+04	**4.1E+04**	**8.5E+04**
12	1.2E+05	2.9E+06	26	**1730**	Yes	290	26	2.8E+05	7.4E+04	1.1E+05	**3.5E+05**	**3.9E+05**
13	2.4E+05	1.1E+07	5	**1390**	-	180	5	-	-	-	-	-
14	4.0E+04	3.9E+05	53	**800**	No	190	53	0.0E+00	5.4E+04	1.1E+05	**5.4E+04**	**1.1E+05**
15	7.9E+04	1.3E+06	41	**1390**	Yes	150	41	3.5E+05	6.8E+03	1.4E+04	**3.6E+05**	**3.7E+05**
16	1.5E+04	8.5E+04	5	**80**	Yes	80	5	2.9E+03	3.0E+04	5.4E+04	**3.3E+04**	**5.7E+04**
17	2.0E+04	1.3E+05	33	**310**	Yes	340	33	5.3E+05	2.3E+04	3.5E+04	**5.5E+05**	**5.6E+05**
18	1.7E+04	1.0E+05	19	**190**	Yes	230	19	1.2E+05	4.8E+04	7.2E+04	**1.6E+05**	**1.9E+05**
19	4.1E+04	4.1E+05	3	**150**	-	110	3	-	-	-	-	-
20	8.0E+04	1.3E+06	1	**150**	Yes	60	1	7.9E+01	7.4E+04	1.1E+05	**7.4E+04**	**1.1E+05**
21	3.0E+04	2.5E+05	33	**450**	No	120	33	0.0E+00	1.4E+04	2.1E+04	**1.4E+04**	**2.1E+04**
22	2.3E+04	1.6E+05	14	**210**	-	110	14	-	-	-	-	-
23	1.0E+04	4.8E+04	90	**310**	No	170	90	0.0E+00	3.3E+04	4.9E+04	**3.3E+04**	**4.9E+04**
24	1.6E+05	4.5E+06	13	**1480**	Yes	50	13	1.1E+04	3.2E+05	6.3E+05	**3.3E+05**	**6.5E+05**
25	3.9E+04	3.8E+05	43	**680**	Yes	140	43	3.6E+05	4.0E+03	6.0E+03	**3.6E+05**	**3.7E+05**
26	1.4E+04	7.7E+04	0	**30**	-	20	0	-	-	-	-	-
27	1.6E+04	9.3E+04	20	**190**	Yes	270	20	1.6E+05	3.4E+04	5.0E+04	**1.9E+05**	**2.1E+05**
28	2.5E+04	1.8E+05	38	**410**	-	180	38	-	-	-	-	-
29	3.8E+04	3.6E+05	8	**240**	-	150	8	-	-	-	-	-
30	1.7E+04	1.0E+05	66	**400**	No	260	66	0.0E+00	2.0E+04	3.0E+04	**2.0E+04**	**3.0E+04**

Appendix D (continued)

No.	Peak discharge estimation data[a] A (m^2)	V (m^3)	Hd (m)	**Qp (m^3/s)**	Maximum debris flow volume estimation data[b] Dam? (-)	W (m)	Hd (m)	Vb (m^3)	Vr_lower (m^3)	Vr_upper (m^3)	**Vm_lower (m^3)**	**Vm_upper (m^3)**
31	3.7E+04	3.5E+05	9	**250**	-	170	9	-	-	-	-	-
32	6.2E+04	8.4E+05	6	**340**	-	110	6	-	-	-	-	-
33	3.8E+04	3.6E+05	7	**220**	-	50	7	-	-	-	-	-
34	1.4E+04	7.7E+04	8	**100**	-	110	8	-	-	-	-	-
35	1.4E+04	7.7E+04	29	**210**	-	120	29	-	-	-	-	-
36	7.7E+04	1.2E+06	4	**340**	-	90	4	-	-	-	-	-
37	4.8E+04	5.4E+05	11	**370**	-	190	11	-	-	-	-	-
38	7.8E+04	1.3E+06	85	**2130**	-	320	85	-	-	-	-	-
39	4.4E+04	4.6E+05	21	**500**	-	110	21	-	-	-	-	-
40	4.4E+04	4.6E+05	11	**340**	Yes	210	11	3.7E+04	6.6E+03	9.8E+03	**4.4E+04**	**4.7E+04**
41	1.1E+04	5.5E+04	86	**320**	-	340	86	-	-	-	-	-
42	1.6E+04	9.3E+04	37	**270**	No	210	37	0.0E+00	4.2E+04	7.0E+04	**4.2E+04**	**7.0E+04**
43	1.0E+04	4.8E+04	4	**50**	-	90	4	-	-	-	-	-
44	1.1E+04	5.5E+04	29	**170**	Yes	130	29	1.5E+05	1.2E+03	1.8E+03	**1.5E+05**	**1.5E+05**
45	1.3E+04	6.9E+04	9	**100**	-	60	9	-	-	-	-	-
46	1.3E+04	6.9E+04	18	**150**	Yes	150	18	7.0E+04	8.7E+03	1.7E+04	**7.8E+04**	**8.7E+04**
47	6.0E+04	7.9E+05	2	**170**	No	40	2	0.0E+00	5.6E+03	9.3E+03	**5.6E+03**	**9.3E+03**
48	4.8E+04	5.4E+05	10	**350**	-	40	10	-	-	-	-	-
49	1.6E+04	9.3E+04	2	**50**	Yes	40	2	2.5E+02	1.4E+03	2.9E+03	**1.7E+03**	**3.1E+03**
50	1.4E+04	7.7E+04	9	**100**	No	60	9	0.0E+00	9.9E+03	2.0E+04	**9.9E+03**	**2.0E+04**
51	1.5E+04	8.5E+04	4	**70**	-	40	4	-	-	-	-	-
52	2.5E+04	1.8E+05	18	**260**	-	250	18	-	-	-	-	-
53	1.7E+04	1.0E+05	7	**100**	-	60	7	-	-	-	-	-
54	1.7E+05	5.2E+06	1	**340**	-	90	1	-	-	-	-	-
55	8.2E+04	1.4E+06	3	**300**	-	20	3	-	-	-	-	-
56	2.0E+04	1.3E+05	15	**190**	Yes	90	15	2.8E+04	4.5E+03	6.7E+03	**3.3E+04**	**3.5E+04**
57	1.3E+04	6.9E+04	33	**210**	Yes	80	33	1.2E+05	9.5E+04	1.4E+05	**2.1E+05**	**2.6E+05**
58	1.7E+04	1.0E+05	2	**50**	Yes	20	2	1.3E+02	2.6E+04	5.1E+04	**2.6E+04**	**5.1E+04**
59	3.9E+04	3.8E+05	23	**470**	Yes	150	23	1.1E+05	2.5E+04	4.9E+04	**1.4E+05**	**1.6E+05**
60	2.0E+06	7.0E+08	3	**12600**	-	140	3	-	-	-	-	-

Appendix D (continued)

	Peak discharge estimation data[a]				Maximum debris flow volume estimation data[b]							
No.	A (m^2)	V (m^3)	Hd (m)	**Qp (m^3/s)**	Dam? (-)	W (m)	Hd (m)	Vb (m^3)	Vr_lower (m^3)	Vr_upper (m^3)	**Vm_lower (m^3)**	**Vm_upper (m^3)**
61	2.0E+04	1.3E+05	33	**310**	No	70	33	0.0E+00	1.0E+05	1.9E+05	**1.0E+05**	**1.9E+05**
62	2.7E+04	2.1E+05	25	**340**	Yes	90	25	7.9E+04	7.3E+03	1.1E+04	**8.6E+04**	**9.0E+04**
63	1.9E+04	1.2E+05	2	**50**	-	100	2	-	-	-	-	-
64	1.4E+04	7.7E+04	3	**50**	Yes	90	3	1.1E+03	1.5E+03	2.3E+03	**2.7E+03**	**3.4E+03**
65	8.0E+04	1.3E+06	24	**1020**	-	160	24	-	-	-	-	-
66	3.6E+04	3.3E+05	1	**70**	Yes	30	1	4.7E+01	2.2E+04	3.3E+04	**2.2E+04**	**3.3E+04**
67	1.2E+05	2.8E+06	2	**360**	No	50	2	0.0E+00	5.8E+04	1.2E+05	**5.9E+04**	**1.2E+05**
68	2.5E+04	1.8E+05	20	**280**	-	150	20	-	-	-	-	-
69	7.4E+04	1.2E+06	12	**620**	-	80	12	-	-	-	-	-
70	1.8E+04	1.1E+05	36	**290**	-	550	36	-	-	-	-	-
71	1.0E+04	4.8E+04	54	**230**	Yes	150	54	6.5E+05	1.4E+04	2.5E+04	**6.6E+05**	**6.7E+05**
72	3.6E+04	3.3E+05	10	**260**	No	240	10	0.0E+00	1.8E+04	3.7E+04	**1.8E+04**	**3.7E+04**
73	7.6E+04	1.2E+06	2	**220**	-	90	2	-	-	-	-	-
74	3.2E+04	2.7E+05	3	**110**	No	110	3	0.0E+00	1.5E+05	2.9E+05	**1.5E+05**	**2.9E+05**
75	1.3E+04	6.9E+04	3	**50**	Yes	720	3	9.2E+03	8.6E+04	1.7E+05	**9.6E+04**	**1.8E+05**
76	1.1E+05	2.4E+06	20	**1320**	-	800	20	-	-	-	-	-
77	5.2E+04	6.2E+05	9	**360**	-	160	9	-	-	-	-	-
78	7.7E+04	1.2E+06	2	**220**	-	140	2	-	-	-	-	-
79	1.2E+05	2.9E+06	4	**560**	Yes	120	4	2.8E+03	3.3E+04	5.4E+04	**3.6E+04**	**5.7E+04**
80	1.8E+04	1.1E+05	4	**80**	Yes	30	4	7.0E+02	2.0E+04	3.4E+04	**2.1E+04**	**3.4E+04**
81	1.5E+05	4.0E+06	23	**1950**	-	490	23	-	-	-	-	-
82	2.0E+05	7.6E+06	4	**1000**	-	80	4	-	-	-	-	-
83	1.9E+06	6.1E+08	5	**15890**	-	320	5	-	-	-	-	-
84	3.5E+04	3.2E+05	29	**480**	Yes	170	29	2.1E+05	6.9E+03	1.4E+04	**2.1E+05**	**2.2E+05**
85	8.3E+04	1.4E+06	2	**240**	-	260	2	-	-	-	-	-
86	1.8E+05	5.9E+06	60	**4340**	-	390	60	-	-	-	-	-
87	1.2E+05	2.8E+06	5	**630**	-	150	5	-	-	-	-	-
88	2.1E+05	8.0E+06	38	**3970**	-	350	38	-	-	-	-	-
89	8.2E+04	1.4E+06	5	**410**	Yes	80	5	2.9E+03	9.8E+04	1.9E+05	**1.0E+05**	**1.9E+05**
90	3.0E+04	2.5E+05	13	**260**	No	110	13	0.0E+00	8.3E+03	1.7E+04	**8.3E+03**	**1.7E+04**

Appendix D (continued)

No.	Peak discharge estimation data[a] A (m^2)	V (m^3)	Hd (m)	**Qp (m^3/s)**	Maximum debris flow volume estimation data[b] Dam? (-)	W (m)	Hd (m)	Vb (m^3)	Vr_lower (m^3)	Vr_upper (m^3)	**Vm_lower (m^3)**	**Vm_upper (m^3)**
91	1.9E+04	1.2E+05	14	**180**	Yes	140	14	4.0E+04	2.2E+05	3.2E+05	**2.6E+05**	**3.6E+05**
92	1.3E+05	3.4E+06	3	**520**	No	140	3	0.0E+00	3.0E+04	5.9E+04	**3.0E+04**	**5.9E+04**
93	1.1E+04	5.5E+04	112	**380**	Yes	420	112	7.6E+06	1.6E+04	2.4E+04	**7.6E+06**	**7.6E+06**
94	1.0E+04	4.8E+04	22	**130**	Yes	110	22	7.8E+04	1.0E+04	1.5E+04	**8.8E+04**	**9.3E+04**
95	2.8E+04	2.2E+05	25	**360**	No	310	25	0.0E+00	2.1E+04	4.3E+04	**2.1E+04**	**4.3E+04**
96	2.1E+05	8.4E+06	2	**700**	-	30	2	-	-	-	-	-
97	6.9E+05	8.3E+07	1	**1820**	-	20	1	-	-	-	-	-
98	5.8E+05	5.8E+07	14	**7190**	-	210	14	-	-	-	-	-
99	2.7E+04	2.1E+05	3	**100**	Yes	110	3	1.4E+03	1.3E+04	2.7E+04	**1.4E+04**	**2.8E+04**
100	1.6E+05	4.9E+06	18	**1890**	-	260	18	-	-	-	-	-
101	1.9E+04	1.2E+05	11	**150**	Yes	60	11	1.1E+04	1.5E+05	3.0E+05	**1.6E+05**	**3.1E+05**
102	2.3E+04	1.6E+05	2	**70**	Yes	150	2	8.8E+02	6.0E+04	9.0E+04	**6.1E+04**	**9.1E+04**
103	1.4E+04	7.7E+04	2	**40**	-	60	2	-	-	-	-	-
104	2.1E+04	1.4E+05	30	**300**	Yes	190	30	2.5E+05	5.4E+04	9.4E+04	**3.0E+05**	**3.4E+05**
105	4.0E+04	3.9E+05	12	**330**	No	80	12	0.0E+00	1.5E+05	2.2E+05	**1.5E+05**	**2.2E+05**
106	8.4E+04	1.5E+06	72	**2090**	-	330	72	-	-	-	-	-
107	1.5E+04	8.5E+04	20	**180**	No	170	20	0.0E+00	2.1E+04	3.1E+04	**2.1E+04**	**3.1E+04**
108	2.5E+04	1.8E+05	2	**70**	No	60	2	0.0E+00	1.6E+04	2.4E+04	**1.6E+04**	**2.4E+04**
109	7.2E+04	1.1E+06	2	**210**	Yes	130	2	7.4E+02	1.5E+04	2.2E+04	**1.5E+04**	**2.3E+04**
110	1.8E+04	1.1E+05	8	**120**	Yes	140	8	1.3E+04	9.8E+03	1.5E+04	**2.3E+04**	**2.8E+04**
111	5.3E+04	6.4E+05	5	**260**	Yes	80	5	3.0E+03	7.0E+03	1.0E+04	**1.0E+04**	**1.4E+04**
112	1.1E+05	2.4E+06	1	**220**	-	300	1	-	-	-	-	-
113	4.9E+04	5.6E+05	66	**1120**	No	360	66	0.0E+00	6.9E+04	1.4E+05	**7.0E+04**	**1.4E+05**
114	1.4E+05	3.5E+06	7	**870**	No	160	7	0.0E+00	1.9E+04	3.8E+04	**1.9E+04**	**3.8E+04**
115	2.6E+04	1.9E+05	4	**110**	No	60	4	0.0E+00	1.9E+04	3.8E+04	**1.9E+04**	**3.8E+04**
116	2.0E+05	7.5E+06	8	**1500**	-	80	8	-	-	-	-	-
117	3.6E+04	3.3E+05	17	**360**	Yes	290	17	1.2E+05	4.3E+04	6.7E+04	**1.6E+05**	**1.8E+05**
118	2.5E+04	1.8E+05	5	**120**	-	40	5	-	-	-	-	-
119	1.2E+05	2.6E+06	94	**3500**	-	630	94	-	-	-	-	-
120	1.0E+05	2.0E+06	43	**1860**	-	140	43	-	-	-	-	-

Appendix D (continued)

No.	Peak discharge estimation data[a] A (m^2)	V (m^3)	Hd (m)	**Qp (m^3/s)**	Maximum debris flow volume estimation data[b] Dam? (-)	W (m)	Hd (m)	Vb (m^3)	Vr_lower (m^3)	Vr_upper (m^3)	**Vm_lower (m^3)**	**Vm_upper (m^3)**
121	2.6E+04	1.9E+05	11	**200**	No	150	11	0.0E+00	4.6E+04	9.1E+04	**4.6E+04**	**9.1E+04**
122	9.0E+04	1.6E+06	27	**1250**	-	320	27	-	-	-	-	-
123	1.1E+04	5.5E+04	29	**170**	-	110	29	-	-	-	-	-
124	1.1E+04	5.5E+04	46	**220**	No	180	46	0.0E+00	2.9E+04	5.8E+04	**2.9E+04**	**5.8E+04**
125	1.7E+04	1.0E+05	7	**100**	No	110	7	0.0E+00	2.7E+04	4.1E+04	**2.7E+04**	**4.1E+04**
126	2.1E+05	8.2E+06	4	**1040**	Yes	50	4	1.0E+03	1.2E+04	1.8E+04	**1.3E+04**	**1.9E+04**
127	2.0E+04	1.3E+05	3	**70**	No	30	3	0.0E+00	7.1E+03	2.4E+04	**7.1E+03**	**2.4E+04**
128	1.8E+05	6.0E+06	73	**4950**	-	560	73	-	-	-	-	-
129	5.0E+04	5.8E+05	3	**180**	-	70	3	-	-	-	-	-
130	8.0E+04	1.3E+06	8	**530**	-	490	8	-	-	-	-	-
131	1.0E+04	4.8E+04	79	**290**	-	130	79	-	-	-	-	-
132	2.8E+04	2.2E+05	121	**920**	-	250	121	-	-	-	-	-
133	2.0E+04	1.3E+05	4	**90**	-	170	4	-	-	-	-	-
134	6.6E+04	9.4E+05	49	**1280**	Yes	440	49	1.5E+06	3.9E+04	5.8E+04	**1.6E+06**	**1.6E+06**
135	1.4E+04	7.7E+04	9	**100**	Yes	110	9	1.3E+04	9.8E+04	1.5E+05	**1.1E+05**	**1.6E+05**
136	2.4E+05	1.1E+07	4	**1230**	-	350	4	-	-	-	-	-
137	2.7E+05	1.3E+07	105	**9780**	-	680	105	-	-	-	-	-
138	2.4E+04	1.7E+05	80	**620**	Yes	220	80	2.0E+06	6.2E+04	1.2E+05	**2.1E+06**	**2.1E+06**
139	1.6E+04	9.3E+04	7	**100**	No	50	7	0.0E+00	4.6E+04	8.1E+04	**4.6E+04**	**8.1E+04**
140	1.8E+05	6.1E+06	20	**2290**	-	170	20	-	-	-	-	-
141	1.2E+04	6.2E+04	13	**110**	-	120	13	-	-	-	-	-
142	5.7E+04	7.3E+05	4	**240**	No	80	4	0.0E+00	2.8E+04	4.5E+04	**2.8E+04**	**4.5E+04**
143	6.7E+04	9.7E+05	33	**1020**	No	140	33	0.0E+00	2.8E+04	4.5E+04	**2.8E+04**	**4.5E+04**
144	3.5E+04	3.2E+05	19	**380**	No	90	19	0.0E+00	1.8E+04	3.6E+04	**1.8E+04**	**3.6E+04**
145	2.0E+04	1.3E+05	10	**150**	-	70	10	-	-	-	-	-
146	2.4E+04	1.7E+05	6	**130**	No	110	6	0.0E+00	7.6E+04	1.1E+05	**7.6E+04**	**1.1E+05**
147	8.4E+04	1.5E+06	24	**1080**	Yes	160	24	1.3E+05	1.7E+04	2.6E+04	**1.4E+05**	**1.5E+05**
148	7.0E+04	1.0E+06	49	**1360**	-	400	49	-	-	-	-	-
149	1.0E+04	4.8E+04	16	**110**	-	150	16	-	-	-	-	-
150	2.1E+04	1.4E+05	24	**270**	No	230	24	0.0E+00	8.3E+04	1.7E+05	**8.3E+04**	**1.7E+05**

Appendix D (continued)

	Peak discharge estimation data[a]				Maximum debris flow volume estimation data[b]							
No.	A (m^2)	V (m^3)	Hd (m)	**Qp (m^3/s)**	Dam? (-)	W (m)	Hd (m)	Vb (m^3)	Vr_lower (m^3)	Vr_upper (m^3)	**Vm_lower (m^3)**	**Vm_upper (m^3)**
151	5.6E+04	7.0E+05	12	**460**	No	230	12	0.0E+00	0.0E+00	2.0E+04	**0.0E+00**	**2.0E+04**
152	2.6E+04	1.9E+05	6	**140**	No	90	6	0.0E+00	1.2E+04	2.3E+04	**1.2E+04**	**2.3E+04**
153	2.5E+04	1.8E+05	24	**310**	-	110	24	-	-	-	-	-
154	4.4E+04	4.6E+05	2	**120**	-	40	2	-	-	-	-	-
155	2.7E+04	2.1E+05	77	**680**	Yes	220	77	1.9E+06	1.1E+04	2.3E+04	**1.9E+06**	**1.9E+06**
156	5.0E+04	5.8E+05	14	**450**	No	100	14	0.0E+00	2.8E+05	4.2E+05	**2.8E+05**	**4.2E+05**
157	1.6E+04	9.3E+04	54	**340**	Yes	130	54	5.6E+05	2.6E+03	4.0E+03	**5.6E+05**	**5.6E+05**
158	1.5E+04	8.5E+04	42	**270**	Yes	110	42	2.8E+05	1.9E+03	2.9E+03	**2.8E+05**	**2.8E+05**
159	1.1E+04	5.5E+04	126	**410**	Yes	360	126	8.2E+06	4.2E+03	6.2E+03	**8.2E+06**	**8.2E+06**
160	1.2E+04	6.2E+04	21	**150**	-	170	21	-	-	-	-	-
161	1.3E+04	6.9E+04	12	**110**	-	200	12	-	-	-	-	-
162	2.1E+04	1.4E+05	27	**280**	-	90	27	-	-	-	-	-
163	2.5E+04	1.8E+05	21	**290**	No	120	21	0.0E+00	1.7E+04	2.6E+04	**1.7E+04**	**2.6E+04**
164	1.5E+04	8.5E+04	35	**250**	-	240	35	-	-	-	-	-
165	1.3E+04	6.9E+04	16	**140**	Yes	60	16	2.4E+04	1.5E+04	2.5E+04	**3.8E+04**	**4.9E+04**
166	1.5E+04	8.5E+04	8	**100**	Yes	120	8	1.1E+04	7.9E+03	1.2E+04	**1.9E+04**	**2.3E+04**
167	2.0E+04	1.3E+05	4	**90**	-	40	4	-	-	-	-	-
168	2.1E+04	1.4E+05	7	**130**	-	750	7	-	-	-	-	-
169	1.5E+04	8.5E+04	1	**30**	Yes	90	1	1.2E+02	6.6E+03	9.9E+03	**6.7E+03**	**1.0E+04**
170	8.7E+04	1.5E+06	1	**170**	Yes	120	1	1.8E+02	1.5E+04	2.4E+04	**1.6E+04**	**2.4E+04**
171	1.2E+04	6.2E+04	13	**110**	Yes	220	13	5.4E+04	1.0E+05	1.9E+05	**1.6E+05**	**2.5E+05**
172	1.1E+04	5.5E+04	4	**50**	-	60	4	-	-	-	-	-
173	5.3E+04	6.4E+05	18	**560**	No	60	18	0.0E+00	1.8E+04	3.6E+04	**1.8E+04**	**3.6E+04**
174	5.6E+04	7.0E+05	34	**860**	Yes	120	34	2.0E+05	2.5E+04	3.7E+04	**2.3E+05**	**2.4E+05**
175	2.8E+04	2.2E+05	5	**140**	-	120	5	-	-	-	-	-

(-) indicates datum not applicable to lake because its hypothetical outburst would not generate a debris flow.
Data for drained lakes based on pre-outburst conditions.
[a] No. = Lake ID number; A = lake area; V = lake volume, from equation (7); Hd = dam height to lake surface; Qp = peak discharge, from equation (8).
[b] Dam? = breach material reaches runout zone?; W = moraine width; Vb = breach volume, from equation (9); Vr_lower = total reach contribution volume (lower yield rate estimate), from equation (10); Vr_upper = total reach contribution volume (upper yield rate estimate), from equation (10); Vm_lower = maximum volume (lower yield rate estimate), from equation (11); Vm_upper = maximum volume (upper yield rate estimate), from equation (11).

Appendix D (continued)

No.	Maximum debris flow runout estimation data[c] Dflow? (-)	Lk_elev (m)	End_elev (m)	PremTerm? (-)	**Runout (m)**	Maximum debris flow area of inundation estimation data[d] **Bm_lower (ha)**	**Bm_upper (ha)**	Probability estimation data[e] Mhw (-)	IceC (-)	Area (ha)	Geol (-)	**Prob (%)**	**Prob_cat (-)**
1	Yes	1870	1160	Yes (15)	**2710**	**2.7**	**3.5**	0.22	1	2.0	1	**9.E-01**	**very low**
2	No	1699	-	-	-	-	-	0.06	0	65.3	1	**6.E+00**	**low**
3	No	1630	-	-	-	-	-	0.16	0	23.0	1	**8.E+00**	**low**
4	No	1649	-	-	-	-	-	0.34	0	9.4	1	**3.E+01**	**very high**
5	No	1722	-	-	-	-	-	0.10	0	8.5	1	**4.E+00**	**very low**
6	No	1875	-	-	-	-	-	0.08	0	1.2	1	**3.E+00**	**very low**
7	Yes	2090	1880	No	**1230**	**3.6**	**3.9**	0.12	0	1.5	3	**3.E+01**	**very high**
8	Yes	2330	2060	No	**1500**	**6.0**	**6.2**	0.38	1	1.3	2	**2.E+01**	**medium**
9	No	2090	-	-	-	-	-	0.03	0	4.3	3	**1.E+01**	**medium**
10	Yes	1818	1380	No	**2380**	**1.6**	**2.2**	0.04	0	5.0	1	**2.E+00**	**very low**
11	Yes	1932	1400	No	**3090**	**2.4**	**3.9**	0.01	0	3.5	1	**2.E+00**	**very low**
12	Yes	1377	660	No	**4000**	**10.0**	**10.7**	0.09	0	12.3	1	**4.E+00**	**very low**
13	No	756	-	-	-	-	-	0.03	0	24.2	1	**3.E+00**	**very low**
14	Yes	2024	860	Yes (14)	**4820**	**2.9**	**4.6**	0.29	0	4.0	2	**5.E+01**	**very high**
15	Yes	1977	1270	Yes (27)	**1400**	**10.2**	**10.3**	0.28	0	7.9	1	**2.E+01**	**medium**
16	Yes	1815	650	Yes (23)	**2780**	**2.1**	**3.0**	0.06	0	1.5	1	**2.E+00**	**very low**
17	Yes	1697	1480	No	**1280**	**13.4**	**13.6**	0.10	0	2.0	1	**3.E+00**	**very low**
18	Yes	1795	1180	Yes (14)	**2410**	**6.0**	**6.6**	0.08	0	1.7	1	**3.E+00**	**very low**
19	No	2154	-	-	-	-	-	0.03	1	4.1	1	**2.E-01**	**very low**
20	Yes	1307	300	Yes (21)	**2590**	**3.5**	**4.6**	0.02	1	8.0	1	**2.E-01**	**very low**
21	Yes	1870	1290	No	**3270**	**1.2**	**1.5**	0.27	0	3.0	1	**2.E+01**	**medium**
22	No	1805	-	-	-	-	-	0.13	0	2.3	1	**5.E+00**	**very low**
23	Yes	1410	1060	No	**2040**	**2.1**	**2.7**	0.54	0	1.0	1	**7.E+01**	**very high**
24	Yes	1667	160	No	**8800**	**9.5**	**14.9**	0.28	0	15.5	1	**2.E+01**	**high**
25	Yes	2187	2020	No	**990**	**10.2**	**10.2**	0.32	1	3.9	2	**1.E+01**	**low**
26	No	2017	-	-	-	-	-	0.00	1	1.4	3	**1.E+00**	**very low**
27	Yes	2215	1210	Yes (15)	**3860**	**6.6**	**7.0**	0.07	1	1.6	3	**2.E+00**	**very low**
28	No	1999	-	-	-	-	-	0.21	0	2.5	2	**3.E+01**	**very high**
29	No	1973	-	-	-	-	-	0.05	1	3.8	2	**9.E-01**	**very low**
30	Yes	2225	1860	No	**2130**	**1.5**	**1.9**	0.25	0	1.7	2	**4.E+01**	**very high**

Appendix D (continued)

No.	Maximum debris flow runout estimation data[c] Dflow?	Lk_elev	End_elev	PremTerm?	Runout	Maximum debris flow area of inundation estimation data[d] Bm_lower	Bm_upper	Probability estimation data[e] Mhw	IceC	Area	Geol	Prob	Prob_cat
	(-)	(m)	(m)	(-)	**(m)**	**(ha)**	**(ha)**	(-)	(-)	(ha)	(-)	**(%)**	**(-)**
31	No	2121	-	-	-	-	-	0.05	1	3.7	2	**9.E-01**	**very low**
32	No	2150	-	-	-	-	-	0.06	1	6.2	3	**2.E+00**	**very low**
33	No	2257	-	-	-	-	-	0.13	1	3.8	3	**4.E+00**	**very low**
34	No	1977	-	-	-	-	-	0.07	1	1.4	2	**1.E+00**	**very low**
35	No	2060	-	-	-	-	-	0.24	1	1.4	2	**5.E+00**	**very low**
36	No	2038	-	-	-	-	-	0.05	1	7.7	2	**1.E+00**	**very low**
37	No	2187	-	-	-	-	-	0.06	1	4.8	2	**1.E+00**	**very low**
38	No	2268	-	-	-	-	-	0.26	1	7.8	2	**7.E+00**	**low**
39	No	2319	-	-	-	-	-	0.20	1	4.4	2	**4.E+00**	**very low**
40	Yes	2291	2160	No	**750**	**2.5**	**2.6**	0.05	1	4.4	2	**9.E-01**	**very low**
41	No	2258	-	-	-	-	-	0.25	1	1.1	2	**6.E+00**	**very low**
42	Yes	2367	1380	No	**5670**	**2.4**	**3.4**	0.17	1	1.6	2	**3.E+00**	**very low**
43	No	2123	-	-	-	-	-	0.05	0	1.0	2	**1.E+01**	**low**
44	Yes	2377	2310	No	**400**	**5.8**	**5.8**	0.23	0	1.1	2	**4.E+01**	**very high**
45	No	2136	-	-	-	-	-	0.14	0	1.3	2	**2.E+01**	**high**
46	Yes	2231	1980	No	**1420**	**3.7**	**3.9**	0.12	0	1.3	2	**2.E+01**	**medium**
47	Yes	2354	2000	No	**1960**	**0.6**	**0.9**	0.05	0	6.0	2	**1.E+01**	**low**
48	No	2272	-	-	-	-	-	0.23	1	4.8	2	**5.E+00**	**very low**
49	Yes	2265	2200	No	**370**	**0.3**	**0.4**	0.05	0	1.6	3	**2.E+01**	**medium**
50	Yes	2137	1700	No	**2580**	**0.9**	**1.5**	0.14	0	1.4	1	**5.E+00**	**very low**
51	No	2335	-	-	-	-	-	0.09	0	1.5	1	**3.E+00**	**very low**
52	No	2227	-	-	-	-	-	0.07	0	2.5	1	**3.E+00**	**very low**
53	No	2225	-	-	-	-	-	0.11	0	1.7	1	**4.E+00**	**very low**
54	No	1950	-	-	-	-	-	0.01	0	16.6	1	**2.E+00**	**very low**
55	No	1990	-	-	-	-	-	0.14	0	8.2	1	**5.E+00**	**very low**
56	Yes	2258	2070	No	**1030**	**2.0**	**2.1**	0.17	0	2.0	1	**7.E+00**	**low**
57	Yes	2162	1400	Yes (15)	**2910**	**7.2**	**8.2**	0.43	0	1.3	1	**4.E+01**	**very high**
58	Yes	2070	1630	Yes (15)	**1690**	**1.7**	**2.7**	0.09	1	1.7	1	**3.E-01**	**very low**
59	Yes	2153	1630	Yes (16)	**1800**	**5.3**	**5.9**	0.15	0	3.9	1	**6.E+00**	**very low**
60	No	1388	-	-	-	-	-	0.02	0	202.3	1	**3.E+01**	**very high**

Appendix D (continued)

No.	Maximum debris flow runout estimation data[c] Dflow?	Lk_elev	End_elev	PremTerm?	Runout	Maximum debris flow area of inundation estimation data[d] Bm_lower	Bm_upper	Probability estimation data[e] Mhw	IceC	Area	Geol	Prob	Prob_cat
	(-)	(m)	(m)	(-)	**(m)**	**(ha)**	**(ha)**	(-)	(-)	(ha)	(-)	**(%)**	**(-)**
61	Yes	2178	760	Yes (14)	**5790**	**4.3**	**6.6**	0.50	0	2.0	1	**6.E+01**	**very high**
62	Yes	2158	1840	No	**1750**	**3.9**	**4.0**	0.28	1	2.7	1	**2.E+00**	**very low**
63	No	2018	-	-	-	-	-	0.02	0	1.9	1	**2.E+00**	**very low**
64	Yes	2162	2040	No	**670**	**0.4**	**0.5**	0.03	0	1.4	1	**2.E+00**	**very low**
65	No	1502	-	-	-	-	-	0.15	0	8.0	1	**6.E+00**	**very low**
66	Yes	1515	1360	No	**910**	**1.6**	**2.1**	0.03	0	3.6	1	**2.E+00**	**very low**
67	Yes	935	0	Yes (12)	**4530**	**3.0**	**4.8**	0.04	0	12.0	1	**2.E+00**	**very low**
68	No	1735	-	-	-	-	-	0.13	0	2.5	1	**5.E+00**	**very low**
69	No	1759	-	-	-	-	-	0.16	0	7.4	2	**3.E+01**	**very high**
70	No	1465	-	-	-	-	-	0.07	1	1.8	1	**2.E-01**	**very low**
71	Yes	1970	1300	Yes (17)	**2170**	**15.2**	**15.3**	0.35	0	1.0	3	**8.E+01**	**very high**
72	Yes	1998	1170	No	**4650**	**1.4**	**2.2**	0.04	0	3.6	2	**9.E+00**	**low**
73	No	1965	-	-	-	-	-	0.02	0	7.6	1	**2.E+00**	**very low**
74	Yes	1797	700	No	**6290**	**5.7**	**8.8**	0.03	0	3.2	1	**2.E+00**	**very low**
75	Yes	1908	930	Yes (12)	**4790**	**4.2**	**6.3**	0.00	0	1.3	1	**1.E+00**	**very low**
76	No	1407	-	-	-	-	-	0.03	0	11.1	1	**2.E+00**	**very low**
77	No	1691	-	-	-	-	-	0.06	0	5.2	1	**3.E+00**	**very low**
78	No	1533	-	-	-	-	-	0.01	0	7.7	1	**2.E+00**	**very low**
79	Yes	1500	1220	No	**3440**	**2.2**	**3.0**	0.03	0	12.2	1	**2.E+00**	**very low**
80	Yes	1755	1370	Yes (15)	**1460**	**1.5**	**2.1**	0.13	0	1.8	1	**5.E+00**	**very low**
81	No	1365	-	-	-	-	-	0.05	0	14.6	1	**3.E+00**	**very low**
82	No	1252	-	-	-	-	-	0.05	0	20.4	2	**1.E+01**	**medium**
83	No	1287	-	-	-	-	-	0.02	0	190.0	1	**3.E+01**	**very high**
84	Yes	1362	830	No	**2990**	**7.1**	**7.3**	0.17	0	3.5	1	**7.E+00**	**low**
85	No	1259	-	-	-	-	-	0.01	0	8.3	1	**2.E+00**	**very low**
86	No	1459	-	-	-	-	-	0.16	0	17.8	1	**8.E+00**	**low**
87	No	1270	-	-	-	-	-	0.03	0	12.0	1	**2.E+00**	**very low**
88	No	918	-	-	-	-	-	0.11	0	20.9	1	**5.E+00**	**very low**
89	Yes	1773	420	Yes (13)	**5660**	**4.3**	**6.6**	0.06	0	8.2	1	**3.E+00**	**very low**
90	Yes	1923	1440	No	**2630**	**0.8**	**1.3**	0.12	0	3.0	1	**4.E+00**	**very low**

Appendix D (continued)

No.	Maximum debris flow runout estimation data[c] Dflow?	Lk_elev	End_elev	PremTerm?	Runout	Maximum debris flow area of inundation estimation data[d] Bm_lower	Bm_upper	Probability estimation data[e] Mhw	IceC	Area	Geol	Prob	Prob_cat
	(-)	(m)	(m)	(-)	**(m)**	**(ha)**	**(ha)**	(-)	(-)	(ha)	(-)	**(%)**	**(-)**
91	Yes	1496	700	No	**4350**	**8.1**	**10.2**	0.10	0	1.9	1	**3.E+00**	**very low**
92	Yes	1578	680	No	**5050**	**1.9**	**3.0**	0.02	0	13.4	1	**2.E+00**	**very low**
93	Yes	1710	1040	No	**3850**	**77.4**	**77.5**	0.26	0	1.1	1	**1.E+01**	**medium**
94	Yes	1560	1060	No	**2860**	**4.0**	**4.1**	0.19	0	1.0	1	**8.E+00**	**low**
95	Yes	1828	620	Yes (18)	**3770**	**1.5**	**2.4**	0.08	0	2.8	1	**3.E+00**	**very low**
96	No	1459	-	-	-	-	-	0.06	0	21.4	1	**3.E+00**	**very low**
97	No	1455	-	-	-	-	-	0.05	0	69.1	1	**6.E+00**	**low**
98	No	1454	-	-	-	-	-	0.07	0	58.0	1	**6.E+00**	**low**
99	Yes	1692	1390	Yes (11)	**1670**	**1.2**	**1.9**	0.03	0	2.7	1	**2.E+00**	**very low**
100	No	1400	-	-	-	-	-	0.07	0	16.2	1	**3.E+00**	**very low**
101	Yes	1975	290	Yes (17)	**5530**	**5.9**	**9.2**	0.18	0	1.9	4	**3.E-04**	**very low**
102	Yes	1558	1060	No	**2870**	**3.1**	**4.0**	0.01	0	2.3	1	**2.E+00**	**very low**
103	No	1624	-	-	-	-	-	0.03	0	1.4	2	**8.E+00**	**low**
104	Yes	1619	870	Yes (16)	**2560**	**9.0**	**9.8**	0.15	0	2.1	2	**2.E+01**	**high**
105	Yes	1652	200	No	**8240**	**5.6**	**7.4**	0.15	0	4.0	1	**6.E+00**	**very low**
106	No	1367	-	-	-	-	-	0.22	0	8.4	1	**1.E+01**	**low**
107	Yes	1842	1380	No	**2510**	**1.5**	**2.0**	0.12	0	1.5	1	**4.E+00**	**very low**
108	Yes	1798	1640	No	**850**	**1.3**	**1.7**	0.03	0	2.5	2	**8.E+00**	**low**
109	Yes	1953	1200	Yes (27)	**1480**	**1.2**	**1.6**	0.02	0	7.2	1	**2.E+00**	**very low**
110	Yes	2048	1840	No	**1150**	**1.6**	**1.8**	0.06	1	1.8	1	**2.E-01**	**very low**
111	Yes	2072	1940	Yes (17)	**420**	**0.9**	**1.1**	0.06	0	5.3	1	**3.E+00**	**very low**
112	No	1687	-	-	-	-	-	0.00	0	11.0	1	**2.E+00**	**very low**
113	Yes	2031	770	No	**6910**	**3.4**	**5.4**	0.18	0	4.9	1	**7.E+00**	**low**
114	Yes	1559	830	Yes (11)	**3930**	**1.4**	**2.3**	0.04	0	13.5	1	**2.E+00**	**very low**
115	Yes	1545	830	Yes (11)	**3600**	**1.4**	**2.3**	0.07	0	2.6	1	**3.E+00**	**very low**
116	No	834	-	-	-	-	-	0.10	0	20.2	1	**5.E+00**	**very low**
117	Yes	1270	480	Yes (21)	**2100**	**5.9**	**6.5**	0.06	0	3.6	1	**2.E+00**	**very low**
118	No	1000	-	-	-	-	-	0.12	1	2.5	1	**4.E-01**	**very low**
119	No	809	-	-	-	-	-	0.15	0	11.6	1	**6.E+00**	**low**
120	No	1004	-	-	-	-	-	0.31	0	10.0	1	**2.E+01**	**high**

Appendix D (continued)

No.	Maximum debris flow runout estimation data[c] Dflow?	Lk_elev	End_elev	PremTerm?	Runout	Maximum debris flow area of inundation estimation data[d] Bm_lower	Bm_upper	Probability estimation data[e] Mhw	IceC	Area	Geol	Prob	Prob_cat
	(-)	(m)	(m)	(-)	**(m)**	**(ha)**	**(ha)**	(-)	(-)	(ha)	(-)	**(%)**	**(-)**
121	Yes	1487	510	Yes (12)	**4740**	**2.5**	**4.0**	0.07	0	2.6	1	**3.E+00**	**very low**
122	No	1628	-	-	-	-	-	0.09	1	9.0	1	**3.E-01**	**very low**
123	No	2025	-	-	-	-	-	0.26	0	1.1	1	**1.E+01**	**medium**
124	Yes	1810	1140	No	**3970**	**1.9**	**3.0**	0.26	0	1.1	1	**1.E+01**	**medium**
125	Yes	2081	1330	Yes (15)	**2730**	**1.8**	**2.4**	0.06	0	1.7	1	**2.E+00**	**very low**
126	Yes	2091	1860	No	**1260**	**1.1**	**1.4**	0.09	1	21.1	1	**4.E-01**	**very low**
127	Yes	1603	1140	No	**2530**	**0.7**	**1.7**	0.09	1	2.0	4	**1.E-05**	**very low**
128	No	1289	-	-	-	-	-	0.13	0	18.0	4	**3.E-04**	**very low**
129	No	1475	-	-	-	-	-	0.04	0	5.0	3	**2.E+01**	**medium**
130	No	941	-	-	-	-	-	0.02	1	8.0	4	**7.E-06**	**very low**
131	No	1212	-	-	-	-	-	0.59	0	1.0	4	**2.E-02**	**very low**
132	No	1298	-	-	-	-	-	0.49	0	2.8	4	**6.E-03**	**very low**
133	No	1175	-	-	-	-	-	0.02	1	2.0	4	**6.E-06**	**very low**
134	Yes	1443	1160	No	**1560**	**26.9**	**27.1**	0.11	1	6.6	4	**2.E-05**	**very low**
135	Yes	1656	1030	Yes (11)	**3080**	**4.6**	**5.9**	0.08	0	1.4	1	**3.E+00**	**very low**
136	No	1034	-	-	-	-	-	0.01	1	24.4	1	**2.E-01**	**very low**
137	No	779	-	-	-	-	-	0.16	0	26.9	1	**9.E+00**	**low**
138	Yes	1890	400	Yes (19)	**4370**	**32.6**	**33.2**	0.36	0	2.4	4	**2.E-03**	**very low**
139	Yes	2150	990	Yes (17)	**3840**	**2.6**	**3.8**	0.15	0	1.6	1	**5.E+00**	**very low**
140	No	1608	-	-	-	-	-	0.12	0	18.1	1	**5.E+00**	**very low**
141	No	2053	-	-	-	-	-	0.11	0	1.2	1	**4.E+00**	**very low**
142	Yes	1851	1140	No	**3860**	**1.8**	**2.5**	0.05	0	5.7	1	**2.E+00**	**very low**
143	Yes	1861	1140	No	**3920**	**1.8**	**2.5**	0.23	0	6.7	1	**1.E+01**	**low**
144	Yes	1870	1000	No	**5140**	**1.4**	**2.2**	0.21	0	3.5	1	**9.E+00**	**low**
145	No	2157	-	-	-	-	-	0.15	0	2.0	3	**3.E+01**	**very high**
146	Yes	1925	1240	No	**3950**	**3.6**	**4.7**	0.05	0	2.4	3	**2.E+01**	**medium**
147	Yes	2165	1790	No	**2150**	**5.5**	**5.7**	0.15	0	8.4	1	**6.E+00**	**low**
148	No	1623	-	-	-	-	-	0.12	0	7.0	1	**5.E+00**	**very low**
149	No	1839	-	-	-	-	-	0.10	0	1.0	1	**3.E+00**	**very low**
150	Yes	2122	1030	No	**5950**	**3.8**	**6.0**	0.10	0	2.1	1	**3.E+00**	**very low**

Appendix D (continued)

	Maximum debris flow runout estimation data[c]					Maximum debris flow area of inundation estimation data[d]		Probability estimation data[e]					
No.	Dflow?	Lk_elev	End_elev	PremTerm?	**Runout**	**Bm_lower**	**Bm_upper**	Mhw	IceC	Area	Geol	**Prob**	**Prob_cat**
	(-)	(m)	(m)	(-)	**(m)**	**(ha)**	**(ha)**	(-)	(-)	(ha)	(-)	**(%)**	**(-)**
151	Yes	1516	1160	No	**1970**	**0.0**	**1.5**	0.05	0	5.6	1	**2.E+00**	**very low**
152	Yes	2088	1640	No	**2560**	**1.0**	**1.6**	0.07	0	2.6	1	**3.E+00**	**very low**
153	No	2290	-	-	-	-	-	0.22	1	2.5	4	**4.E-05**	**very low**
154	No	2292	-	-	-	-	-	0.05	1	4.4	4	**8.E-06**	**very low**
155	Yes	2261	1950	Yes (15)	**1180**	**30.5**	**30.6**	0.35	1	2.7	2	**1.E+01**	**medium**
156	Yes	2188	300	Yes (14)	**7800**	**8.5**	**11.1**	0.14	1	5.0	3	**4.E+00**	**very low**
157	Yes	2235	2060	Yes (15)	**630**	**13.6**	**13.6**	0.40	0	1.6	1	**4.E+01**	**very high**
158	Yes	2353	2160	No	**1040**	**8.6**	**8.6**	0.38	0	1.5	1	**3.E+01**	**very high**
159	Yes	2265	1940	No	**1930**	**81.5**	**81.5**	0.35	1	1.1	1	**3.E+00**	**very low**
160	No	2298	-	-	-	-	-	0.13	0	1.2	1	**5.E+00**	**very low**
161	No	1988	-	-	-	-	-	0.06	0	1.3	1	**2.E+00**	**very low**
162	No	2067	-	-	-	-	-	0.31	0	2.1	1	**2.E+01**	**high**
163	Yes	2082	1740	No	**1930**	**1.3**	**1.7**	0.17	0	2.5	1	**7.E+00**	**low**
164	No	2158	-	-	-	-	-	0.15	1	1.5	1	**5.E-01**	**very low**
165	Yes	2360	1740	No	**3510**	**2.3**	**2.7**	0.25	0	1.3	1	**1.E+01**	**medium**
166	Yes	2018	1880	Yes (13)	**590**	**1.4**	**1.6**	0.07	0	1.5	1	**3.E+00**	**very low**
167	No	1745	-	-	-	-	-	0.10	0	2.0	1	**3.E+00**	**very low**
168	No	2025	-	-	-	-	-	0.01	1	2.1	3	**1.E+00**	**very low**
169	Yes	2427	2270	No	**900**	**0.7**	**0.9**	0.01	1	1.5	2	**6.E-01**	**very low**
170	Yes	1617	990	Yes (19)	**1800**	**1.2**	**1.7**	0.01	0	8.7	1	**2.E+00**	**very low**
171	Yes	1780	420	Yes (13)	**6120**	**5.8**	**7.9**	0.06	0	1.2	1	**2.E+00**	**very low**
172	No	1521	-	-	-	-	-	0.07	0	1.1	2	**1.E+01**	**low**
173	Yes	1990	1000	No	**5620**	**1.4**	**2.2**	0.29	0	5.3	1	**2.E+01**	**high**
174	Yes	2024	1120	No	**4900**	**7.5**	**7.7**	0.28	0	5.6	1	**2.E+01**	**medium**
175	No	2046	-	-	-	-	-	0.04	0	2.8	1	**2.E+00**	**very low**

(-) indicates datum not applicable to lake because its hypothetical outburst would not generate a debris flow.
Data for drained lakes based on pre-outburst conditions.
[c] No. = lake ID number; Dflow? = Will debris flow form?; Lk_elev = lake elevation; End_elev = elevation along channel corresponding to 10° average slope; PremTerm? = Will debris flow terminate "prematurely" due to abrupt path widening or gradient reduction? (average runout slope (°) at termination in brackets); Runout = maximum expected runout distance, corresponding to 10° average slope. [d] Bm_lower = maximum area of inundation (based on lower volume estimate), from equation (12); Bm_upper = maximum area of inundation (based on upper volume estimate), from equation (12). [e] Mhw = moraine height-to-width ratio (to lake surface); IceC = presence/absence of ice core (0 = ice-free; 1 = ice-cored); Area = lake area; Geol = main rock type forming moraine (1=granitic, 2=volcanic, 3=sedimentary, 4=metamorphic); Prob = outburst probability; Prob_cat = outburst probability category.

Appendix E. Supplemental foreign lake data used in statistical database

		Longitude[b]			Latitude						
No.	Lake[a]	Deg	Min	Sec	Deg	Min	Sec	Map sheet[c]	Elev. (m)[d]	Dam type[e]	Outburst date
176	"Patience Mountain"	117	40	39	51	7	52	082N012	2351	1	1951 - 1966
177	"South Macoun"	117	22	44	51	12	48	082N024	1849	1	Before 1949
178	"North Macoun"	117	23	28	51	14	15	082N024	1863	1	July 1983
179	Tide Lake	130	4	9	56	18	20	104B040	655	1	1927 - 1930
180	Tats Lake	137	31	0	59	37	43	114P063	1519	1	June 28, 1990
181	"Ottarasko E Fork"[f]	124	37	8	51	35	58	092N057	2143	1	Sep. 3, 1993 - July 19, 1994
182	"Diller Glacier"	121	46	26	44	8	27	North Sister Quadrangle	2292	1	Sept. 7, 1970
183	"Collier Glacier"	121	47	18	44	11	3	North Sister Quadrangle	2134	1	July 1942, 2nd outburst 1954 - 1956
184	"East Bend Glacier"	121	41	9	44	4	53	Broken Top Quadrangle	2444	1	Oct. 7, 1966
185	Carver Lake	121	45	14	44	6	55	South Sister Quadrangle	2388	1	N/A
186	"Snowking Mountain"	121	17	5	48	23	43	Snowking Mountain	1780	1	Before 1955, 2nd outburst 1980

[a] Lake names in quotations are unofficial, according to Terrain Resource Information Management (TRIM) and United States Geological Survey topographic maps.
[b] West longitude and North latitude, in degrees (Deg), minutes (Min), and seconds (Sec).
[c] Terrain Resource Information Management (TRIM) or United States Geological Survey topographic map on which lake outlet is located.
[d] Approximate lake elevation (m), based on pre-outburst level for drained lakes, interpolated between contours if lake elevation not provided on map.
[e] 1 = "classic" narrow, sharp-crested moraine; 2 = broad, rounded moraine; 3 = low, indefinite moraine.
[f] Lake located within study area, but excluded from inventory because less than 1 ha in size.

Appendix E (continued)

No.	Lake[a]	Roll no.	Date	Scale[b]	Focal (mm)[c]	Film[d]	Frame 1 No.	Frame 1 Altitude[e] (m)	Frame 2 No.	Frame 2 Altitude[e] (m)
176	"Patience Mountain"	BC1382	14-Sep-51	1:30 000	325	B&W	16	6096	15	6096
177	"South Macoun"	30BCB96078	10-Sep-96	1:15 000	306	B&W	76	6403	75	6403
178	"North Macoun"	30BCB96078	10-Sep-96	1:15 000	306	B&W	252	6403	253	6403
179	Tide Lake	BC5504	16-Aug-72	1:30 000	153	B&W	172	6858	173	6858
180	Tats Lake	BC87076	25-Aug-87	1:70 000	152	B&W	189	12802	188	12802
181	"Ottarasko East Fork"[f]	30BCC93106	3-Sep-93	1:15 000	305	colour	66	6096	65	6096
182	"Diller Glacier"	F16 41017 1274	6-Sep-74	1:15 000	208	B&W	98	5184	99	5184
183	"Collier Glacier"	F16 41017 1274	6-Sep-74	1:15 000	208	B&W	101	6109	102	6109
184	"East Bend Glacier"	EGI-47	13-Jul-59	1:12 000	305	B&W	197	5399	198	5399
185	Carver Lake	USDA-F 616180C 1690	14-Sep-90	1:12 000	208	colour	253	5342	252	5342
186	"Snowking Mountain"	F12 616050A 1783	16-Aug-85	1:12 000	208	colour	63	4309	62	4309

[a] Lake names in quotations are unofficial, according to Terrain Resource Information Management (TRIM) and United States Geological Survey topographic maps.
[b] Nominal.
[c] Camera focal length (m).
[d] Film emulsion = colour or black & white (B&W)
[e] Flying altitude above mean sea level (m) from which photograph was taken.
[f] Lake located within study area, but excluded from inventory because less than 1 ha in size.

Appendix E (continued)

No.	*Frbd* (m)	*RlfG* (m)	*FMht* (-)	*Mhw* (-)	*Mdfk* (-)	*LGpx* (m)	*LGsp* (°)	*Calv* (m)	*Lsld* (-)	*Snow* (-)	*IceC* (-)	*Mveg* (-)	*UsLk* (-)	*Crev* (-)	*SnSt* (°)	*Area* (ha)	*Wshd* (ha)	*Geol* (-)	*Lk* (-)
176	0	-	0.00	0.36	0.66	-	-	-	0	1	0	1	0	-	-	1.6	36	3	1
177	0	0	0.00	0.07	0.30	0	0	260	0	1	0	1	0	0	28	5.3	74	3	1
178	3	40	0.10	0.38	0.73	190	11	0	0	0	0	1	0	0	24	2.0	76	3	1
179	0	30	0.00	0.07	0.10	500	3	0	0	1	0	1	1	0	11	250.0	13000	2	3
180	0	0	0.00	0.34	0.38	0	0	170	0	0	0	1	0	0	16	2.5	73	1	1
181	0	50	0.00	0.29	0.39	110	25	0	0	0	0	1	0	1	23	0.4	41	2	1
182	0	0	0.00	0.32	0.45	0	0	140	0	0	0	1	0	0	21	3.1	52	2	1
183	0	10	0.00	0.12	0.17	560	1	0	0	0	0	1	0	1	12	10.0	360	2	1
184	0	0	0.00	0.40	0.56	0	0	110	0	1	0	1	0	0	23	3.6	32	2	1
185	0	70	0.00	0.09	0.64	180	21	0	0	0	0	1	0	1	18	7.0	110	2	1
186	0	0	0.00	0.16	0.29	0	0	370	0	0	0	1	0	1	10	6.0	145	1	1

Notes:
Data for drained lakes based on pre-outburst conditions.
Predictor variable codes (column headings) and units correspond to those in Table 2-1.
(-) indicates particular variable not applicable to lake because no glacier existed in watershed when aerial photograph was taken.
Complete hazard assessment not completed for foreign lakes.